Construction of Hilbert transform pairs of MRA tight frames and its application

DISSERTATION

zur Erlangung des Grades
eines Doktors der Naturwissenschaften
der Technischen Universität Dortmund

Der Fakultät für Mathematik
der Technischen Universität Dortmund
vorgelegt von:

Kyoung-Yong Lee

2007

Tag der mündlichen Prüfung: 22. November 2007
Vorsitzender: Prof. Dr. Norbert Steinmetz,Technische Universität Dortmund
1. Gutachter: Prof. Dr. Joachim Stöckler, Technische Universität Dortmund
2. Gutachter: Prof. Dr. Ole Christensen, Technical University of Denmark, Lyngby

Abstract

Hilbert transform pairs of wavelets, biorthogonal wavelets and frames were found to be attractive in many applications. The Hilbert transform pairs are, however, hardly adoptable for applications, since their two-scale symbols are not trigonometric polynomials. Moreover, the symbols can not be implemented as FIR filters, nor rational IIR filters. That is the reason why approximations are constructed by many researchers in spite of the theoretical existence of the Hilbert transform pairs of wavelets, biorthogonal wavelets, and frames. But these conventional approaches have two drawbacks. Firstly, the wavelets and refinable functions do not have closed forms. Secondly, the symmetry, or "linear phase", of the wavelets and refinable functions is an important constraint in many applications. But, the results, however, show that it is not easy to get symmetric Hilbert transform pairs of wavelets (or generators of frames).

In the first half of this thesis, we study the construction of Hilbert transform pair of MRA tight frames, which overcomes the drawbacks of the conventional constructions. Namely, our first research contributions are as follows:

- We show that for a given MRA tight frame $\{\psi_{j,k,\ell}\}$, the family $\{\mathcal{H}\psi_{j,k,\ell}\}$ is an MRA tight frame as well. Furthermore, we present a general method producing an MRA tight frame $\{T\psi_{j,k,\ell}\}$ from a given one, where T is a linear operator including the Hilbert transform.
- For the sake of the application, we demonstrate an approximate Hilbert transform $\{\tilde{\Psi}_{j,k,\ell}\}$ such that $\tilde{\Psi}_j \approx \mathcal{H}\psi_j$ and $\tilde{\Psi}_j$ has closed form and almost symmetry.

In the second half of this thesis, we focus on the work of Zhao. He constructed the biorthogonal wavelet $\{\Lambda\psi, \Lambda^{-1}\tilde{\psi}\}$ for a given biorthogonal wavelet $\{\psi, \tilde{\psi}\}$ and applied it to the filtered backprojection algorithm of computed tomography. The Λ-operator is defined by $\Lambda = \mathcal{H}\mathcal{D}$, where $\mathcal{D}$ is the differential operator. The Λ-operator appears in the inversion formula for the Radon transform and plays an important role in the filtered backprojection algorithm. His construction is based on the general method of generating a biorthogonal wavelet from a given one. The

associated filters are described by IIR filters and they were approximated by FIR filters by truncation.

We generalize the result of Zhao to MRA bi-frames in association with the first two results of this thesis. Namely, the other main results of this thesis are as follows:

- We show that it is possible to construct the MRA bi-frame $(\{\Lambda\psi_{j,k,\ell}\}, \{\Lambda^{-1}\psi_{j,k,\ell}\})$ for a given MRA tight frame $\{\psi_{j,k,\ell}\}$. In addition, we present a general method generating an MRA bi-frame $\left(\{T\psi_{j,k,\ell}\}, \{T^{-1}\tilde{\psi}_{j,k,\ell}\}\right)$ from a given $\left(\{\psi_{j,k,\ell}\}, \{\tilde{\psi}_{j,k,\ell}\}\right)$, where the linear operator T (possibly unbounded) includes the Hilbert transform, differentiation/integration, and the Λ-operator.
- Using the second result of this thesis, we present an approximation of $(\{\Lambda\psi_{j,k,\ell}\}, \{\Lambda^{-1}\psi_{j,k,\ell}\})$.

In addition to the approximation, we propose an approximation of the Ram-Lak filter. We expect that this result can be employed in the filtered backprojection algorithm of computed tomography.

Acknowledgements

Many people have contributed in various ways to this thesis. First and foremost, I am deeply indebted to Prof. Stöckler for his consistent guidance in my research and his steady support and encouragement as an always thoughtful mentor. In the numerous meetings of the last 4 years, he sparked my interest and let me know the taste of mathematics. To Prof. Christensen I want to express my gratefulness for agreeing to be a reviewer for my thesis and for giving wonderful advices .

I was lucky enough to have the colleagues - especially Michael, Maria, Laura, in Lehrstuhl VIII (Approximationstheorie) of Dortmund, who provided me a very pleasant working atmosphere and unceasing help. It is a wonderful and cherishable memory of my life to work with them.

Family is an important source of motivation of my life. I want to thank my parents who had a deep affection for their children and taught them a sincere and conscientious life. To my wife Hyeyoung and my daughter Jia I would like to show my appreciation for always being with me and going through tough times together.

Contents

CHAPTER 1

Mathematical background

1.1. Introduction

It is well-known that wavelets and frames of $L^2(\mathbb{R})$ have advantages in time-frequency analysis and other applications ([**5, 17, 21, 31**]). In particular, spline wavelets and frames have been of great interest due to their benefits in the following points: size of the time-frequency window, computational complexity and efficiency, simplicity in implementation, smoothness and symmetry of the wavelets, and order of approximation ([**5**]). One of the basic methods for such constructions involves cardinal B-splines, which are taken for the simplest functions with such properties. In addition, they possess 'total positivity' that controls zero-crossing and shapes of the spline curves. Their properties are known to be crucial to computation, graphical display, real-time processing of discrete data ([**5**]).
Chui et al. ([**7, 8**]) constructed spline MRA tight frame whose generators have high order of vanishing moments apart from the good properties of splines. We will recall the approach and demonstrate new examples in chapter 3 and the appendix. These examples will be adopted for the demonstration of the main result of this thesis. In section 3.4, algorithms of DFRT (Discrete Frame Transformation) will be given.

Recently, Hilbert transform pairs of wavelets, biorthogonal wavelets and frames were found to be attractive in many applications ([**15, 16, 18, 26, 27, 28, 30**]). The Hilbert transform pairs are, however, hardly adoptable for applications, since their two-scale symbols are not trigonometric polynomials. Moreover, the symbols can not be implemented as FIR filters, nor rational IIR filters ([**26**]). That is the reason why approximations are constructed by many researchers in spite of the theoretical existence of the Hilbert transform pairs of wavelets, biorthogonal wavelets, frames, see e.g. [**15, 16, 18, 26, 27, 28**]. Kingsbury proposed the dual-tree wavelet transform in [**18**], where he constructed a pair of wavelet frames, each having 2 generators, and such that the generators of one frame are approximate Hilbert transforms

of the generators of the other. Selesnick ([**26**]) showed that, when an MRA (Multiresolution analysis) wavelet ψ is given, $\mathcal{H}\psi$ is an MRA wavelet as well, where $\mathcal{H}$ denotes the Hilbert transform. The relations between the two refinable functions and two-scale symbols are given. Furthermore, he imposed several constraints on the two-scale symbols in order to obtain approximate Hilbert transform pairs of wavelets ([**26**]), biorthogonal wavelets ([**27**]), and frames ([**28**]). He calls the corresponding discrete transform the *double-density dual-tree DWT* ([**28**]). Gopinath generalized the result of Kingsbury ([**18**]) and Selesnick ([**26, 27, 28**]) to an approximately shift invariant redundant dyadic wavelet transform - the *phaselet transform* ([**15, 16**]). For biorthogonal wavelets, these constructions are special cases of a general approach of Zhao, who showed how one can construct new MRA biorthogonal wavelets $\{T\psi_{j,k}, T^{-1}\tilde{\psi}_{j,k}\}$ from given ones ([**30**]), where T is a linear (possibly unbounded) operator and $\psi_{j,k} = 2^{j/2}\psi(2^j \cdot -k)$. In his work, the Hilbert transform pair of the given MRA biorthogonal wavelet was demonstrated as a special case.
All these approaches have two drawbacks. Firstly, the wavelets and refinable functions do not have closed forms. Similar to the construction of Daubechies wavelets, the two-scale symbols are found so that the resulting wavelets form a Hilbert transform pair. Then the function values of the corresponding wavelets and refinable functions at the dyadic points are computed by the cascade algorithm. But, in some applications and industry standards, explicit analytic formulation of the functions are required ([**7**]). Secondly, the symmetry, or "linear phase", of the wavelets and refinable functions is an important constraint in many applications ([**27, 28**]). The results ([**15, 16, 26, 27, 28**]), however, show that it is not easy to get symmetric Hilbert transform pairs of wavelets (or generators of frames).

The first half of this thesis is devoted to the generalization and development of these results to the MRA tight frames. First, we introduce the definition and several properties of the Hilbert transform in chapter 2. In addition, some basic notions and formulas relating to the filtered backprojection algorithm of computed tomography are given. Then we examine the existence of the MRA tight frame $\{\mathcal{H}\psi_{j,k,\ell}\}$ as well as its approximation under the assumption that an MRA tight frame $\{\psi_{j,k,\ell} := 2^{k/2}\psi_j(2^k \cdot -\ell),\ 1 \le j \le r, k, \ell \in \mathbb{Z}\}$ is given. In particular, we are interested in the MRA tight frames which are characterized by [**7**] and [**13**], that

enable the generators to have a high order of vanishing moments. We will recall the characterizations in chapter 4.
In summary, we study the solutions of the following questions.

(Q 1) For a given MRA tight frame $\{\psi_{j,k,\ell}\}$, is the family $\{\mathcal{H}\psi_{j,k,\ell}\}$ an MRA tight frame as well? Furthermore, can we find a general method producing an MRA tight frame $\{T\psi_{j,k,\ell}\}$ from a given one, where T is a linear operator including the Hilbert transform?

(Q 2) Can we find an approximate Hilbert transform $\{\tilde{\Psi}_{j,k,\ell}\}$ such that $\tilde{\Psi}_j \approx \mathcal{H}\psi_j$ and $\tilde{\Psi}_j$ has closed form and symmetry?

For the solution of (Q 1) we adopt the approaches of Selesnick ([**26, 27, 28**]) and Zhao ([**30**]) and show in chapter 4 that they work for MRA tight frames as well. In addition, a general way will be given, that enables us to go from an MRA tight frame to another. Furthermore, in Theorem 4.12 we suggest an alternative description (4.20)-(4.23) of Selesnick's approach. On the basis of our new description, we suggest an answer of (Q 2) in chapter 5 using Thiran allpass filters which were employed in [**15, 16, 26, 27, 28**]. In particular, our new description contains a formulation of the Hilbert transform pair in terms of B-splines of order m and $m+1$. When we adopt some examples of the spline MRA tight frames of order m, we find their approximate Hilbert transforms as finite linear combinations of B-splines of order $m+1$ as well, i.e. they have closed forms, and are almost symmetric unlike the afore-mentioned approaches. Furthermore, our approximate Hilbert transforms have compact support, high order of vanishing moments, and enough regularity.
On the other hand, we show that $\tilde{\Psi}_j$ satisfies the characterizing identities of MRA tight frames approximately. From this fact, we introduce the notion of approximate MRA tight frames in chapter 5. In chapter 6, we lay emphasis on the tightness of the approximate Hilbert transforms. Namely, for given spline MRA tight frames we search their approximate Hilbert transforms which are themselves spline MRA tight frames. For examples, we take some spline MRA tight frames from chapter 3 and the appendix and demonstrate their approximate Hilbert transforms.

Next, we take the operator $\Lambda = \mathcal{H}\mathcal{D}$ into account, where $\mathcal{D}$ is the differential operator. The Λ-operator appears in the inversion formula for the Radon transform and plays an important role in the filtered backprojection algorithm. In the second half of this thesis, we focus on the work of Zhao ([**30**]). He constructed the biorthogonal wavelet $\{\Lambda\psi, \Lambda^{-1}\tilde{\psi}\}$ for a given biorthogonal wavelet $\{\psi, \tilde{\psi}\}$ and applied it to the filtered backprojection algorithm of computed tomography. His construction is based on the general method of generating a biorthogonal wavelet from a given one ([**30**, Theorem 4.1]). The associated filters are described by IIR filters and they were approximated by FIR filters by truncation. Our study is devoted to the generalization of Zhao's result to MRA bi-frames in association with the solutions of (Q 1) and (Q 2). Namely, we will seek the solutions of the following problems.

(Q 3) Can we construct the MRA bi-frame $(\{\Lambda\psi_{j,k,\ell}\}, \{\Lambda^{-1}\psi_{j,k,\ell}\})$ for a given MRA tight frame $\{\psi_{j,k,\ell}\}$? In addition, can we find a general method generating an MRA bi-frame $\Big(\{T\psi_{j,k,\ell}\}, \{T^{-1}\tilde{\psi}_{j,k,\ell}\}\Big)$ from a given $\Big(\{\psi_{j,k,\ell}\}, \{\tilde{\psi}_{j,k,\ell}\}\Big)$, where the linear operator T (possibly unbounded) includes the Hilbert transform, differentiation/integration, and the Λ-operator?

(Q 4) Can we find an approximation of $(\{\Lambda\psi_{j,k,\ell}\}, \{\Lambda^{-1}\psi_{j,k,\ell}\})$?

In the study of the solution of (Q 3), we begin with the characterization of MRA bi-frames which will be given in Proposition 7.1. After that we take a close look at the formulation of the Λ-operator and we reveal that the commutation of the MRA tight frame $\{\mathcal{H}\psi_{j,k,\ell}\}$ brings us the desired MRA bi-frame. For the general method in (Q 3), we generalize the result of [**30**, Theorem 4.1] and extend the solution of (Q 1). These results will be given in Theorem 7.9. In section 7.5, we deal with the lifting scheme for MRA bi-frames, which is not included as a special case of Theorem 7.9. Furthermore, we show in chapter 8 that (Q 4), again, is answered by the commutation of the proposed solution of (Q 2). As in the case of approximate MRA tight frames, we introduce the notion of approximate MRA bi-frames. Using the approximation, we propose an approximation of the Ram-Lak filter. We expect that this result can be employed in the filtered backprojection algorithm of computed tomography.

1.2. Orthonormal wavelets

In this section we give some basic notions which will be used throughout this dissertation. The Fourier transform of $f \in L^2(\mathbb{R})$ is defined as

$$\hat{f}(\xi) = \int_{\mathbb{R}} f(x) e^{-ix\xi} dx, \quad \xi \in \mathbb{R}.$$

The inner product and norm for the space $L^2(\mathbb{R})$ are

$$\langle f, g \rangle = \int_{-\infty}^{\infty} f(x)\overline{g(x)}dx, \quad \|f\|_{L^2(\mathbb{R})} = \langle f, f \rangle^{1/2}.$$

A function $\psi \in L^2(\mathbb{R})$ is an *orthonormal wavelet* provided that the system $\{\psi_{j,k} : j, k \in \mathbb{Z}\}$ is an orthonormal basis for $L^2(\mathbb{R})$, where

$$\psi_{j,k}(x) = 2^{j/2}\psi(2^j x - k) \quad \text{for all } j, k \in \mathbb{Z}.$$

In other words, $\psi \in L^2(\mathbb{R})$ is an orthonormal wavelet if

$$\langle \psi_{j,k}, \psi_{\ell,m} \rangle = \delta_{j,\ell}\delta_{k,m} \quad \forall\ j, k, \ell, m \in \mathbb{Z} \tag{1.1}$$

and every $f \in L^2(\mathbb{R})$ can be written as

$$f = \sum_{j,k=-\infty}^{\infty} c_{j,k}\psi_{j,k}, \quad c_{j,k} = \langle f, \psi_{j,k} \rangle \tag{1.2}$$

with strong convergence in $L^2(\mathbb{R})$. A *multiresolution analysis* (MRA) consists of a sequence of closed subspaces V_j, $j \in \mathbb{Z}$, of $L^2(\mathbb{R})$ satisfying ([**17**, p.44])

(1) $V_j \subset V_{j+1}$ for all $j \in \mathbb{Z}$,
(2) $f(\cdot) \in V_j \Leftrightarrow f(2\cdot) \in V_{j+1}$ for all $j \in \mathbb{Z}$,
(3) $\bigcap_{j\in\mathbb{Z}} V_j = \{0\}$,
(4) $\overline{\bigcup_{j\in\mathbb{Z}} V_j} = L^2(\mathbb{R})$,
(5) There exists a function $\phi \in V_0$, such that $\{\phi(\cdot - k) | k \in \mathbb{Z}\}$ is an orthonormal basis for V_0.

The function ϕ is called *scaling* (or *refinable*) *function* of the MRA. The condition (5) can be weakened to $\{\phi(\cdot - k) | k \in \mathbb{Z}\}$ being a *Riesz basis* for V_0, viz. for every $f \in V_0$ there exists a unique sequence $(\alpha_n)_{n\in\mathbb{Z}} \in \ell^2(\mathbb{Z})$ such that

$$f(x) = \sum_{n\in\mathbb{Z}} \alpha_n \phi(x - n),$$

with convergence in $L^2(\mathbb{R})$, and

$$A\sum_{n\in\mathbb{Z}}|\alpha_n|^2 \le \left\|\sum_{n\in\mathbb{Z}}\alpha_n\phi(x-n)\right\|^2_{L^2(\mathbb{R})} \le B\sum_{n\in\mathbb{Z}}|\alpha_n|^2$$

with constants $0 < A \le B < \infty$ independent of f. It is known ([**17**]) that condition (3) is obsolete.

We say that the wavelet ψ is associated with an MRA, or that ψ is an *MRA wavelet*, if there exists a function $\phi \in L^2(\mathbb{R})$ such that the system $\{\phi(\cdot - k)|k \in \mathbb{Z}\}$ is an orthonormal basis for V_0, where

$$V_j := \bigoplus_{k=-\infty}^{j-1} W_k, \quad W_k = \mathrm{clos}_{L^2(\mathbb{R})}\mathrm{span}\{\psi_{k,\ell} : \ell \in \mathbb{Z}\}. \tag{1.3}$$

(Note that V_j satisfies (1) to (4) automatically from its definition, since $\{\psi_{j,k} : j, k \in \mathbb{Z}\}$ is an orthonormal basis for $L^2(\mathbb{R})$.) Shortly, ψ is an MRA wavelet if the sequence of the spaces $(V_j)_{j\in\mathbb{Z}}$ constitutes an MRA. If we have such an MRA wavelet, every function $f \in L^2(\mathbb{R})$ can be approximated as closely as desired by $f_n \in V_n$ for some $n \in \mathbb{Z}$, by the property (4). By the fact that $V_n = V_{n-1} \bigoplus W_{n-1}$, we obtain

$$\begin{aligned} f_n &= f_{n-1} + g_{n-1} \\ &= f_{n-\ell} + g_{n-\ell} + \cdots + g_{n-1}, \end{aligned} \tag{1.4}$$

where $g_k \in W_k, k = n-1, \ldots, n-\ell$. The decomposition in (1.4) is called *wavelet decomposition*. The function $f_{n-\ell}$ is a coarse approximation of f and $g_{n-1}, \ldots, g_{n-\ell}$, are differences or details of f ([**5**, p.19]). This decomposition provides a multilevel description of f, which has very important applications in signal/image processing ([**31**, p.151, 214]).

Now from the fact that $\phi \in V_0$, $\psi \in W_0$ and $V_1 = V_0 \bigoplus W_0$, ϕ and ψ are linear combinations of $\phi_{1,k} = 2^{1/2}\phi(2\cdot - k), k \in \mathbb{Z}$. That is to say, there exist two sequences $\{p_k\}$ and $\{q_k\} \in \ell^2(\mathbb{Z})$ such that

$$\phi(x) = \sum_{k\in\mathbb{Z}} p_k\phi(2x-k), \tag{1.5}$$

$$\psi(x) = \sum_{k\in\mathbb{Z}} q_k\phi(2x-k), \tag{1.6}$$

for all $x \in \mathbb{R}$. The formulas (1.5) and (1.6) are called *two-scale relations* of the refinable function and wavelet, respectively ([**5**, p.19]). Each of the sequences $\{p_k\}$ and $\{q_k\}$ is called *two-scale sequence* of the refinable function and wavelet, respectively. If we take Fourier transforms, the formulas (1.5) and (1.6) are equivalent to

$$\begin{aligned} \hat{\phi}(\xi) &= P(\xi/2)\hat{\phi}(\xi/2), \quad P(\xi) := \frac{1}{2}\sum_{k\in\mathbb{Z}} p_k e^{-ik\xi}, \\ \hat{\psi}(\xi) &= Q(\xi/2)\hat{\phi}(\xi/2), \quad Q(\xi) := \frac{1}{2}\sum_{k\in\mathbb{Z}} q_k e^{-ik\xi}. \end{aligned}$$

We call P and Q the *two-scale symbols* of the refinable function and wavelet, respectively ([**5**, p.122]).

It is well known that the constructions of such ϕ and ψ are based on the periodic function $P(\xi)$ such that

$$P(0) = 1 \tag{1.7}$$

and

$$|P(\xi)|^2 + |P(\xi+\pi)|^2 = 1, \quad Q(\xi) = e^{-i\xi}\overline{P(\xi+\pi)}. \tag{1.8}$$

We call P and Q that satisfy (1.7) and (1.8) *conjugate quadrature filters* (CQF) ([**4**, p.313]). In addition, P and Q are called *finite impulse response* (FIR) filters, if only finitely many coefficients p_k (resp. q_k) are nonzero. They are called infinite impulse response (IIR) filters otherwise. The associated refinable function ϕ and wavelet ψ are defined by

$$\hat{\phi}(\xi) = \prod_{k=1}^{\infty} P(2^{-k}\xi)$$

and

$$\hat{\psi}(\xi) = Q(\xi/2)\hat{\phi}(\xi/2) = e^{-i\xi/2}\overline{P(\xi/2+\pi)}\hat{\phi}(\xi/2).$$

For efficiency in computation and applications, wavelets with the following properties are desirable,

- ϕ and ψ have compact support and are smooth,
- ψ has L *vanishing moments*, i.e.

$$\int_{-\infty}^{\infty} t^k \psi(t)dt = 0, \quad for\ 0 \le k < L,$$

- ψ is symmetric or antisymmetric,

- ϕ and ψ have finite two-scale sequences, i.e. the two-scale symbols P and Q are trigonometric polynomials.

1.3. Biorthogonal wavelets

It is known that the CQF's have some disadvantages for practical design and applications. One of them is that they cannot be both FIR and linear phase (real and symmetrical coefficients) ([**4**, p.314]). This is one of the reasons so-called biorthogonal wavelets are considered. A pair $\{\psi, \tilde{\psi}\}$ of functions is called *biorthogonal wavelet*, if each set $\{\psi_{j,k} : j,k \in \mathbb{Z}\}$ and $\{\tilde{\psi}_{j,k} : j,k \in \mathbb{Z}\}$ is a Riesz basis of $L^2(\mathbb{R})$ and they are biorthogonal to each other in the sense ([**17**, p.423])

$$\langle \psi_{j,k}, \tilde{\psi}_{\ell,m} \rangle = \delta_{j,\ell}\delta_{k,m} \quad \forall\ j,k,\ell,m \in \mathbb{Z}.$$

For any $f \in L^2(\mathbb{R})$ two possible decompositions exist in these bases ([**21**, p.266]), namely

$$f = \sum_{j\in\mathbb{Z}}\sum_{k\in\mathbb{Z}} \langle f, \tilde{\psi}_{j,k}\rangle \psi_{j,k} = \sum_{j\in\mathbb{Z}}\sum_{k\in\mathbb{Z}} \langle f, \psi_{j,k}\rangle \tilde{\psi}_{j,k}.$$

A biorthogonal wavelet $\{\psi, \tilde{\psi}\}$ is called an *MRA biorthogonal wavelet*, when a pair of associated scaling functions $\{\phi, \tilde{\phi}\}$ in $L^2(\mathbb{R})$ exists, with ([**21**, p.266])

$$\langle \phi_{0,k}, \tilde{\phi}_{0,m} \rangle = \delta_{k,m} \quad \forall\ k,m \in \mathbb{Z}.$$

In other words, the spaces V_j and $\tilde{V}_j$ which are defined as in (1.3) define two MRA's of $L^2(\mathbb{R})$

$$\{0\} \subset \ldots \subset V_{-1} \subset V_0 \subset V_1 \subset \ldots \subset L^2(\mathbb{R}),$$

$$\{0\} \subset \ldots \subset \widetilde{V}_{-1} \subset \widetilde{V}_0 \subset \widetilde{V}_1 \subset \ldots \subset L^2(\mathbb{R}),$$

where $\{\phi(\cdot - k) | k \in \mathbb{Z}\}$ is a Riesz basis of V_0, and $\{\widetilde{\phi}(\cdot - k) | k \in \mathbb{Z}\}$ is a Riesz basis of $\widetilde{V}_0$. For every $j \in \mathbb{Z}$ the biorthogonality implies that

$$V_j \perp \widetilde{W}_j, \quad \widetilde{V}_j \perp W_j, \quad V_{j+1} = V_j \bigoplus W_j, \quad \widetilde{V}_{j+1} = \widetilde{V}_j \bigoplus \widetilde{W}_j,$$

$$V_j \cap W_j = \{0\}, \quad \widetilde{V}_j \cap \widetilde{W}_j = \{0\}$$

and thus

$$L^2(\mathbb{R}) = \bigoplus_{j\in\mathbb{Z}} W_j = \bigoplus_{j\in\mathbb{Z}} \widetilde{W}_j.$$

The corresponding two-scale relations are:

$$\phi(x) = \sum_{k\in\mathbb{Z}} p_k \phi(2x-k), \quad \psi(x) = \sum_{k\in\mathbb{Z}} q_k \phi(2x-k),$$
$$\tilde{\phi}(x) = \sum_{k\in\mathbb{Z}} \tilde{p}_k \tilde{\phi}(2x-k), \quad \tilde{\psi}(x) = \sum_{k\in\mathbb{Z}} \tilde{q}_k \tilde{\phi}(2x-k).$$

When an MRA biorthogonal wavelet is given, every $f \in L^2(\mathbb{R})$ can be decomposed by both

$$f = \sum_{j\in\mathbb{Z}}\sum_{k\in\mathbb{Z}} \langle f, \widetilde{\psi}_{j,k}\rangle \psi_{j,k} = \sum_{k\in\mathbb{Z}} \langle f, \widetilde{\phi}_{m,k}\rangle \phi_{m,k} + \sum_{j\geq m}\sum_{k\in\mathbb{Z}} \langle f, \widetilde{\psi}_{j,k}\rangle \psi_{j,k} \tag{1.9}$$

and

$$f = \sum_{j\in\mathbb{Z}}\sum_{k\in\mathbb{Z}} \langle f, \psi_{j,k}\rangle \widetilde{\psi}_{j,k} = \sum_{k\in\mathbb{Z}} \langle f, \phi_{m,k}\rangle \widetilde{\phi}_{m,k} + \sum_{j\geq m}\sum_{k\in\mathbb{Z}} \langle f, \psi_{j,k}\rangle \widetilde{\psi}_{j,k}, \tag{1.10}$$

for every $m \in \mathbb{Z}$.

As in the case of the MRA wavelets, we can construct an MRA biorthogonal wavelet using the set of two-scale symbols. An MRA biorthogonal wavelet $\{\psi, \tilde{\psi}\}$ with refinable functions $\{\phi, \tilde{\phi}\}$ can be constructed by two-scale symbols $\{P, \tilde{P}, Q, \tilde{Q}\}$ if each of $\{\psi_{j,k}, j, k \in \mathbb{Z}\}$ and $\{\tilde{\psi}_{j,k}, j, k \in \mathbb{Z}\}$ forms a Riesz bases of $L^2(\mathbb{R})$ and the two-scale symbols

$$P(\xi) := \frac{1}{2}\sum_{k\in\mathbb{Z}} p_k e^{-ik\xi}, \quad \tilde{P}(\xi) := \frac{1}{2}\sum_{k\in\mathbb{Z}} \tilde{p}_k e^{-ik\xi},$$
$$Q(\xi) := e^{-i\xi}\overline{\tilde{P}(\xi+\pi)}, \quad \tilde{Q}(\xi) := e^{-i\xi}\overline{P(\xi+\pi)}, \tag{1.11}$$

satisfy

$$P(\xi)\overline{\tilde{P}(\xi)} + P(\xi+\pi)\overline{\tilde{P}(\xi+\pi)} = 1, \quad \text{for a.e. } \xi \in \mathbb{R}, \tag{1.12}$$

$$P(0) = 1 = \tilde{P}(0), \quad Q(0) = 0 = \tilde{Q}(0). \tag{1.13}$$

In this case, the pairs $\{\psi, \tilde{\psi}\}$ and $\{\phi, \tilde{\phi}\}$ are determined by the two-scale symbols

$$\hat{\phi}(\xi) = \prod_{j=1}^{\infty} P(2^{-j}\xi), \quad \hat{\psi}(\xi) = Q(\xi/2)\prod_{j=2}^{\infty} P(2^{-j}\xi),$$

$$\widehat{\tilde{\phi}}(\xi) = \prod_{j=1}^{\infty} \tilde{P}(2^{-j}\xi), \quad \widehat{\tilde{\psi}}(\xi) = \tilde{Q}(\xi/2)\prod_{j=2}^{\infty} \tilde{P}(2^{-j}\xi).$$

Now we introduce the decomposition and reconstruction algorithms of MRA biorthogonal wavelets. When $f \in L^2(\mathbb{R})$ is given, we have from (1.9)

$$f(x) = \sum_{k\in\mathbb{Z}} \tilde{c}_{m,k}\phi_{m,k}(x) + \sum_{j\geq m}\sum_{k\in\mathbb{Z}} \tilde{d}_{j,k}\psi_{j,k}(x),$$

where $\tilde{c}_{m,k} := \langle f, \tilde{\phi}_{m,k}\rangle$, $\tilde{d}_{j,k} := \langle f, \tilde{\psi}_{j,k}\rangle$. The following decomposition and reconstruction algorithms are well known ([**30**, p.358]):

Decomposition:

$$\tilde{c}_{m-1,k} = \sum_{\ell\in\mathbb{Z}} \overline{\tilde{p}_{\ell-2k}}\tilde{c}_{m,\ell}, \qquad \tilde{d}_{m-1,k} = \sum_{\ell\in\mathbb{Z}} \overline{\tilde{q}_{\ell-2k}}\tilde{c}_{m,\ell}$$

Reconstruction:

$$\tilde{c}_{m,k} = \sum_{\ell\in\mathbb{Z}} (p_{k-2\ell}\tilde{c}_{m-1,\ell} + q_{k-2\ell}\tilde{d}_{m-1,\ell})$$

1.4. Frames

Now we introduce the notion of a *frame* which allows us to replace the orthonormality condition (1.1) by a weaker one ([**21**, p.397]). Recall that, if $\psi \in L^2(\mathbb{R})$ is an orthonormal wavelet, we have for every $f \in L^2(\mathbb{R})$

$$\sum_{j,k\in\mathbb{Z}} |\langle f, \psi_{j,k}\rangle|^2 = \|f\|^2_{L^2(\mathbb{R})}. \tag{1.14}$$

Moreover, the function f can be recovered from the numbers $c_{j,k} = \langle f, \psi_{j,k}\rangle$ and the function $\psi_{j,k}$ as in (1.2). It is particularly useful for applications, such as encoding and reconstructing sounds and other signals ([**17**, p.397]), to relax condition (1.1) and to allow redundancy of such systems, and yet still be able to recover f, as in (1.2). These considerations lead us to the notion of a frame. In general, a family of functions $\{\varphi_j : j \in \mathbb{J}\} \subset L^2(\mathbb{R})$ is called *a frame* of the Hilbert space $L^2(\mathbb{R})$, if there exist two constants A and B, $0 < A \leq B < \infty$, such that

$$A\|f\|^2_{L^2(\mathbb{R})} \leq \sum_{j\in\mathbb{J}} |\langle f, \varphi_j\rangle|^2 \leq B\|f\|^2_{L^2(\mathbb{R})} \quad \text{for all } f \in L^2(\mathbb{R}). \tag{1.15}$$

If the family $\{\varphi_j : j \in \mathbb{J}\}$ satisfies only

$$\sum_{j\in\mathbb{J}} |\langle f, \varphi_j\rangle|^2 \leq B\|f\|^2_{L^2(\mathbb{R})} \quad \text{for all } f \in L^2(\mathbb{R}),$$

we call it a *Bessel family*. The constants A and B in (1.15) are called *frame bounds*. When $A = B$ we say that the frame is *tight*. If we have a tight frame, we can recover every $f \in L^2(\mathbb{R})$ by

$$f = \frac{1}{A} \sum_{j \in \mathbb{J}} \langle f, \varphi_j \rangle \varphi_j. \tag{1.16}$$

A tight frame in which the family $\{\varphi_j, j \in \mathbb{J}\}$ is composed of shifts and scales of r (in our work $r = 2$ or 3) generators, i.e.

$$\{\varphi_j, j \in \mathbb{J}\} = \{\psi_{j,k,\ell} := 2^{k/2} \psi_j(2^k \cdot -\ell),\ 1 \le j \le r, k, \ell \in \mathbb{Z}\},$$

is called a wavelet tight frame. Moreover, if the generators are associated with a refinable function, we call it an MRA tight frame. In chapter 4, we deal with such MRA tight frames having high order of vanishing moments. Even if a frame is not tight, we have a reconstruction formula similar to (1.16) using its *dual frame*. For details see [**17**, Chapter 8].

Now, we introduce the notion of *bi-frame* ([**13**]) which can be understood as a generalization of biorthogonal wavelets. When $\{\psi_1, \ldots, \psi_r, \}$ and $\{\tilde{\psi}_1, \ldots, \tilde{\psi}_r, \}$ are two families in $L^2(\mathbb{R})$, the pair of systems

$$\Big(\{\psi_{j,k,\ell}, 1 \le j \le r, k, \ell \in \mathbb{Z}\}, \{\tilde{\psi}_{j,k,\ell}, 1 \le j \le r, k, \ell \in \mathbb{Z}\} \Big)$$

is called a *bi-frame*, if each of the two systems is a Bessel family, and they present the perfect reconstruction formula

$$f = \sum_{j,k,\ell} \langle f, \tilde{\psi}_{j,k,\ell} \rangle \psi_{j,k,\ell} = \sum_{j,k,\ell} \langle f, \psi_{j,k,\ell} \rangle \tilde{\psi}_{j,k,\ell}, \text{ for all } f \in L^2(\mathbb{R}).$$

Note that each of the two systems is necessarily a frame. When each of two systems is a frame with an underlying MRA, the system is called an MRA bi-frame. MRA bi-frames will be dealt with in chapter 7.

CHAPTER 2

Hilbert transform and filtered backprojection

The Hilbert transform appears in the inversion formula for the Radon transform as well as in the filtered backprojection algorithm of computed tomography. We introduce the definitions and basic properties of the Hilbert transform, Radon transform, and the filtered backprojection algorithm. These properties will be used for the generation of Hilbert transform pairs of MRA tight frames in chapter 4 and for the construction of approximate MRA tight frames in chapter 5.

2.1. Hilbert transform

In this section we introduce the notion of Hilbert transform and its basic properties. The terminology in this section is mainly taken from [**3**, Chapter 8].

Definition 2.1. [**3**, p.306] *The Hilbert transform of a function $f \in L^p, 1 \leq p < \infty$, is defined as the Cauchy principal value,*

$$(\mathcal{H}f)(x) = PV\left[\frac{1}{\pi}\int_{-\infty}^{\infty}\frac{f(u)}{x-u}du\right] \equiv \lim_{\delta\to 0+} f_\delta^\sim(x), \tag{2.1}$$

$$\text{where } f_\delta^\sim(x) = \frac{1}{\pi}\int_{|u|\geq\delta}\frac{f(u)}{x-u}du.$$

From the definition we have the following basic properties of the Hilbert transform for $f, g \in L^p, 1 \leq p < \infty$ ([**3**, pp.310-315]):

(i) The Hilbert transform $\mathcal{H}f$ exists a.e.

(ii) (Linearity) $\mathcal{H}(\alpha f + \beta g) = \alpha\mathcal{H}f + \beta\mathcal{H}g$ a.e. for $\alpha, \beta \in \mathbb{C}$.

(iii) (Shift-invariance) $\mathcal{H}(f(\cdot + h))(x) = \mathcal{H}f(x + h)$ a.e. for each $h \in \mathbb{R}$.

(iv) (Homogeneity) $\mathcal{H}(f(\alpha\cdot))(x) = \mathcal{H}f(\alpha x)$, for $\alpha > 0$.

(v) If f is an even (resp. odd) function, then $\mathcal{H}f$ is odd (resp. even).

Some further results which are useful in forthcoming chapters are presented in the next Proposition ($(a) - (c)$ are from [**3**, pp.311-323] and (d) is from [**2**]).

Proposition 2.2. *Let $f \in L^p(\mathbb{R}), 1 < p < \infty$. Then*
(a) $\mathcal{H}f$ belongs to $L^p(\mathbb{R})$ and satisfies

$$\|\mathcal{H}f\|_{L^p} \leq C_p \|f\|_{L^p}$$

with some constant C_p independent of f. Moreover,

$$\lim_{\delta \to 0+} \|\mathcal{H}f - f_\delta^\sim\|_{L^p} = 0,$$

i.e. the limit (2.1) exists not only pointwise a.e. but also in the L^p-norm. Especially for $f \in L^2(\mathbb{R})$, we have

$$\|f\|_{L^2(\mathbb{R})} = \|\mathcal{H}f\|_{L^2(\mathbb{R})}.$$

(b)(Hilbert formula) For every $g \in L^{p'}(\mathbb{R})$, $\frac{1}{p} + \frac{1}{p'} = 1$,

$$\int_{\mathbb{R}} f(x)\overline{g(x)}dx = \int_{\mathbb{R}} \mathcal{H}f(x)\overline{\mathcal{H}g(x)}dx.$$

In particular, for $p = p' = 2$, we have

$$\langle f, g\rangle_{L^2(\mathbb{R})} = \langle \mathcal{H}f, \mathcal{H}g\rangle_{L^2(\mathbb{R})}.$$

(c) $\mathcal{H}(\mathcal{H}f)(x) = -f(x)$ a.e. and generally,

$$\mathcal{H}^r f = (-1)^{\lfloor r/2 \rfloor} \cdot \begin{cases} f, & r \text{ even}, \\ \mathcal{H}f, & r \text{ odd}. \end{cases} \tag{2.2}$$

(d) If $f, \ldots, f^{(k-1)} \in \mathbf{AC}(\mathbb{R})$ and $f^{(k)} \in L^p(\mathbb{R})$, then $\mathcal{H}f, \ldots, (\mathcal{H}f)^{(k-1)} \in \mathbf{AC}(\mathbb{R})$ and

$$\mathcal{D}^k \mathcal{H}f = \mathcal{H}\mathcal{D}^k f \text{ a.e.} \tag{2.3}$$

Note that (a) doesn't hold, in general, for $f \in L^1(\mathbb{R})$. For example, when $f(x) = \frac{1}{(1+x^2)} \in L^1$, its Hilbert transform $\mathcal{H}f(x) = \frac{x}{1+x^2}$ is not in $L^1(\mathbb{R})$ any more ([**3**, p.315]). Furthermore, (a) means that the Hilbert transform defines a bounded linear mapping from L^p to L^p. In particular, for $L^2(\mathbb{R})$ it preserves the norm. It follows from (b) that $\mathcal{H}$ is a unitary operator on $L^2(\mathbb{R})$, and (c) implies that $\mathcal{H} : L^p \to L^p$ is bounded, linear, onto ([**3**, p.323]) and invertible with

$$\mathcal{H}^{-1} = -\mathcal{H}.$$

In (d) the notation $\mathbf{AC}(\mathbb{R})$ means the space of all absolutely continuous functions, and $\mathcal{D}$ is the differential operator. Hence, $\mathcal{H}f$ inherits the regularity of the function f, and the Hilbert transform and the differential operator commute under the given regularity condition. This commutation property will contribute to the construction of our MRA bi-frames in chapter 7.

Instead of Definition 2.1, we can give another formulation through the Fourier transform. In the distributional sense, Definition 2.1 is expressed as ([**3**, p.324])

$$(\mathcal{H}f)(x) = \left(\frac{1}{\pi u} * f\right)(x). \tag{2.4}$$

For $f \in L^2(\mathbb{R})$, this gives us

$$(\mathcal{H}f)\hat{}(\xi) = \left(\frac{1}{\pi u}\right)\hat{}(\xi)\hat{f}(\xi) = -i\ \mathrm{sgn}(\xi)\hat{f}(\xi). \tag{2.5}$$

Sometimes (2.5) is used as the definition of the Hilbert transform of $f \in L^p(\mathbb{R})$, $1 < p \leq 2$ ([**26**]).

Next, let us look at the close connection between the Hilbert transform and wavelets. Firstly, if $\psi \in L^2(\mathbb{R})$ is an orthonormal wavelet, so is $\mathcal{H}\psi$. Indeed, if we combine the properties (ii)-(iv), we have for an orthonormal wavelet $\psi \in L^2(\mathbb{R})$ that

$$\begin{aligned} \mathcal{H}(\psi_{j,k}) &= \mathcal{H}(2^{j/2}\psi(2^j \cdot -k)) = 2^{j/2}\mathcal{H}(\psi(2^j \cdot -k)) \quad \text{by (ii)} \\ &= 2^{j/2}(\mathcal{H}\psi)(2^j \cdot -k) \quad \text{by (iii) and (iv)} \\ &= (\mathcal{H}\psi)_{j,k}. \end{aligned} \tag{2.6}$$

The unitarity of $\mathcal{H}$ implies that $\mathcal{H}\psi$ is also an orthonormal wavelet. Furthermore, when two wavelets ψ_1 and ψ_2 are given satisfying $\psi_2 = \mathcal{H}\psi_1$, then the function $\eta := \psi_1 + i\psi_2$ satisfies

$$\hat{\eta}(\xi) = \begin{cases} 2\hat{\psi}_1(\xi)\ a.e. & \xi > 0, \\ 0 \qquad a.e. & \xi \leq 0, \end{cases} \tag{2.7}$$

since

$$\hat{\psi}_2(\xi) = \begin{cases} -i\hat{\psi}_1(\xi)\ a.e. & \xi > 0, \\ i\hat{\psi}_1(\xi)\ a.e. & \xi \leq 0. \end{cases}$$

It is well-known that $\{\eta_{j,k} | j,k \in \mathbb{Z}\}$ is an orthonormal basis of the Hardy space $H^2(\mathbb{R}) := \{f \in L^2(\mathbb{R}) | \hat{f}(\xi) = 0,\ a.e.\ \xi \leq 0\}$. η is called a Hardy wavelet ([**15**]).

The support behavior of Hardy wavelets in the Fourier domain made them useful in many applications ([**15**]), and several results appeared recently dealing with (approximate) Hilbert transform pairs of wavelets ([**15, 16, 18, 26, 27, 28**]). One of our main results is devoted to finding Hilbert transform pairs of MRA tight frames and their approximations. One of the applications of Hilbert transform pairs of wavelets/frames is the algorithm of filtered backprojection of computerized tomography ([**30**]), since the operator $\mathcal{H}$ appears in the inversion formula of the Radon transform, as will be explained in the next section.

2.2. Algorithm of filtered backprojection of computerized tomography

In this section we present some background on the filtered backprojection algorithm. Not only the definitions of the Radon transform and its dual but also the inversion formula of the Radon transform and the filtered backprojection algorithm will be presented. The notations in this section are taken from [**22, 23**]. As the domain of the Radon transform, one usually defines the *Schwartz space* ([**22**, p.180])

$$\mathcal{S}(\mathbb{R}^n) = \{f \in C^\infty(\mathbb{R}^n) : \sup_{\mathbf{x}\in\mathbb{R}^n} |\mathbf{x}^{\mathbf{j}} D^{\mathbf{k}} f(\mathbf{x})| < +\infty \ \forall\, \mathbf{j}, \mathbf{k} \in \mathbb{Z}_+^n\}.$$

The $(n-1)$-dimensional unit sphere in $\mathbb{R}^n$ is denoted by S^{n-1}.

Definition 2.3. [**23**, p.9] *The Radon transform*

$$\mathcal{R}f(\theta, s) = \int_{H(\theta,s)} f(\mathbf{x})d\mathbf{x} = \int_{\theta^\perp} f(s\theta + \mathbf{y})d\mathbf{y} \tag{2.8}$$

is the integral of $f \in \mathcal{S}(\mathbb{R}^n)$ over the hyperplane $H(\theta, s) := \{\mathbf{x} \in \mathbb{R}^n : \mathbf{x} \cdot \theta = s\}$ perpendicular to $\theta \in S^{n-1}$ with (signed) distance $s \in \mathbb{R}$ from the origin, where $\theta^\perp := \{\mathbf{x} \in \mathbb{R}^n : \mathbf{x} \cdot \theta = 0\}$.

Note that for $n = 2$, $\mathcal{R}f$ is the integral over a straight line. Furthermore, $\mathcal{R}f$ is a function on the unit cylinder

$$C^n = \{(\theta, s) : \theta \in S^{n-1}, s \in \mathbb{R}\} \subset \mathbb{R}^n$$

and $\mathcal{R}f \in \mathcal{S}(C^n)$ ([**23**, pp.9-10]), where

$$\mathcal{S}(C^n) = \{g \in C^\infty(C^n) : s^j \frac{\partial^k}{\partial s^k} g(\theta, s) < +\infty \ \forall\ j, k = 0, 1, 2, \ldots\}.$$

The dual operator $\mathcal{R}^\sharp$, called *backprojection*, is known as

$$\mathcal{R}^\sharp g(\mathbf{x}) = \int_{S^{n-1}} g(\theta, \mathbf{x}\cdot\theta)\ d\theta, \quad \mathbf{x}\in\mathbb{R}^n,\ g\in\mathcal{S}(C^n).$$

Thus if we have $g = \mathcal{R}f$, the value $(\mathcal{R}^\sharp g)(\mathbf{x})$ is the average of the integrals of f over all hyperplanes (straight lines for $n = 2$) which contains $\mathbf{x}$ ([**23**, p.10]). Furthermore, we have the following inversion formula for the Radon transform for an arbitrary dimension $n \geq 2$ ([**23**, p.11]),

$$f = \frac{1}{2}(2\pi)^{-n+1}\mathcal{I}^{-\alpha}\mathcal{R}^\sharp\mathcal{I}^{\alpha+1-n}\mathcal{R}f, \tag{2.9}$$

where $\mathcal{I}^{-\alpha}$ and $\mathcal{I}^{\alpha+1-n}$ are the *Riesz potentials* in $\mathbb{R}^n$ and C^n, respectively. Note that the *Riesz potential* $\mathcal{I}^\alpha$ *in* $\mathbb{R}^n$ is defined by ([**23**, pp.5-11])

$$(\mathcal{I}^\alpha f)^\wedge(\xi) = |\xi|^{-\alpha}\hat{f}(\xi),\ \alpha < n,$$

and the *Riesz potential* $\mathcal{I}^\alpha$ *in* C^n by

$$(\mathcal{I}^\alpha g)^\wedge(\theta,\sigma) = |\sigma|^{-\alpha}\hat{g}(\theta,\sigma),\ \alpha < 1,$$

where the univariate Fourier transform with respect to s is used. For $n = 2$ and $\alpha = 0$, we have in (2.9) ([**23**])

$$f = \frac{1}{4\pi}\mathcal{R}^\sharp\mathcal{I}^{-1}\mathcal{R}f,$$

where $\mathcal{I}^{-1}$ is the Riesz potential in C^2. Note that

$$(\mathcal{I}^{-1}g)^\wedge(\theta,\sigma) = |\sigma|\hat{g}(\theta,\sigma) = \mathrm{sgn}(\sigma)\sigma\hat{g}(\theta,\sigma) = (\mathcal{H}\mathcal{D}g)^\wedge(\theta,\sigma).$$

Hence, we have

$$\mathcal{I}^{-1} = \mathcal{H}\mathcal{D},$$

where both the Hilbert transform $\mathcal{H}$ and the differential operator $\mathcal{D}$ are with respect to the second variable $s\in\mathbb{R}$ of g ([**23**]). From now on we set for convenience

$$\Lambda := \mathcal{I}^{-1}, \tag{2.10}$$

and use it in our inversion formula ([**22**]),

$$f(\mathbf{x}) = \frac{1}{4\pi}(\mathcal{R}^\sharp\Lambda\mathcal{R}f)(\mathbf{x}) = \frac{1}{4\pi}(\mathcal{R}^\sharp\mathcal{H}\mathcal{D}\mathcal{R}f)(\mathbf{x}) \tag{2.11}$$

$$= \frac{1}{4\pi}\int_{S^1}(\mathcal{H}\frac{\partial}{\partial s}g)(\theta,\mathbf{x}\cdot\theta)d\theta,\ g = \mathcal{R}f,\ \mathbf{x}\in\mathbb{R}^2. \tag{2.12}$$

If we apply the definition of the Hilbert transform, we get *Radon's inversion formula* ([**23**, p.12])

$$f(\mathbf{x}) = \frac{1}{4\pi^2}\int_{\mathbb{R}}\frac{1}{t}\int_{S^1}\frac{\partial}{\partial s}g(\theta,\mathbf{x}\cdot\theta+t)d\theta dt. \tag{2.13}$$

From Radon's inversion formula we want to point out an important practical aspect. Note that $g(\theta,\mathbf{x}\cdot\theta)$ is the integral of f over the straight line perpendicular to θ through $\mathbf{x}$ ([**22**]). If we want to recover f at some point $\mathbf{x}\in\mathbb{R}^2$ using (2.13), we should compute the integrals along all straight lines through $\mathbf{x}+t\theta$ for each $\theta\in S^1$ and $t\in\mathbb{R}$. In other words, computing f at some point $\mathbf{x}\in\mathbb{R}^2$ requires the integrals along all straight lines through the support of f ([**22**]). In this sense Radon's inversion formula is not local, and, generally, neither are the inversion formulas in even dimensions ([**22, 23**]). This is the reason why some alternative reconstruction algorithms are developed. The standard reconstruction algorithm in two dimensions is the *filtered backprojection algorithm* ([**22**]). It is based on the formula ([**22, 23**])

$$(\mathcal{R}^\sharp g)*f=\mathcal{R}^\sharp(g*\mathcal{R}f),$$

where $f\in\mathcal{S}(\mathbb{R}^n)$ and $g\in\mathcal{S}(C^n)$. Let $g=w_b$ and $W_b=\mathcal{R}^\sharp w_b$. Then the *filtered backprojection algorithm* is obtained as

$$W_b*f=\mathcal{R}^\sharp(w_b*\mathcal{R}f).$$

The main idea is to choose W_b as an approximation of the δ-distribution and to determine w_b by $W_b=\mathcal{R}^\sharp w_b$ ([**23**]). Usually W_b is chosen to be the low-pass filter with cut-off frequency b. Then W_b*f is an approximation to f which is computed by convolving ("filtering") the given data $\mathcal{R}f$ by w_b, followed by the backprojection operator $\mathcal{R}^\sharp$ ("backprojection") ([**22**, pp.102-103], [**23**, p.81]). On the other hand, there are several wavelet-based reconstruction algorithms (see [**30**]). For example, Zhao ([**30**]) constructed an MRA biorthogonal wavelet $\{\Phi,\tilde{\Phi},\Lambda\psi,\Lambda^{-1}\psi\}$ and applied it to the decomposition of the given $\mathcal{R}f$ and the reconstruction of $\Lambda\mathcal{R}f$. Finally the backprojection $\mathcal{R}^\sharp$ was applied to get the original f. This approach motivated our study of construction of MRA bi-frames $(\{\Lambda\psi_{j,k,\ell}\},\{\Lambda^{-1}\psi_{j,k,\ell}\})$ and its approximation.

CHAPTER 3

MRA tight frames of splines on an interval

Recently Chui et al. ([**8, 11**]) constructed MRA tight frames of splines on an interval. The frame elements have compact support and a high order of vanishing moments up to the order of the splines. In addition, the examples in [**8, 11**] reveal that 2 or 3 symmetric/antisymmetric frame elements of the tight frame on an interval can be adopted as frame generators of $L^2(\mathbb{R})$. In other words, the technique of the construction of the MRA tight frames on an interval is available for the construction of tight frames of $L^2(\mathbb{R})$ ([**8**]). In this chapter, we present several examples of MRA tight frames on an interval using the approach in [**8**]. In particular, we address that 2 or 3 interior wavelets generate a tight frame of $L^2(\mathbb{R})$ and they will be employed in the examples of coming chapters.

3.1. Background on spline MRA tight frames on an interval

In this section we introduce basic notions and notations which are required for the construction of spline MRA tight frames on an interval. Furthermore, we recall several facts regarding the construction. They are mainly taken from [**8, 11**].
Let $I = [a, b]$ be a bounded interval and $m \geq 2$ be the order of the B-splines which will be used as refinable functions for the description of the frame elements. Furthermore, let $(\mathbf{t}_j)_{j\geq 0}$ be a sequence of knot vectors such that

$$\mathbf{t}_0 \subset \mathbf{t}_1 \subset \cdots \subset I, \ \overline{\bigcup_{j\geq 0} \mathbf{t}_j} = I, \tag{3.1}$$

$$\lim_{j\to\infty} h(\mathbf{t}_j) = 0, \ \text{where } h(\mathbf{t}_j) := \max_k\{t_{k+1}^{(j)} - t_k^{(j)}\}. \tag{3.2}$$

Each knot vector

$$\mathbf{t}_j := \{t_k^{(j)} : -m+1 \leq k \leq M_j\}, \quad M_j \in \mathbb{N} \tag{3.3}$$

is assumed to have m stacked knots at the boundaries of the interval I, and their interior knots may be nonuniformly spaced and have multiplicities from 1 to m. In other words, we consider each knot vector $\mathbf{t}_j$ as an ordered set whose elements may have multiplicities up to m such that

$$t_k^{(j)} \le t_{k+1}^{(j)} \quad \text{and} \quad t_k^{(j)} < t_{k+m}^{(j)} \quad \text{for all } k, \tag{3.4}$$

$$t_{-m+1}^{(j)} = \cdots = t_0 = a \quad \text{and} \quad t_{M_j-m+1}^{(j)} = \cdots = t_{M_j}^{(j)} = b. \tag{3.5}$$

For each $\mathbf{t}_j$, we consider the normalized B-splines of order m defined by

$$N_{\mathbf{t}_j;m,k}(x) := (t_{k+m}^{(j)} - t_k^{(j)})[t_k^{(j)}, \ldots, t_{k+m}^{(j)}](\cdot - x)_+^{m-1}, \tag{3.6}$$

where $-m+1 \le k \le M_j - m$ and $[t_k^{(j)}, \ldots, t_{k+m}^{(j)}]$ denotes the divided difference of order m. Note that $N_{\mathbf{t}_j;m,k}$ is strictly positive on its support $[t_k^{(j)}, t_{k+m}^{(j)}]$ and is a polynomial of degree $m-1$ in each interval $(t_i^{(j)}, t_{i+1}^{(j)})$, $k \le i \le k+m-1$. In addition, it has $m - \mu_i^{(j)} - 1$ continuous derivatives at each $t_i^{(j)}$, where $\mu_i^{(j)}$ is the multiplicity of the knot $t_i^{(j)} \in \mathbf{t}_j$. Now, we define $V_j, j \ge 0$, to be the space of splines of order m, generated by the family

$$\Phi_j := \left[N_{\mathbf{t}_j;m,k}; -m+1 \le k \le M_j - m\right]$$

of the normalized B-splines with respect to $\mathbf{t}_j$. We have generally $M_j = \sharp(\mathbf{t}_j) - m$ denoting the number of the normalized B-splines over the knot vector $\mathbf{t}_j$. The sequence of spaces $\{V_j\}_{j\ge 0}$ is called a nonstationary MRA of $L^2(I)$ ([**8, 11**]). Each family Φ_j is also considered as a row vector.

Example 3.1. *We look at the quadratic B-splines, of order $m = 3$, over*

$$\mathbf{t} := \{0, 0, 0, 0.5, 1, 1.5, \ldots, 4, 4.5, 5, 5, 5\}$$

and

$$\tilde{\mathbf{t}} := \{0, 0, 0, 0.7, 1.2, 1.2, 1.8, 2, 2, 3.1, 3.7, 4.7, 5, 5, 5\}.$$

The knot vector $\mathbf{t}$ is equidistant and has simple knots except at the boundaries, whereas $\tilde{\mathbf{t}}$ is non-equidistant and has multiplicity 2 at the knot 1.2. Figure 3.1 shows the families, say Φ and $\tilde{\Phi}$, of the normalized B-splines with respect to $\mathbf{t}$ and $\tilde{\mathbf{t}}$, respectively. Note that the interior functions of Φ are composed of shifts of a single function, but those of $\tilde{\Phi}$ are not.

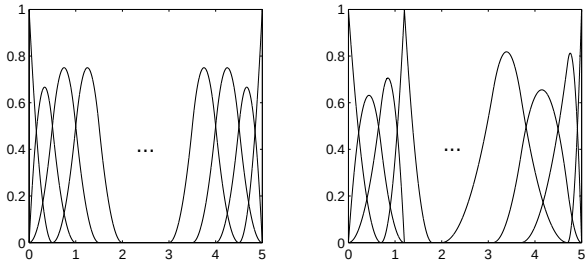

FIGURE 3.1. B-splines of order 3 over $\mathbf{t}$ (left) and $\tilde{\mathbf{t}}$ (right).

From the fact that V_j and V_{j+1} are nested we have the refinement relation

$$\Phi_j = \Phi_{j+1} P_j. \tag{3.7}$$

Namely, each $N_{\mathbf{t}_j;m,k}$, $-m+1 \le k \le M_j - m$, is a linear combination of $N_{\mathbf{t}_{j+1};m,k}$, $-m+1 \le k \le M_{j+1} - m$. The $M_{j+1} \times M_j$ matrix P_j is sparse and can be computed by the *Oslo-algorithm* ([**8**]). Chui et al. ([**8**]) constructed families

$$\Psi_j := [\psi_{j,k}; 1 \le k \le n_j] = \Phi_{j+1} Q_j, \quad j \ge 0, \tag{3.8}$$

that generate a so called *MRA tight frame of $L^2(I)$ (with respect to a quadratic form T_0)*. We give its definition first.

Definition 3.2. [**8**] *Assume that $\{\Phi_j\}_{j\ge 0}$ is a locally supported family. Let S_0 be a spsd (symmetric positive semi-definite) matrix, that defines the quadratic form T_0*

$$T_0 f := \langle f, \Phi_0 \rangle S_0 \langle f, \Phi_0 \rangle^T, \quad f \in L^2(I). \tag{3.9}$$

Then the family $\{\Psi_j\}_{j\ge 0}$ constitutes an MRA tight frame of $L^2(I)$ (with respect to T_0), if

$$T_0 f + \sum_{j\ge 0} \sum_{k=1}^{n_j} |\langle f, \psi_{j,k} \rangle_{L^2(I)}|^2 = \|f\|^2_{L^2(I)} \ \textit{for all} \ f \in L^2(I). \tag{3.10}$$

Note that this definition is slightly different from that of usual MRA tight frames of $L^2(\mathbb{R})$. If $S_0 = I$, the identity matrix, then $\{\Psi_j\}_{j\ge 0} \cup \{\Phi_0\}$ is a tight frame in the usual sense. Now we introduce the notion *locally supported*. A function family $\{\Phi_j\}_{j\ge 0}$ is said to be *locally supported*, if the sequence

$$h(\Phi_j) := \max_{k \in \mathbb{M}_j} \text{length}(\text{supp}\phi_{j,k})$$

converges to zero. If the sequence of knot vectors $(\mathbf{t}_j)_{j\geq 0}$ satisfies (3.2) and Φ_j is the family of the normalized B-splines over $\mathbf{t}_j$ in (3.6), then it is known that $\{\Phi_j\}_{j\geq 0}$ is locally supported ([**8**]). A general characterization of the MRA tight frame (with respect to T_0) is also provided in [**8**], and we present it here for the next section.

Theorem 3.3. [**8**] *Let $\{\Phi_j\}_{j\geq 0}$ be a locally supported family and S_0 an spsd matrix such that $\|T_0 f\|_{L^2(I)} \leq \|f\|^2_{L^2(I)}$ for all $f \in L^2(I)$. Then $\{\Psi_j\}_{j\geq 0} = \{\Phi_{j+1}Q_j\}_{j\geq 0}$ defines an MRA tight frame with respect to T_0, in the sense of Definition 3.2, if and only if there exist spsd matrices S_j of dimensions $M_j \times M_j$, $j \geq 1$, such that the following conditions hold:*

(i) *The quadratic forms*

$$T_j = \langle f, \Phi_j\rangle S_j \langle f, \Phi_j\rangle^T$$

satisfy

$$\lim_{j\to\infty} T_j f = \|f\|^2_{L^2(I)}, \quad f \in L^2(I).$$

(ii) *For each $j \geq 0$, we have the identity*

$$S_{j+1} - P_j S_j P_j^T = Q_j Q_j^T. \tag{3.11}$$

3.2. Stationary spline MRA tight frames on an interval

For a given m, the order of the B-spline, and L, the order of vanishing moments, and an interval $I = [0, n], n \in \mathbb{N}$, we want to look at the practical aspect of the construction of spline MRA tight frames (with respect to T_0) of $L^2(I)$ using Theorem 3.3. In particular, we are interested in the *stationary case*, where

$$\mathbf{t}_j = I \cap 2^{-j}\mathbb{Z}, \ j \geq 0, \tag{3.12}$$

and both boundary points 0 and n have multiplicity m. Throughout our work, we will deal with the stationary case only (for the general case see [**8, 11**]). It is clear that the nested sequence of knot vectors $\mathbf{t}_j, j \geq 0$, in (3.12) satisfies (3.1) and (3.2). Now, the family Φ_j of B-splines in (3.6) provides the basis of the MRA spline space $V_j, j \geq 0$. First, the matrices $P_j, j \geq 0$, are computed by the Oslo-algorithm as we already mentioned. Then spsd matrices $S_j, j \geq 0$, are obtained by the method

in [**8**] so that condition (i) of Theorem 3.3 holds. Moreover, the matrix on the left hand side of condition (ii) in Theorem 3.3 is positive semi-definite. Finally, each matrix Q_j is obtained by a factorization of the matrix $S_{j+1} - P_j S_j P_j^T$ and defines the family $\Psi_j = \Phi_{j+1} Q_j,\ j \geq 0$. We have, in the end, an MRA tight frame $\{\Psi_j\}_{j\geq 0} = \{\Phi_{j+1} Q_j\}_{j\geq 0}$ (with respect to T_0) of $L^2(I)$.

The very core of the work of Chui et al. ([**8**]) is the construction of such S_j's that eventually provide an MRA tight frame with L vanishing moments. Indeed, the $M_j \times M_j$ matrix S_j is designed to be an approximate inverse of the *Gramian matrix* $\Gamma(\mathbf{t}_j) := [\langle N_{\mathbf{t}_j;m,k}, N_{\mathbf{t}_j;m,\ell}\rangle]$ so that $\Phi_j S_j$ defines an approximate dual of Φ_j (for further details see [**8**]).

Note that each family Φ_j is composed of $2m-2$ "boundary functions" (B-splines with a multiple boundary knot) and $M_j - (2m-2)$ "interior functions" (B-splines with simple knots only). For example, the family Φ in Figure 3.1 has 4 boundary functions and 8 interior functions. In the stationary case, the boundary functions of $\Phi_j, j \geq 1$, are just scales of those of Φ_0 and the interior functions of Φ_j are also shifts and scales of those of Φ_0. More precisely, the first $m-1$ B-splines $N_{\mathbf{t}_j;m,-m+1}, \cdots, N_{\mathbf{t}_j;m,-1}$, ("left boundary functions") have a multiple knot 0, and the last $m-1$ B-splines $N_{\mathbf{t}_j;m,M_j-2m+2}$, $\cdots$, $N_{\mathbf{t}_j;m,M_j-m}$, ("right boundary functions") have a multiple knot n. Moreover, these boundary functions are dilates of $N_{\mathbf{t}_0;m,-m+1}, \cdots, N_{\mathbf{t}_0;m,-1}$, and $N_{\mathbf{t}_0;m,M_j-2m+2}, \cdots, N_{\mathbf{t}_0;m,M_j-m}$. Note that the right boundary functions are reflection of the left boundary functions, as

$$N_{\mathbf{t}_j;m,M_j-2m+1-k}(x) = N_{\mathbf{t}_j;m,k}(n-x), \quad -m+1 \leq k \leq -1.$$

The interior B-splines $N_{\mathbf{t}_j;m,0}, \cdots, N_{\mathbf{t}_j;m,M_j-2m+1}$, satisfy

$$N_{\mathbf{t}_j;m,k}(x) = N_{\mathbf{t}_0;m,0}(2^j x - k), 0 \leq k \leq M_j - 2m + 1,$$

i.e. they are shifts and dilates of a single cardinal B-spline. The families Ψ_j in (3.8) which we will construct have a similar structure; there is a fixed number $s \in \mathbb{N}$ of "boundary wavelets" satisfying $\psi_{j,k}(x) = 2^{j/2}\psi_{0,k}(2^j x), \quad 1 \leq k \leq s$, at the left boundary and

$$\psi_{j,n_j+1-k}(x) = \psi_{j,k}(n-x), \quad 1 \leq k \leq s,$$

at the right boundary. All other functions $\psi_{j,k}$ ("interior wavelets") are dilates and shifts of a fixed small number $r = 2$ or 3 of interior wavelets of Ψ_0. Namely, in the stationary case,

$$\psi_{j,s+rk+\ell} = 2^{j/2}\psi_{0,s+\ell}(2^j \cdot -k), \quad 1 \le \ell \le r,$$

holds and we call $\psi_{0,s+1}, \ldots, \psi_{0,s+r}$, the generators of the interior wavelets.
This structure does not depend on the stepsize 2^{-j} if the interval $I = [0, n]$ is large enough such that the boundary scaling functions/wavelets at the left and right boundary do not overlap. In this sense we call this construction *scaling-invariant*. Hence, due to the scaling-invariant construction, we only need to find the family Ψ_0 for an MRA tight frame (with respect to T_0) of $L^2(I)$. In other words, we will find just a factorization $Q_0 Q_0^T$ of the matrix $S_1 - P_0 S_0 P_0^T$. The matrix Q_0 has s first columns defining the boundary wavelets, its s last columns are the reflection of the first s columns, and the "interior" columns are shifted versions of r generating columns.

There is a close connection between spline MRA tight frames (with respect to T_0) on an interval and spline MRA tight frames on the real line. In the stationary case, the examples of spline MRA tight frames (with respect to T_0) ([**8, 11**]) suggest that the interior wavelets of Ψ_0 are splines with simple integer knots obtained as shifts of 3 fixed symmetric generators $\psi_1,\ \psi_2,\ \psi_3$, for $m = 4,\ L = 4$ ([**8, 11**]) (or two symmetric generators for $m = 2,\ L = 2$ ([**7, 8, 11**])). Moreover, it was revealed ([**8, 11**]) that these 3 (or 2) generators constitute a spline MRA tight frame of $L^2(\mathbb{R})$

$$\{\psi_{j,k,\ell} = 2^{k/2}\psi_j(2^k \cdot -\ell) : j = 1, 2, 3 \text{ (or } j = 1, 2),\ k, \ell \in \mathbb{Z}\}$$

in the sense of

$$\sum_{j=1}^{3 \text{ (or } 2)} \sum_{k\in\mathbb{Z}} \sum_{\ell\in\mathbb{Z}} |\langle f, \psi_{j,k,\ell}\rangle_{L^2(\mathbb{R})}|^2 = \|f\|^2_{L^2(\mathbb{R})}.$$

In other words, these 3 (or 2) generators satisfy both of the characterizations [**11**, Theorem 1] and [**13**, Proposition 1.11 (OEP)] of MRA tight frames of splines in $L^2(\mathbb{R})$. These recently developed characterizations will be recalled in section 4.1. In the next section and in the appendix, we extend the results. Namely, we construct MRA tight frames on an interval of order $m = 3, 4, 5, 6$, and take $r = 2$ or 3 symmetric/antisymmetric generators $\psi_1, \cdots, \psi_r$, of interior wavelets of Ψ_0. In the

next chapter, we point out that the generators constitute an MRA tight frame of $L^2(\mathbb{R})$.

3.3. Examples of stationary spline MRA tight frames on an interval

We develop some new examples of the spline MRA tight frames on an interval which were not given in the work of Chui et al. ([**8, 11**]). For the construction, we employ the method introduced in [**8**] for $m = 3$ $(L = 1, 3)$, 4 $(L = 2)$, 5 $(L = 3, 5)$, 6 $(L = 4, 6)$, where m denotes the order of the spline and L is the order of vanishing moments of the frame elements. Although the approach in [**8**] includes the nonstationary case, we consider only the stationary case for the sake of the scaling-invariant construction and a simple algorithm of DFRT (Discrete Frame Transformation).

In this section, we briefly present the general approach of the construction. The main process of the construction is devoted to the factorization of the spsd matrix in (3.11) for $j = 0$

$$S_1 - P_0 S_0 P_0^T = Q_0 Q_0^T.$$

In each case, we consider the following two equidistant and simple knot vectors on $I = [0, n]$

$$\mathbf{t}_0 = \{\underbrace{0, \cdots, 0}_{m}, 1, 2, \cdots, n-1, \underbrace{n, \cdots, n}_{m}\}, \tag{3.13}$$

$$\mathbf{t}_1 = \{\underbrace{0, \cdots, 0}_{m}, 0.5, 1, \cdots, n-1, n-0.5, \underbrace{n, \cdots, n}_{m}\}. \tag{3.14}$$

We define the families Φ_0 and Φ_1 of normalized B-splines of order m over the knot vectors. The interval $I = [0, n]$ is chosen so that the left and right boundary functions of Φ_0 do not overlap and 2 or 3 generators of the interior wavelets are apparently seen. For given m and L, the scaling-invariant construction reveals the same generators for different values of n, if n is large enough.

First, we compute the matrix P_0 for the two knot vectors $\mathbf{t}_0$ and $\mathbf{t}_1$. The matrices S_0 and S_1 depend on m, L, and the knot vectors $\mathbf{t}_0$ and $\mathbf{t}_1$, respectively and they are computed by matlab routines in [**20**]. It is shown in [**8**, Theorem 5.7] that the matrix $S_1 - P_0 S_0 P_0^T$ is positive semi-definite and has the representation

$$S_1 - P_0 S_0 P_0^T = E_{\mathbf{t}_1;m,L} Z_L E_{\mathbf{t}_1;m,L}^T, \tag{3.15}$$

where $E_{\mathbf{t}_1;m,L}$ is used for the description of the Lth order derivatives of the B-splines of order $m+L$ ([**8**, p.155]). The matrix Z_L is sparse, symmetric, and can be factorized on the basis of [**8**, Theorem 6.2] and consequently reads $Z_L := \hat{Q}\hat{Q}^T$. As a result we have the representation

$$S_1 - P_0 S_0 P_0^T = E_{\mathbf{t}_1;m,L} Z_L E_{\mathbf{t}_1;m,L}^T \tag{3.16}$$

$$= E_{\mathbf{t}_1;m,L} \hat{Q}\hat{Q}^T E_{\mathbf{t}_1;m,L}^T = Q_0 Q_0^T, \tag{3.17}$$

where the matrix $Q_0 := E_{\mathbf{t}_1;m,L}\hat{Q}$ defines the family Ψ_0. We obtain the factorization of Z_L in a similar way as in the examples in [**8**] so that the interior wavelets of Ψ_0 are symmetric/antisymmetric. In order to simplify the computation of the factorization we employ the symmetric reductions suggested in [**8**]. Namely, we multiply tridiagonal matrices $(I - K_i)$ and $(I - K_i^T)$ to the left and right side of Z_L to get a matrix $\tilde{Z}_L$ with a smaller bandwidth. In the examples, the symmetric reductions are performed $0 \le j \le 3$ times to get a matrix $\tilde{Z}_L$

$$\tilde{Z}_L = (I - K_j)\cdots(I - K_1) Z_L (I - K_1^T)\cdots(I - K_j^T). \tag{3.18}$$

Each matrix $I - K_i$ will be precisely given in each example and has the inverse

$$(I - K_i)^{-1} = I + K_i. \tag{3.19}$$

Finally, we find a factorization $\tilde{Z}_L = BB^T$, with $B = [B_\ell, B_i, B_r]$, where B_ℓ and B_r are, so called, the left and right blocks of B, and B_i is the interior block matrix. In the factorization we determine the block B_i first, and then find the other blocks from

$$\tilde{Z}_L - B_i B_i^T = B_\ell B_\ell^T + B_r B_r^T.$$

Namely, the matrix B_i will be determined so that the elements of the matrix $\tilde{Z}_L - B_i B_i^T$ are zero except at the blocks in the first and last diagonal corners. Moreover, the right block is positive semi-definite and the 180°-rotation of the left. Through the Cholesky factorization we get a matrix B_ℓ, and rotate it to get B_r. Hence, from (3.18) and (3.19), we have

$$Z_L = (I + K_1)\cdots(I + K_j) BB^T (I + K_j)\cdots(I + K_1)^T,$$

and from (3.16) and (3.17)

$$\begin{aligned} & S_1 - P_0 S_0 P_0^T \\ = \; & E_{\mathbf{t}_1;m,L}(I+K_1)\cdots(I+K_j)BB^T(I+K_j)^T\cdots(I+K_1)^T E_{\mathbf{t}_1;m,L}^T \\ = \; & E_{\mathbf{t}_1;m,L}\hat{Q}\hat{Q}^T E_{\mathbf{t}_1;m,L}^T = Q_0 Q_0^T. \end{aligned}$$

As mentioned in [**8**], we have two representations of the elements of Ψ_0. One is from the matrix Q_0 using $\Psi_0 = \Phi_1 Q_0$, namely

$$\psi_{0,k}(x) = \sum_{i=-m+1}^{M_1-m} q_{i,k} N_{\mathbf{t}_1,m;i}(x), \;\; k = 1,\ldots,n_1, \tag{3.20}$$

where, for convenience, the elements $q_{i,k}$ of Q_0 carry the row index $-m+1 \le i \le M_1 - m$. The second equivalent representation is from the matrix $\hat{Q} = (I + K_1)\cdots(I+K_j)B$

$$\psi_{0,k}(x) = \sum_{i=-m+1}^{M_1-m-L} \hat{q}_{i,k} \frac{d^L}{dx^L} N_{\mathbf{t}_1,m+L,i}(x), \;\; k = 1,\ldots,n_1, \tag{3.21}$$

with respect to the Lth order derivatives of the B-splines of order $m+L$. We employ the latter since it requires fewer coefficients and shows clearly that both the boundary and interior wavelets have L vanishing moments. The matrices $(I+K_1)\cdots(I+K_j)B_\ell$ and $(I+K_1)\cdots(I+K_j)B_i$ give the coefficients of the left boundary wavelets and the interior wavelets, respectively. The right boundary wavelets are reflections of the left.

Note that each frame element has L vanishing moments and compact support. Particularly, the interior wavelets are $m-2$ times continuously differentiable and consist of shifts and dilates of the 2 or 3 symmetric/antisymmetric generators. The coefficients of the 2 or 3 interior wavelets and those of left boundary wavelets will be given in expansion (3.21) in each example. For convenience, we give three examples for $(m,L) = (3,3), (5,5)$, and $(6,4)$ in this chapter and further examples for $(m,L) = (3,1), (4,2), (5,3)$, and $(6,6)$ in the appendix.

3.3.1. Construction of a quadratic spline tight frame with 3 vanishing moments ($m = 3,\ L = 3$).

For the construction we take $I = [0,6]$, i.e. $n = 6$ in (3.13) and (3.14). Then from

representation (3.15) we have the 11×11 matrix

$$Z_3 = \frac{1}{100}\begin{pmatrix}
0.085938 & 0.052083 & 0.008681 & 0 & 0 & 0 & \\
0.052083 & 0.262587 & 0.167191 & 0.063477 & 0.010579 & 0 & \\
0.008681 & 0.167191 & 0.673289 & 0.385132 & 0.125902 & 0.031738 & \\
0 & 0.063477 & 0.385132 & 0.723877 & 0.490926 & 0.190430 & \\
\vdots & 0.010579 & 0.125902 & 0.490926 & 0.948385 & 0.498861 & \\
 & 0 & 0.031738 & 0.190430 & 0.498861 & 0.771484 & \cdots \\
 & \vdots & 0.005290 & 0.031738 & 0.144857 & 0.498861 & \\
 & & 0 & 0 & 0.031738 & 0.190430 & \\
 & & 0 & 0 & 0.005290 & 0.031738 & \\
 & & 0 & 0 & 0 & 0 & \\
 & & 0 & 0 & 0 & 0 &
\end{pmatrix}.$$

Note that the last 5 columns of Z_3 are the 180°-rotation of the first 5 columns. Now, we employ the symmetric reductions by

$$\tilde{Z}_3 = (I - K_1)Z_3(I - K_1^T), \tag{3.22}$$

where

$$\tilde{Z}_3 = \frac{1}{100}\begin{pmatrix}
0.085938 & 0.052083 & 0 & 0 & 0 & 0 & 0 & \\
0.052083 & 0.262587 & 0.112847 & 0.063477 & 0 & 0 & 0 & \\
0 & 0.112847 & 0.520110 & 0.253906 & 0 & 0 & 0 & \\
0 & 0.063477 & 0.253906 & 0.723877 & 0.338542 & 0.190430 & 0 & \\
\vdots & 0 & 0 & 0.338542 & 0.670573 & 0.338542 & 0 & \\
 & 0 & 0 & 0.190430 & 0.338542 & 0.771484 & 0.338542 & \cdots \\
 & \vdots & \vdots & 0 & 0 & 0.338542 & 0.670573 & \\
 & & & 0 & 0 & 0.190430 & 0.338542 & \\
 & & & 0 & 0 & 0 & 0 & \\
 & & & 0 & 0 & 0 & 0 & \\
 & & & 0 & 0 & 0 & 0 &
\end{pmatrix}.$$

and

$$I - K_1 = \begin{pmatrix}
1 & & & & & & & & & & \\
 & 1 & & & & & & & & & \\
 & -1/6 & 1 & -1/6 & & & & & & & \\
 & & & 1 & & & & & & & \\
 & & & -1/6 & 1 & -1/6 & & & & & \\
 & & & & & 1 & & & & & \\
 & & & & & -1/6 & 1 & -1/6 & & & \\
 & & & & & & & 1 & & & \\
 & & & & & & & -1/6 & 1 & -1/6 & \\
 & & & & & & & & & 1 & \\
 & & & & & & & & & & 1
\end{pmatrix}. \tag{3.23}$$

The last 11×4 block of the $\tilde{Z}_3$ is the 180°-rotation of the first 11×4 block. Each matrix $I - K_i$ that appears in our work has the same structure as $I - K_1$. Thus, for convenience, we use the notation $T_{11,1,-1/6}$ for this matrix. Generally, $T_{j,k,\alpha}$ denotes

a tridiagonal matrix of dimensions $j \times j$ that has exactly the same structure as the matrix (3.23) with $k \times k$ unit block matrix at both diagonal ends. In addition, $T_{j,k,\alpha}$ has α instead of $-1/6$ in (3.23). The relation $(I - K_j)^{-1} = I + K_j$ in (3.19) reads as $T_{j,k,\alpha}^{-1} = T_{j,k,-\alpha}$. Now for the factorization of $\tilde{Z}_3 = BB^T$, with $B = [B_l, B_i, B_r]$, we suggest the 11×7 block matrix B_i given by

$$B_i = \begin{pmatrix} 0 & & & & & & \\ 0 & & & & & & \\ 0 & & & & & & \\ a & b & & & & & \\ & c & d & & & & \\ & b & & a & b & & \\ & & & c & d & & \\ & & & b & & a & \\ & & & & & 0 & \\ & & & & & 0 & \\ & & & & & 0 & \end{pmatrix}. \tag{3.24}$$

The 3 repeating columns of B_i will result in 3 antisymmetric interior wavelets in the end. We compare the 5th and 6th columns of the matrices $\tilde{Z}_3$ and $B_i B_i^T$ to determine a, b, c, d as in Table 3.1.

13/3840	bc	39/20480	b^2
103/15360	$c^2 + d^2$	13/3840	bc
13/3840	bc	79/10240	$a^2 + 2b^2$
0	0	13/3840	bc
0	0	39/20480	b^2

TABLE 3.1. The 5th and 6th columns of $\tilde{Z}_3$ and $B_i B_i^T$.

Then we have,

$$b = \sqrt{39/20480}, \qquad c = 13/(3840 \times b),$$

$$a = \sqrt{79/10240 - 2b^2}, \qquad d = \sqrt{103/15360 - c^2}.$$

as one possible solution. Hence, we have

$$\tilde{Z}_3 - B_i B_i^T = B_\ell B_\ell^T + B_r B_r^T,$$

and the elements of $\tilde{Z}_3 - B_i B_i^T$ are zero except at the first and last 4×4 blocks at both diagonal corners. The first block is positive definite and its 180°-rotation is the last block. Through the Cholesky factorization of the first block we get the 11×4 matrix B_ℓ, and rotate it to get B_r. Now, the matrix $T_{11,1,1/6} B_i$ gives the coefficients of 7 interior wavelets

$$\psi_j(\cdot - k), \quad 1 \le j \le 3, \ 0 \le k \le 1, \quad \psi_1(\cdot - 2),$$

which are given by 3 generators $\psi_1 := \psi_{0,5},\ \psi_2 := \psi_{0,6}$, and $\psi_3 := \psi_{0,7}$. Table 3.2 gives their coefficients in expansion (3.21).

i	$\hat{q}_{0,4+i}$	$\hat{q}_{1,4+i}$	$\hat{q}_{2,4+i}$	$\hat{q}_{3,4+i}$	$\hat{q}_{4,4+i}$
1	25/24	25/4	25/24		
2	0.727304	4.363825	9.212519	4.363825	0.727304
3			2.621470		

TABLE 3.2. Coefficients (*100) of interior wavelets $\psi_{0,4+i}, i = 1, 2, 3$, in expansion (3.21).

The supports of $\psi_1,\ \psi_2,\ \psi_3$, are

$$\text{supp } \psi_1 = [0, 4], \quad \text{supp } \psi_2 = [0, 5], \quad \text{supp } \psi_3 = [1, 4].$$

The graphs of the three generators are shown in Figure 3.2.

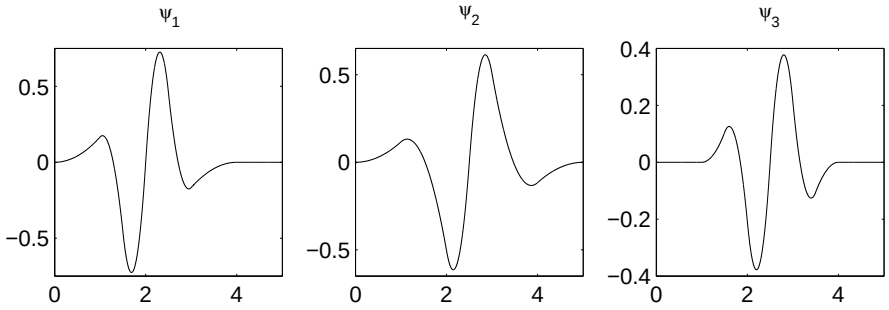

FIGURE 3.2. Three antisymmetric generators of the quadratic spline tight frame with 3 vanishing moments and simple interior knots.

Table 3.3 lists the coefficients in (3.21) of the 4 boundary wavelets for the left endpoint of the interval. The reflections of these functions give the 4 boundary

i	$\hat{q}_{-2,i}$	$\hat{q}_{-1,i}$	$\hat{q}_{0,i}$	$\hat{q}_{1,i}$	$\hat{q}_{2,i}$
1	2.931510	1.776673	0.296112		
2		4.806466	3.369007	1.320649	0.220108
3			7.363799	3.268805	0.544801
4			0.226876	1.361258	0.226876

TABLE 3.3. Coefficients($\times$100) of boundary wavelets $\psi_{0,i}, i = 1, \ldots, 4$, in expansion (3.21).

wavelets at the other endpoint 6. The graphs of the boundary wavelets for the left endpoint are shown in Figure 3.3.

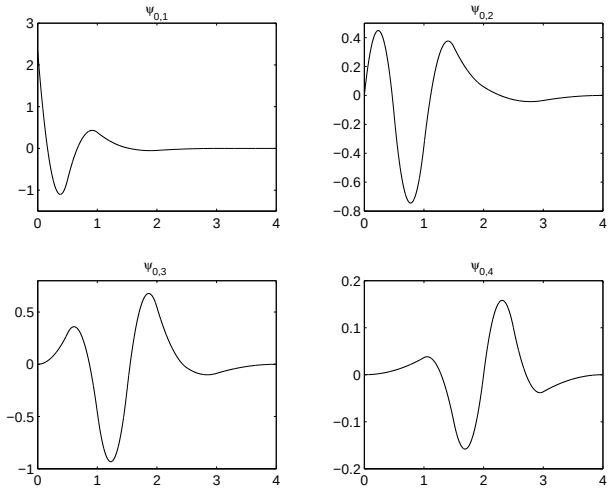

FIGURE 3.3. Boundary wavelets of the quadratic spline tight frame with 3 vanishing moments and simple interior knots.

3.3.2. Construction of a quartic spline tight frame with 5 vanishing moments ($m = 5,\ L = 5$).

We take $n = 11$ in (3.13) and (3.14) for the construction. For a factorization of the 21×21 matrix Z_5 in (3.15) we get

$$\tilde{Z}_5 = T_{21,4,-5/16} T_{21,3,-1/10} Z_5 T_{21,3,-1/10}^T T_{21,4,-5/16}^T,$$

by two symmetric reductions. Now we are going to get a factorization $\tilde{Z}_5 = BB^T$, where $B = [B_l, B_i, B_r]$. We take the 21×10 block matrix B_i given by

$$B_i = \begin{pmatrix} 0 & & & & & & & & & \\ \vdots & & & & & & & & & \\ 0 & & & & & & & & & \\ a & & e & & & & & & & \\ b & c & f & & & & & & & \\ a & d & g & a & & & & & & \\ & c & f & b & & & & & & \\ & & e & a & & & & & & \\ & & & & \ddots & & & & & \\ & & & & & e & & & & \\ & & & & & c & f & & & \\ & & & & & d & g & a & & \\ & & & & & c & f & b & & \\ & & & & & & e & a & & \\ & & & & & & & 0 & & \\ & & & & & & & \vdots & & \\ & & & & & & & 0 & & \end{pmatrix},$$

where B_i has 6 null rows at the top and the bottom, and find a solution similarly to the previous example. A numerical solution is

$$a = 0.366152 \times 10^{-2},\ b = 1.152073 \times 10^{-2},\ c = 0.059178 \times 10^{-2},\ d = 0.284117 \times 10^{-2},$$
$$e = 0.571251 \times 10^{-2},\ f = 0.999690 \times 10^{-2},\ g = 2.402380 \times 10^{-2}.$$

From the columns of the matrix $T_{21,3,1/10}T_{21,4,5/16}B_i$ we obtain the coefficients (see Table 3.4) of 10 interior wavelets

$$\psi_j(\cdot - k),\quad 1 \le j \le 3,\ 0 \le k \le 2,\quad \psi_1(\cdot - 3),$$

which are given by 3 antisymmetric generators $\psi_1 := \psi_{0,10},\ \psi_2 := \psi_{0,11}$, and $\psi_3 := \psi_{0,12}$. Their supports are

$$\text{supp } \psi_1 = [0, 8],\quad \text{supp } \psi_2 = [1, 8],\quad \text{supp } \psi_3 = [0, 9],$$

and their graphs are shown in Figure 3.4.

i	$\hat{q}_{0,9+i}$	$\hat{q}_{1,9+i}$	$\hat{q}_{2,9+i}$	$\hat{q}_{3,9+i}$	$\hat{q}_{4,9+i}$	$\hat{q}_{5,9+i}$	$\hat{q}_{6,9+i}$	$\hat{q}_{7,9+i}$	$\hat{q}_{8,9+i}$
1	0.011442	0.114422	0.515686	1.380918	0.515686	0.114422	0.011442		
2			0.014796	0.147964	0.313710	0.147964	0.014796		
3	0.017852	0.178516	0.781998	1.928950	2.788170	1.928950	0.781998	0.178516	0.017852

TABLE 3.4. Coefficients(*100) of interior wavelets $\psi_{0,9+i},\ i = 1, 2, 3$, in expansion (3.21).

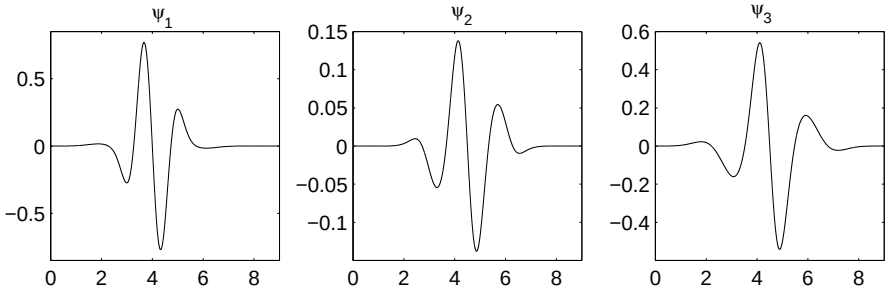

FIGURE 3.4. Three antisymmetric generators of interior wavelets of the quartic tight frame with 5 vanishing moments and simple interior knots.

i	$\hat{q}_{-4,i}$	$\hat{q}_{-3,i}$	$\hat{q}_{-2,i}$	$\hat{q}_{-1,i}$	$\hat{q}_{0,i}$	$\hat{q}_{1,i}$	$\hat{q}_{2,i}$	$\hat{q}_{3,i}$	$\hat{q}_{4,i}$	$\hat{q}_{5,i}$	$\hat{q}_{6,i}$
1	0.083801	0.129096	0.080878	0.022197	0.002220						
2		0.268477	0.371396	0.278256	0.114840	0.026368	0.002637				
3			0.651194	0.800265	0.509584	0.217970	0.067069	0.013719	0.001372		
4				1.000536	1.325019	0.963876	0.456642	0.149937	0.036015	0.006370	0.000637
5					1.298451	1.525510	1.069101	0.522368	0.178372	0.038223	0.003822
6					0.149179	1.491788	1.508878	0.940359	0.364858	0.082067	0.008207
7					0.050778	0.507781	1.818456	1.427776	0.598845	0.138202	0.013820
8							0.009743	0.097426	0.086200	0.023169	0.002317
9							0.000335	0.003345	0.011374	0.003345	0.000335

TABLE 3.5. Coefficients (*100) of the 9 boundary wavelets $\psi_{0,i}, i = 1, \ldots, 9$, in expansion (3.21).

Furthermore, the columns of the matrix $T_{21,3,1/10}T_{21,4,5/16}B_\ell$ give the coefficients (see Table 3.5) of the 9 boundary wavelets for the left endpoint of the interval. The graphs of them are shown in Figure 3.5.

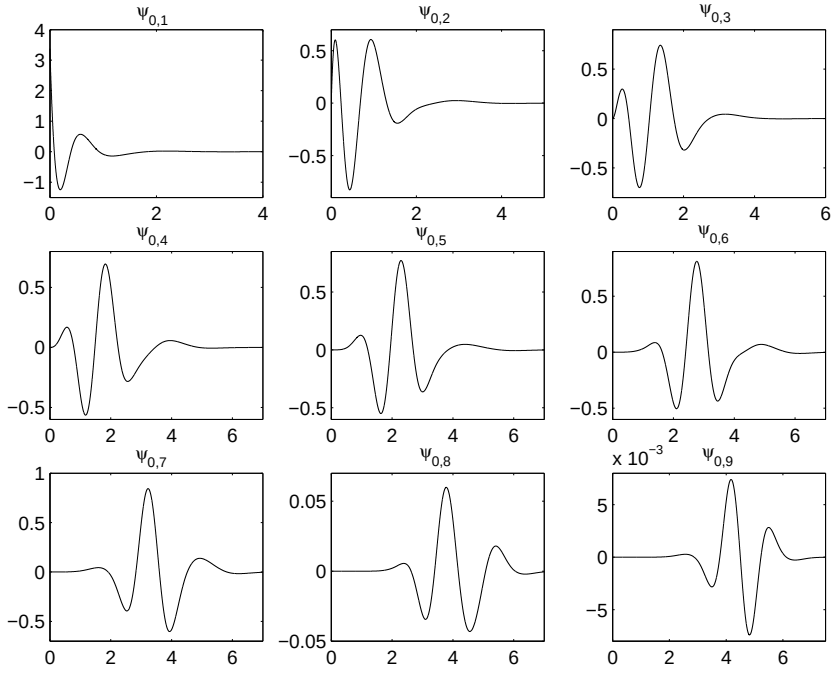

FIGURE 3.5. Boundary wavelets of the quartic tight frame with 5 vanishing moments and simple interior knots.

3.3.3. Construction of a quintic spline tight frame with 4 vanishing moments ($m = 6, L = 4$).

We consider $n = 12$ in (3.13)-(3.14) and search for a factorization of the 25×25 matrix Z_4 from representation (3.15). First, we get

$$\tilde{Z}_4 = T_{25,5,-5/16} T_{25,4,-1/10} Z_4 T_{25,4,-1/10}^T T_{25,5,-5/16}^T$$

by two symmetric reductions. In order to get a factorization of $\tilde{Z}_4$ we set

$$\tilde{Z}_4 = BB^T,$$

where $B = [B_\ell, B_i, B_r]$ and B_i is the 25×13 block matrix given by

$$B_i = \begin{pmatrix}
0 & & & & & & & & & & & & \\
\vdots & & & & & & & & & & & & \\
0 & & & & & & & & & & & & \\
a & e & & & & & & & & & & & \\
b & c & f & & & & & & & & & & \\
a & d & g & a & & & & & & & & & \\
 & c & f & b & & & & & & & & & \\
 & & e & a & & & & & & & & & \\
 & & & & \ddots & & & & & & & & \\
 & & & & & e & & & & & & & \\
 & & & & & c & f & & & & & & \\
 & & & & & d & g & a & & & & & \\
 & & & & & c & f & b & & & & & \\
 & & & & & & e & a & & & & & \\
 & & & & & & & 0 & & & & & \\
 & & & & & & & \vdots & & & & & \\
 & & & & & & & 0 & & & & &
\end{pmatrix}.$$

In addition, B_i has 7 null rows at the top and bottom. A solution is

$$a = 0.742456 \times 10^{-2},\ b = 3.700562 \times 10^{-2},\ c = 0.285988 \times 10^{-2},\ d = 1.520220 \times 10^{-2},$$
$$e = 1.398466 \times 10^{-2},\ f = 2.447316 \times 10^{-2},\ g = 6.367207 \times 10^{-2}.$$

The columns of the 25×13 matrix $T_{25,4,1/10} T_{25,5,5/16} B_i$ represent the coefficients (see Table 3.6) of the 13 interior wavelets

$$\psi_j(\cdot - k), \quad j = 1, 2, 3,\ 0 \le k \le 3, \quad \psi_1(\cdot - 4).$$

They are shifts of the 3 symmetric generators $\psi_1 := \psi_{0,11},\ \psi_2 := \psi_{1,12}$, and $\psi_3 := \psi_{0,13}$, whose supports are

$$\text{supp } \psi_1 = [0, 8], \quad \text{supp } \psi_2 = [1, 8], \quad \text{supp } \psi_3 = [0, 9].$$

The three generators are shown in Figure 3.6.

The columns of the 25×10 matrix $T_{25,4,1/10} T_{25,5,5/16} B_\ell$ give the coefficients (see Table 3.7) of the 10 boundary wavelets for the left endpoint of the interval. Figure 3.7 shows them.

Remark 3.4. *1. If we extend the bounded intervals to* $\mathbb{R}$*, each matrix* B_i *has infinite dimension and* 2 *or* 3 *columns (from the bounded interval case) are repeated with their nonzero entries shifted by* 2 *rows at a time. Eventually, no boundary*

i	$\hat{q}_{0,i+10}$	$\hat{q}_{1,i+10}$	$\hat{q}_{2,i+10}$	$\hat{q}_{3,i+10}$	$\hat{q}_{4,i+10}$	$\hat{q}_{5,i+10}$	$\hat{q}_{6,i+10}$	$\hat{q}_{7,i+10}$	$\hat{q}_{8,i+10}$
1	0.023202	0.232018	1.182118	4.164597	1.182118	0.232018	0.023202		
2			0.076106	0.761056	1.672431	0.761056	0.076106		
3	0.043702	0.437021	1.929577	4.874089	7.342024	4.874089	1.929577	0.437021	0.043702

TABLE 3.6. Coefficients(*100) of interior wavelets $\psi_{0,10+i}, i = 1, 2, 3$, in expansion (3.21).

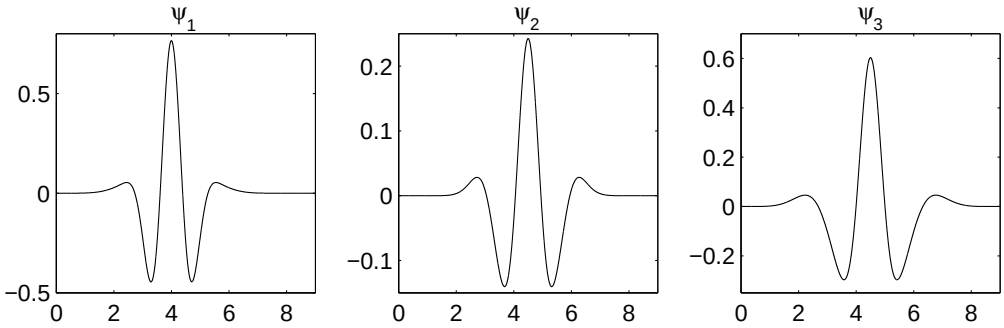

FIGURE 3.6. Three symmetric generators of the interior wavelets of the quintic spline tight frame with 4 vanishing moments and simple interior knots.

i	$\hat{q}_{-5,i}$	$\hat{q}_{-4,i}$	$\hat{q}_{-3,i}$	$\hat{q}_{-2,i}$	$\hat{q}_{-1,i}$	$\hat{q}_{0,i}$	$\hat{q}_{1,i}$	$\hat{q}_{2,i}$	$\hat{q}_{3,i}$	$\hat{q}_{4,i}$	$\hat{q}_{5,i}$	$\hat{q}_{6,i}$
1	0.17537	0.18268	0.06905	0.00863								
2		0.54686	0.58634	0.32338	0.08574	0.00857						
3			1.32579	1.23516	0.66480	0.22620	0.04840	0.00484				
4				2.35354	2.32681	1.27944	0.47586	0.12939	0.02479	0.00248		
5					3.35991	3.41191	2.14596	0.93804	0.29198	0.06671	0.01137	0.00114
6						4.13071	3.98100	2.46809	1.09545	0.35095	0.07315	0.00732
7						0.45761	4.57611	3.57169	1.99741	0.73193	0.16127	0.01613
8						0.15721	1.57207	5.58467	3.96854	1.55834	0.35197	0.03520
9								0.04454	0.44540	0.39910	0.10744	0.01074
10								0.00142	0.01422	0.04836	0.01422	0.00142

TABLE 3.7. Coefficients (*100) of the 10 boundary wavelets $\psi_{0,i}, i = 1, \ldots, 10$, in expansion (3.21).

*matrices B_ℓ, B_r, occur. In other words, our construction of interior frame elements reveals 2 or 3 generators of a tight frame of $L^2(\mathbb{R})$. For details, see the work of Chui et al. ([**9**]). Through numerical computations using the characterizations* [**7, 11, 13**]

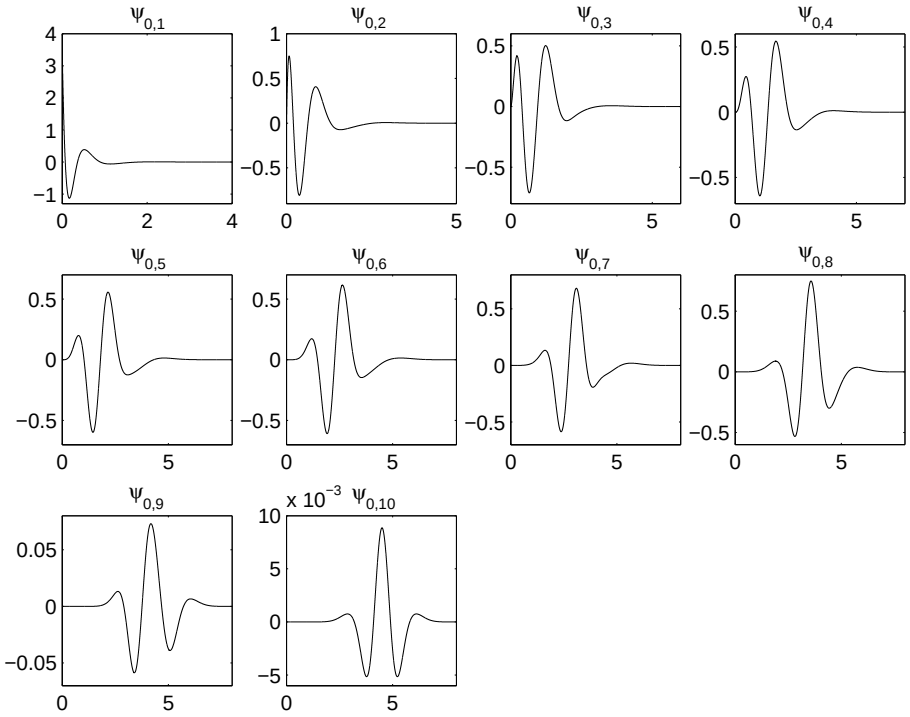

FIGURE 3.7. Boundary wavelets of the quintic spline tight frame with 4 vanishing moments and simple interior knots.

of MRA tight frames that will be introduced later, we will verify that they are actually MRA tight frames of $L^2(\mathbb{R})$.

3.4. Discrete frame transformation (DFRT)

Once we have an MRA tight frame on an interval, we can construct the so-called DFRT (Discrete Frame Transformation) in a similar fashion as the DWT (Discrete Wavelet Transformation). Namely, for a given input signal $[c_k]_{k=1,\dots,M_j} \in \ell^2(\mathbb{M}_j),\ j > 0,\quad \mathbb{M}_j = \{1, 2, \dots, M_j\}$, we can compute the coefficient sequences $C_{j-J} \in \ell^2(\mathbb{M}_{j-J}),\ J \le j$, and $D_i \in \ell^2(\mathbb{N}_i), j - J \le i \le j - 1,\ \mathbb{N}_i = \{1, 2, \dots, n_i\}$, of the decomposition and, likewise, the reconstruction by a pyramidal algorithm. Depending on the nature of the input data we divide the algorithms into *simple DFRT* and *preprocessed DFRT*. We deal with the stationary case consistently as in the previous section.

3.4.1. Simple DFRT decomposition and reconstruction.

Let a spline MRA tight frame, with splines of order m on some interval $I =$

$[a,b], a, b \in \mathbb{R}$, be given. Moreover, the associated knot vectors $\mathbf{t}_j, j \geq 0$, are assumed to have the form (3.3) and satisfy (3.4), (3.5), and (3.12). The B-splines $\phi_{j,k}$'s are defined on these vectors. Now we suppose that input data $[c_k]_{k=1,2,\cdots,M_j}$ are given with

$$c_k := c_{j,k} = \langle f, \phi_{j,k} \rangle, \quad k \in \{1, \ldots, M_j\},$$

for some $f \in L^2(I)$. The knot sequences of coarser levels $\mathbf{t}_{j-1}, \mathbf{t}_{j-2}, \cdots, \mathbf{t}_{j-J}$, determine the matrices P_{j-k} of the refinement relations $\Phi_{j-k} = \Phi_{j-k+1} P_{j-k}$ in (3.7) and S_{j-k} in (3.11). Moreover, the frame elements are defined by the matrices Q_{j-k} as in (3.8). For convenience, we employ the notions of row vectors $C_j := [c_{j,k}]_k = [\langle f, \phi_{j,k} \rangle]_k = \langle f, \Phi_j \rangle$ and $D_j := [d_{j,k}]_k = [\langle f, \psi_{j,k} \rangle]_k = \langle f, \Psi_j \rangle$, which are called *core* and *detail part* of the input at depth j, respectively. Using these notations we describe the algorithms of decomposition and reconstruction.

Theorem 3.5. *Let $j > 0$ and $C_j := [c_{j,k}]_k = \langle f, \Phi_j \rangle$ be given for some $f \in L^2(I)$. Then we have*

(i) [Decomposition] $C_{j-1} = C_j P_{j-1}, \quad D_{j-1} = C_j Q_{j-1}$.

(ii) [Reconstruction] $C_j S_j = C_{j-1} S_{j-1} P_{j-1}^T + D_{j-1} Q_{j-1}^T$.

Proof.

We begin with the decomposition. From the definition of C_j and the refinement relation (3.7) we have

$$C_j P_{j-1} = \langle f, \Phi_j \rangle P_{j-1} = \langle f, \Phi_j P_{j-1} \rangle = \langle f, \Phi_{j-1} \rangle = C_{j-1}$$

The identity $D_{j-1} = C_j Q_{j-1}$ follows analogously using (3.8).
The reconstruction algorithm follows from (i) and (3.11),

$$C_{j-1} S_{j-1} P_{j-1}^T + D_{j-1} Q_{j-1}^T = C_j (P_{j-1} S_{j-1} P_{j-1}^T + Q_{j-1} Q_{j-1}^T) = C_j S_j. \qquad \square$$

Remark 3.6. *1. C_j is obtained from (ii), if S_j is invertible.*
2. If we want to reconstruct C_j from its decomposition $C_{j-J}, D_i, i = j-1, j-2, \ldots, j-J$, we do not need to compute the inverse of S_j at each level. Namely, if we employ the notation $C_j^S := C_j S_j$, (ii) is equivalent to

$$C_j^S = C_{j-1}^S P_{j-1}^T + D_{j-1} Q_{j-1}^T. \tag{3.25}$$

We get C^S_{j-J} by multiplying C_{j-J} by S_{j-J} at the coarsest level, and apply (3.25) until we obtain C^S_j. Finally we obtain $C_j = C^S_j S_j^{-1}$. (see Figure 3.9).

We present the diagrams of the simple DFRT decomposition and reconstruction.

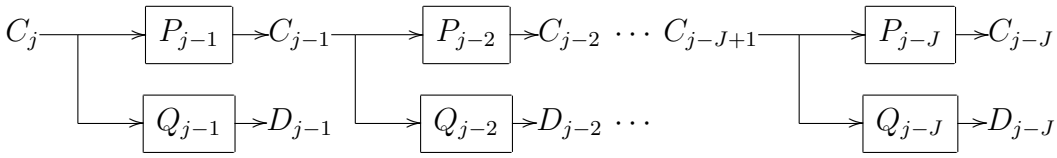

FIGURE 3.8. Simple DFRT decomposition.

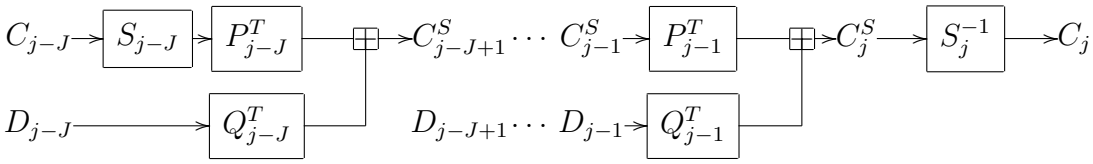

FIGURE 3.9. Simple DFRT reconstruction.

3.4.2. Preprocessed DFRT decomposition/reconstruction.

We suppose, as in the previous section, that we have an MRA tight frame on an interval. Now let the input $\hat{C}_j := [\hat{c}_{j,k}]_k$ be a row vector in $\mathbb{R}^{M_j}$ whose entries are the coefficients of some function $f \in V_j$ for some $j > 0$,

$$f = \sum_{k=1}^{M_j} \hat{c}_{j,k}\phi_{j,k} = \hat{C}_j \Phi_j^T. \tag{3.26}$$

In order to apply the algorithm of the decomposition as in (i) of Theorem 3.5, however, we need the coefficients

$$C_j = \langle f, \Phi_j \rangle.$$

Namely, we are required to transform the input $\hat{C}_j$ to C_j before we perform the decomposition. This is the reason why we call this algorithm 'preprocessed DFRT'. In the next theorem we are going to deal with the preprocessed DFRT decomposition and reconstruction. Here, Γ_j denotes the Gramian matrix of the basis Φ_j of V_j, i.e.

$$\Gamma_j = \langle \Phi_j^T, \Phi_j \rangle.$$

Theorem 3.7. *Let $\hat{C}_j$ be the row vector in (3.26). Then we have*

(i) [Decomposition] $C_j = \hat{C}_j\Gamma_j,\ C_{j-1} = C_jP_{j-1},\ D_{j-1} = C_jQ_{j-1}$.

(ii) [Reconstruction] $C_jS_j = C_{j-1}S_{j-1}P_{j-1}^T + D_{j-1}Q_{j-1}^T,\ \hat{C}_j = C_j\Gamma_j^{-1}$.

Proof.

The definition of Γ_j directly implies $C_j = \hat{C}_j\Gamma_j$. The decomposition in (i) is identical to (i) of Theorem 3.5. The first part of the reconstruction is also the same as that of Theorem 3.5, and $\hat{C}_j = C_j\Gamma_j^{-1}$ is obvious. □

Remark 3.8. *If we want to reconstruct $\hat{C}_j$ from C_{j-J} and $D_i, i = j-1, \ldots, j-J$, we compute C_iS_i using (ii) in each step until we get C_jS_j. Then the last step of the reconstruction is to get $\hat{C}_j$ using $\hat{C}_j = C_j^SS_j^{-1}\Gamma_j^{-1}$. Namely, the matrices S_j^{-1} and Γ_j^{-1} are necessary only one time at the end of the algorithm.*

In order to reconstruct $\hat{C}_j$ in (ii) we need to compute two inverse matrices S_j^{-1}, Γ_j^{-1}, in which the computational complexity is high. For a simpler algorithm, we recall that the spsd matrix S_j is designed as an approximation of Γ_j^{-1}, i.e. $S_j^{-1} \approx \Gamma_j$ or $S_j^{-1}\Gamma_j^{-1} \approx I$. If we apply this property to the given function f in (3.26), we have an alternative decomposition/reconstruction algorithm. Namely, we define $\tilde{f} := \hat{C}_jS_j^{-1}\Gamma_j^{-1}\Phi_j^T$ and $\tilde{C}_j := \langle\tilde{f}, \Phi_j\rangle$, where $\tilde{f}$ is taken for an approximation to f and brings us

$$\tilde{C}_j = \langle\tilde{f}, \Phi_j\rangle = \hat{C}_jS_j^{-1}\Gamma_j^{-1}\langle\Phi_j^T, \Phi_j\rangle = \hat{C}_jS_j^{-1}\Gamma_j^{-1}\Gamma_j = \hat{C}_jS_j^{-1}.$$

This relation allows us to describe the algorithms without use of the matrix Γ_j^{-1}.

Theorem 3.9. *Let $\hat{C}_j$ be the row vector in (3.26) and $\tilde{C}_j = \langle\tilde{f}, \Phi_j\rangle,\ \tilde{D}_j = \langle\tilde{f}, \Psi_j\rangle$. Then we have*

(i) [Decomposition] $\tilde{C}_j = \hat{C}_jS_j^{-1},\ \tilde{C}_{j-1} = \tilde{C}_jP_{j-1},\ \tilde{D}_{j-1} = \tilde{C}_jQ_{j-1}$.

(ii) [Reconstrucion] $\hat{C}_j = \tilde{C}_{j-1}S_{j-1}P_{j-1}^T + \tilde{D}_{j-1}Q_{j-1}^T$.

Proof.

Firstly, at the beginning of the decomposition we compute $\tilde{C}_j = \hat{C}_jS_j^{-1}$ and then analogously to the proof of Theorem 3.5 we have the decomposition (i). For the reconstruction we have

$$\tilde{C}_jS_j = \tilde{C}_{j-1}S_{j-1}P_{j-1}^T + \tilde{D}_{j-1}Q_{j-1}^T,$$

which is identical with

$$\hat{C}_j = \tilde{C}_{j-1} S_{j-1} P_{j-1}^T + \tilde{D}_{j-1} Q_{j-1}^T.$$

Hence, we have (ii). □

Remark 3.10. *If we want to decompose the input $\hat{C}_j$ to the $(j-J)$th level, we perform the preprocessing $\tilde{C}_j = \hat{C}_j S_j^{-1}$ in advance. Then we have the core and detail parts only by multiplying $\tilde{C}_{j-k+1}$ by the matrices P_{j-k}'s and Q_{j-k}'s for $k = 1, \ldots, J$, (see Figure 3.10). On the other hand, if we want to reconstruct $\hat{C}_j$ from the $\tilde{C}_{j-J}$ and $\tilde{D}_{j-k}$'s for $k = 1, \ldots, J$, we multiply $\tilde{C}_{j-J}$ by S_{j-J} at the coarsest level, and then reconstruct the original $\hat{C}_j$ with the ordinary pyramidal scheme (see Figure 3.11).*

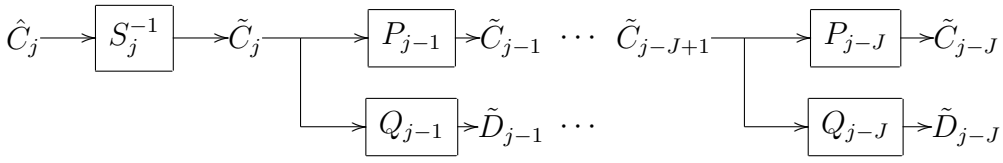

FIGURE 3.10. Preprocessed DFRT decomposition.

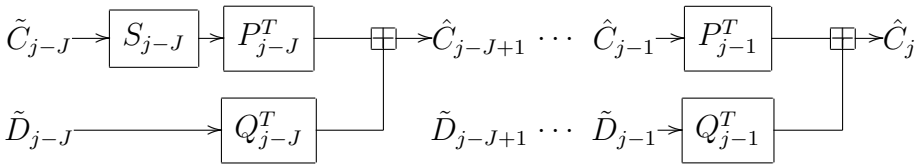

FIGURE 3.11. Preprocessed DFRT reconstruction.

CHAPTER 4

Generation of Hilbert transform pairs of MRA tight frames

This chapter is devoted to the study of Hilbert transform pairs of MRA tight frames of $L^2(\mathbb{R})$. We suppose that an MRA tight frame $\{\psi_{j,k,\ell}\}$ of $L^2(\mathbb{R})$ is given. Then we construct its Hilbert transform $\{\mathcal{H}\psi_{j,k,\ell}\}$ that is also an MRA tight frame of $L^2(\mathbb{R})$. For the construction we will show that Selesnick's ([**26, 27**]) and Zhao's ([**30**]) approaches can be extended to MRA tight frames of $L^2(\mathbb{R})$. At the end, we reveal a general method generating an MRA tight frame from a given one. This method covers the generation of the Hilbert transform of a given MRA tight frame. We begin with the recently developed characterizations of MRA tight frames of $L^2(\mathbb{R})$.

4.1. Characterizations of MRA tight frames of $L^2(\mathbb{R})$

The characterizations of MRA tight frames were developed in parallel and independently in [**7, 11, 13**]. The characterization of Daubechies et al. ([**13**]) is more general and includes that of Chui et al. ([**7, 11**]). One of the salient differences is that the latter requires a compactly supported refinable function. Since we want to develop the Hilbert transform of frames, we need the more general characterization in [**13**]. By [**11**, Theorem 1] and [**7**, Theorem 1], one can characterize the tight frames generated by a compactly supported refinable function.

Assumption 4.1. [**7**] *(a) The refinable function ϕ is compactly supported, real-valued, piecewise* Lip α *for some $\alpha > 0$, and satisfies $\hat{\phi}(0) = 1$. Furthermore, it satisfies a two-scale relation*

$$\phi(x) = \sum_{k=n_1}^{n_2} p_k \phi(2x-k), \quad a.e.\ x \in \mathbb{R},$$

for some real numbers p_k. In other words,

$$\hat{\phi}(\xi) = p(\xi/2)\hat{\phi}(\xi/2), \quad a.e.\ \xi \in \mathbb{R}, \tag{4.1}$$

where the corresponding two-scale trigonometric polynomial p is defined by

$$p(\xi) := \frac{1}{2}\sum_{k=n_1}^{n_2} p_k e^{-ik\xi},\ \xi \in \mathbb{R}.$$

We further assume that

$$p(\xi) = \left(\frac{1+e^{-i\xi}}{2}\right)^m p_0(\xi),$$

for some $m \geq 1$, with a trigonometric polynomial p_0 that satisfies $p_0(\pi) \neq 0$.

Next, we consider a finite family $\{\psi_j \in L^2(\mathbb{R}), j = 1, \ldots, r\}$ defined by two-scale relations

$$\hat{\psi}_j(\xi) = q_j(\xi/2)\hat{\phi}(\xi/2),\quad j = 1, \ldots, r, \tag{4.2}$$

where q_j are trigonometric polynomials that have real coefficients and vanish at $\xi = 0$. Namely,

$$q_j(\xi) = \left(1 - e^{-i\xi}\right)^{L_j} q_0^j(\xi), \tag{4.3}$$

where $L_j \geq 1$ and q_0^j are trigonometric polynomials as well and satisfy $q_0^j(0) \neq 0$. Each of the functions ψ_j has, as a result, compact support and at least one vanishing moment. The next characterization asserts when the family of shifts and dilates

$$\{\psi_{j,k,\ell} = 2^{k/2}\psi_j(2^k \cdot -\ell) : 1 \leq j \leq r, k, \ell \in \mathbb{Z}\}$$

is an MRA tight frame of $L^2(\mathbb{R})$.

Proposition 4.2. [**11**, Theorem 1] *Let ϕ be a refinable function with compact support and two-scale trigonometric polynomial p with real coefficients such that Assumption 4.1 is satisfied. Let q_j be trigonometric polynomials with real coefficients vanishing at $\xi = 0$. Then the functions $\psi_j, j = 1, \cdots, r$, defined in (4.2) generate a tight frame of $L^2(\mathbb{R})$, if and only if there exists a VMR (Vanishing Moment Recovery) function S, defined a.e. in $\mathbb{R}$, that satisfies the following properties:*
(i) *S is a trigonometric polynomial with real coefficients and nonnegative values for all $\xi \in \mathbb{R}$, and $S(0) = 1$;*
(ii) *for a.e. $\xi \in \mathbb{R}$ the following two equations hold;*

$$S(2\xi)\left|p(\xi)\right|^2 + \sum_{j=1}^{r}\left|q_j(\xi)\right|^2 = S(\xi), \tag{4.4}$$

$$S(2\xi)p(\xi)\overline{p(\xi+\pi)}+\sum_{j=1}^{r}q_j(\xi)\overline{q_j(\xi+\pi)}=0. \tag{4.5}$$

Remark 4.3. *1. If we take N_m, the cardinal B-spline of order m (degree $m-1$), as our refinable function for $m \geq 2$, it satisfies all conditions in Assumption 4.1. Namely, we have*

$$\hat{N}_m(\xi)=\left(\frac{1-e^{-i\xi}}{i\xi}\right)^m,$$

and its two-scale symbol is

$$p_m(\xi)=\left(\frac{1+e^{-i\xi}}{2}\right)^m.$$

2. Furthermore, the VMR functions S of N_m were presented in [**7, 11**] *so that S satisfy (i) and (ii) of Proposition 4.2. They were designed for given m and $1 \leq L \leq m$ so that each q_j has the form (4.3).*

3. Note that the r ($r = 2$ or 3) generators of the interior wavelets in the examples of the previous section have equivalent expansions to those in (3.20) and (3.21). From now on, we use the notation $\psi_j^{m,L}$, $j = 1, \ldots, r$, for the generators of order m and having L vanishing moments. The expansion (3.20) in the time domain is equivalent to the representation

$$\hat{\psi}_j^{m,L}(\xi)=q_j^{m,L}(\xi/2)\hat{N}_m(\xi/2), \quad 1 \leq j \leq r, \tag{4.6}$$

in the frequency domain, where the two-scale symbols $q_j^{m,L}$ are trigonometric polynomials,

$$q_j^{m,L}(\xi):=\frac{1}{2}\sum_{\ell=-m+1}^{M_1-m}q_{\ell,k_0+j}e^{-i(\ell+m-1)\xi}, \quad 1 \leq j \leq r, \tag{4.7}$$

and where $k_0 \in \mathbb{N}$ denotes the number of "left boundary wavelets" in (3.20) (q_{ℓ,k_0+j} are the elements of the (k_0+j)th column of the matrix Q_0 in (3.17)). If we employ the expansion (3.21), each $q_j^{m,L}$ is given by

$$q_j^{m,L}(\xi)=2^L\hat{q}_j^{m,L}(\xi)(1-e^{-i\xi})^L, \tag{4.8}$$

where the trigonometric polynomial $\hat{q}_j^{m,L}$ is defined similarly to (4.7) using the coefficients of expansion (3.21). Note that $\hat{q}_j^{m,L}(0) \neq 0$ since its coefficients are positive (see section 3.3).

4. Numerical computations verify that the above mentioned p_m, $q_j^{m,L}$, and the associated VMR function, say $s_{m,L}$, satisfy (i) and (ii) of the Proposition 4.2 for all examples of section 3.3 and the appendix, which was already pointed out in Remark 3.4.

Another characterization, Oblique Extension Principle (OEP) ([**13**]), of tight frames with MRA is given under the following assumptions on the two-scale symbols and the refinable functions. The notation $\tau := (p, q_1, \cdots, q_r)$ denotes *the combined MRA mask*.

Assumption 4.4. [**13**] *All MRA-based constructions that are considered in* [**13**] *are assumed to satisfy the following:*
(a) The combined MRA mask τ is measurable and (essentially) bounded.
(b) The refinable function ϕ satisfies $\lim_{\xi\to 0}\hat{\phi}(\xi) = 1$.
(c) The function $[\hat{\phi},\hat{\phi}] := \sum_{k\in\mathbb{Z}^d}|\hat{\phi}(\cdot + 2\pi k)|^2$ *is essentially bounded.*

Now, we give several definitions and notations taken from [**13**] before the characterization is presented. Let the family $\{\psi_j, j = 1, \cdots, r\}$ constitute an MRA tight frame and ϕ be the corresponding refinable function. The *fundamental function* Θ of the *parent wavelet vector* $F := (\phi, \psi_1, \ldots, \psi_r)$ is defined by

$$\Theta(\xi) := \sum_{k=0}^{\infty}\sum_{j=1}^{r}|q_j(2^k\xi)|^2\prod_{m=0}^{k-1}|p(2^m\xi)|^2. \tag{4.9}$$

From this definition, it follows that

$$\Theta(\xi) = \sum_{j=1}^{r}|q_j(\xi)|^2 + |p(\xi)|^2\Theta(2\xi), \tag{4.10}$$

which is identical with (4.4), if $\Theta = S$. (We accept the identity $\Theta = S$ a priori, and deal with it later in detail.) The notation for the *spectrum* of the shift-invariant space V_0

$$\sigma(V_0) := \{\omega \in [-\pi,\pi]^d : \hat{\phi}(\omega + 2\pi k) \neq 0, \text{for some } k \in \mathbb{Z}^d\}$$

appears in the following propositions. Note that if the refinable function ϕ has compact support, $\hat{\phi}$ is entire. Hence, $\sigma(V_0) := [-\pi,\pi]^d \setminus \mathcal{N}$, where $\mathcal{N}$ is a null set.

Proposition 4.5. [**13**, Proposition1.7] *Assume that the combined MRA mask* $\tau = (p, q_1, \ldots, q_r)$ *is bounded and, furthermore,* $\hat{\phi}$ *is continuous at the origin and* $\hat{\phi}(0) = 1$. *Define* Θ *as in (4.9). Then the following conditions are equivalent:*
(a) The corresponding wavelet system $\{\psi_{j,k,\ell}, 1 \le j \le r, k, \ell \in \mathbb{Z}\}$ *is a tight frame.*
(b) For almost all $\xi \in \sigma(V_0)$, *the function* Θ *satisfies:*
(b1) $\lim_{j\to-\infty} \Theta(2^j\xi) = 1$.
(b2) For $\xi + \pi \in \sigma(V_0)$

$$\Theta(2\xi)p(\xi)\overline{p(\xi+\pi)} + \sum_{j=1}^{r} q_j(\xi)\overline{q_j(\xi+\pi)} = 0. \tag{4.11}$$

For the construction, however, it is not easy to build the masks $p, q_j, j = 1, \ldots, r$, so that the fundamental function Θ and the masks satisfy all conditions of Proposition 4.5 ([**13**]). For that reason the following sufficient condition is proposed ([**13**]).

Proposition 4.6. [**13**, Proposition 1.11]*(Oblique extension principle (OEP)) Let* τ *be the combined mask of an MRA that satisfies Assumption 4.4. Suppose that there exists a* $2\pi-$*periodic function* Θ *that satisfies the following:*
(i) Θ *is non-negative, essentially bounded, continuous at the origin, and* $\Theta(0) = 1$.
(ii) *If* $\xi, \xi + \pi \in \sigma(V_0)$, *then*

$$\Theta(2\xi)p(\xi)\overline{p(\xi+\nu)} + \sum_{j=1}^{r} q_j(\xi)\overline{q_j(\xi+\nu)} = \begin{cases} \Theta(\omega), & \text{if } \nu = 0, \\ 0, & \text{if } \nu = \pi. \end{cases} \tag{4.12}$$

Then the wavelet system $\{\psi_{j,k,\ell}, 1 \le j \le r, k, \ell \in \mathbb{Z}\}$ *defined by* τ *is a tight frame.*

Remark 4.7. *1. Note that Proposition 4.5 does not require that the two-scale symbols are trigonometric polynomials nor the refinable function is compactly supported. Furthermore, condition (b1) is milder than (i) of Proposition 4.2. In this sense Proposition 4.5 is more general than Proposition 4.2. As for the two identities (4.4) and (4.5) of the first characterization, (4.4) is the same as (4.10) and (4.5) equals (4.11).*
2. Now we need to clarify the difference between the functions S *and* Θ, *although they are in many cases identical as we accepted a priori. The VMR function* S *is defined through the equations (4.4) and (4.5), while the fundamental function* Θ *is defined by the masks in (4.9). We show that these two functions are identical when*

S is bounded. Note that the boundedness of S follows from the stability of ϕ *([**7**]). If we apply (4.4) recursively, we have*

$$\begin{aligned} S(\xi) &= \left(S(4\xi) \left|P(2\xi)\right|^2 + \sum_{j=1}^{r} \left|Q_j(2\xi)\right|^2 \right) \left|P(\xi)\right|^2 + \sum_{j=1}^{r} \left|Q_j(\xi)\right|^2 \\ &= \left(S(8\xi) \left|P(4\xi)\right|^2 + \sum_{j=1}^{r} \left|Q_j(4\xi)\right|^2 \right) \left|P(2\xi)\right|^2 \left|P(\xi)\right|^2 \\ &+ \left|P(\xi)\right|^2 \sum_{j=1}^{r} \left|Q_j(2\xi)\right|^2 + \sum_{j=1}^{r} \left|Q_j(\xi)\right|^2 \end{aligned}$$

and generally

$$S(\xi) = S(2^K\xi) \prod_{\ell=0}^{K-1} \left|P(2^\ell\xi)\right|^2 + \sum_{k=0}^{K-1} \sum_{j=1}^{r} \left|Q_j(2^k\xi)\right|^2 \prod_{m=0}^{k-1} \left|P(2^m\xi)\right|^2 .$$

Finally, using (4.1), we obtain

$$S(\xi) = S(2^K\xi) \left| \frac{\hat{\phi}(2^K\xi)}{\hat{\phi}(\xi)} \right|^2 + \sum_{k=0}^{K-1} \sum_{j=1}^{r} \left|Q_j(2^k\xi)\right|^2 \prod_{m=0}^{k-1} \left|P(2^m\xi)\right|^2 . \tag{4.13}$$

First, we show that

$$S(2^K\xi) \left| \frac{\hat{\phi}(2^K\xi)}{\hat{\phi}(\xi)} \right|^2 \to 0, \ as \ K \to \infty \ for \ \xi \in \sigma(V_0).$$

Since S is bounded, it suffices to show that $|\hat{\phi}(2^K\xi)| \to 0$ *a.e. as* $K \to \infty$*. This follows from the Riemann-Lebesgue lemma, if* ϕ *has compact support. In general, if* $\phi \in L^2(\mathbb{R})$*, then*

$$\int_1^\infty |\hat{\phi}(\xi)|^2 d\xi = \sum_{j\geq 0} \int_{2^j}^{2^{j+1}} |\hat{\phi}(\xi)|^2 d\xi = \sum_{j\geq 0} 2^j \int_1^2 |\hat{\phi}(2^j\xi)|^2 d\xi < \infty.$$

Hence, we conclude that $\sum_{j\geq 0} |\hat{\phi}(2^j\xi)|^2 < \infty$ *for a.e.* $\xi \in [1,2]$*, and, a fortiori,*

$$\sum_{j\geq 0} |\hat{\phi}(2^j\xi)|^2 < \infty \ a.e. \ \xi \in [1,2].$$

This implies $\lim_{j\to\infty} \hat{\phi}(2^j\xi) = 0$ *for a.e.* $\xi \in [1,2]$*. The same argument holds for the interval* $[-2,-1]$*, and this gives*

$$\lim_{j\to\infty} \hat{\phi}(2^j\xi) = 0 \quad for \ a.e. \ \xi \in \mathbb{R} \setminus \{0\}.$$

Now, it follows from (4.13) that

$$\begin{aligned} S(\xi) &= \lim_{K\to\infty}\left(S(2^K\xi)\left|\frac{\hat{\phi}(2^K\xi)}{\hat{\phi}(\xi)}\right|^2 + \sum_{k=0}^{K-1}\sum_{j=1}^{r}\left|Q_j(2^k\xi)\right|^2\prod_{m=0}^{k-1}\left|P(2^m\xi)\right|^2\right) \\ &= \sum_{k=0}^{\infty}\sum_{j=1}^{r}\left|Q_j(2^k\xi)\right|^2\prod_{m=0}^{k-1}\left|P(2^m\xi)\right|^2 = \Theta(\xi),\ \xi\in\sigma(V_0). \end{aligned}$$

*As a result, S is real and positive on $\sigma(V_0)$. If, in addition, ϕ has compact support, $S=\Theta$ almost everywhere. In the work of Chui et al. ([**7**]) B-splines were chosen as the refinable function and the associated VMR function S is constructed as a trigonometric polynomial. Since S is bounded and satisfies all conditions of Proposition 4.5 the same MRA tight frames are generated by both characterizations Proposition 4.2 and Proposition 4.5. In the rest of this thesis, for convenience, we use the notation S for the fundamental function (VMR functions will be called fundamental functions as well).*

4.2. Construction of Hilbert transform pairs of MRA tight frames

In this section we present an important result of this thesis which asserts that the Hilbert transform of a given MRA tight frame of $L^2(\mathbb{R})$ is an MRA tight frame of $L^2(\mathbb{R})$ as well. For the proof we employ the approach introduced in [**30, 26**]. Namely, we suppose that an MRA tight frame of $L^2(\mathbb{R})$ is given which is generated by r generators ψ_j. They satisfy the two characterizations (see Remark 4.3). Let s be the associated fundamental function. Now we show how to multiply a certain function to the two-scale symbols of the given MRA tight frame, in order that the new two-scale symbols define the generators $\{\mathcal{H}\psi_j, j=1,\ldots,r\}$ of an MRA tight frame of $L^2(\mathbb{R})$ with a new refinable function Φ. The new refinable function Φ does not have compact support, in general, although the given refinable function has compact support. This is the reason why we use Proposition 4.5 for the proof.

Theorem 4.8. *Let $\{\psi_j, j=1,\ldots,r\}$ be the generators of an MRA tight frame of $L^2(\mathbb{R})$ defined by the two-scale symbols $q_j, j=1,\ldots,r$. Furthermore, suppose that the associated refinable function ϕ and its corresponding two-scale symbol p satisfy the assumptions of Proposition 4.5. In addition, let s be the associated fundamental*

function defined in (4.9). If we define new symbols

$$P(\xi) := e^{-i\theta(\xi)}p(\xi), \quad Q_j(\xi) := e^{i\theta(\xi-\pi)}q_j(\xi), \quad j = 1, \cdots, r, \tag{4.14}$$

where θ is 2π-periodic and $\theta(\xi) = \xi/2$ on $[-\pi, \pi)$, the refinable function Φ with $\hat{\Phi}(\xi) = \prod_{j=1}^{\infty} P(2^{-j}\xi)$ is in $L^2(\mathbb{R})$, and $\{\Psi_j, j = 1, \cdots, r\}$ with $\hat{\Psi}_j(\xi) = Q_j(\xi/2)\hat{\Phi}(\xi/2)$ are the generators of an MRA tight frame of $L^2(\mathbb{R})$ and $\Psi_j = \mathcal{H}\psi_j, j = 1, \cdots, r$.

Proof.

As we mentioned above, we employ Proposition 4.5 for the proof. Firstly, it is clear that $P, Q_j, j = 1, \cdots, r$, are measurable, since $p, q_j, j = 1, \cdots, r$, are measurable and the function $e^{-i\theta(\xi)}$ is piecewise continuous with has jumps at $\pi(2k+1), k \in \mathbb{Z}$ (see [**26**]). In addition, $P, Q_j, j = 1, \cdots, r$, are bounded, since $|P| = |p|,\ |Q_j| = |q_j|,\ j = 1, \ldots, r$. Note that the combined mask $(P, Q_1, \ldots, Q_r)$ gives the same fundamental function s as the combined mask $(p, q_1, \ldots, q_r)$. Hence, (b1) holds trivially. Secondly, from the two-scale relation of the refinable function we have

$$\begin{aligned} \hat{\Phi}(\xi) &= \prod_{k=1}^{\infty} P(2^{-k}\xi) = \prod_{k=1}^{\infty} p(2^{-k}\xi) \prod_{\ell=1}^{\infty} e^{-i\theta(2^{-\ell}\xi)} \\ &= \hat{\phi}(\xi) e^{-i\sum_{\ell=1}^{\infty}\theta(2^{-\ell}\xi)}, \quad a.e.\ \xi \in \mathbb{R}. \end{aligned} \tag{4.15}$$

The pointwise convergence of $-\sum_{\ell=1}^{\infty}\theta(2^{-\ell}\xi)$ is shown in [**26**] and can be demonstrated as in Figure 4.2. Furthermore, Φ is in $L^2(\mathbb{R})$ due to $|\hat{\Phi}| = |\hat{\phi}|$ and $\hat{\Phi}$ is continuous at the origin since the functions $\hat{\phi}$ and $e^{-i\sum_{\ell=1}^{\infty}\theta(2^{-\ell}\cdot)}$ are continuous at zero as well, and clearly has value 1 at zero (see Figure 4.1).

As the next step, we show that the fundamental function s satisfies (b2) with the two-scale symbols $P, Q_1, \ldots, Q_r$. From the definitions of P and $Q_j, j = 1, \ldots, r$, we have

$$\begin{aligned} & s(2\xi)P(\xi)\overline{P(\xi+\pi)} + \sum_{j=1}^{r} Q_j(\xi)\overline{Q_j(\xi+\pi)} \\ = \ & s(2\xi)p(\xi)\overline{p(\xi+\pi)}e^{-i\theta(\xi)}e^{i\theta(\xi-\pi)} + \sum_{j=1}^{r} q_j(\xi)\overline{q_j(\xi+\pi)}e^{i\theta(\xi-\pi)}e^{-i\theta(\xi)} \\ = \ & e^{i\theta(\xi-\pi)}e^{-i\theta(\xi)}\left(s(2\xi)p(\xi)\overline{p(\xi+\pi)} + \sum_{j=1}^{r} q_j(\xi)\overline{q_j(\xi+\pi)}\right) = 0, \quad a.e.\ \xi \in \mathbb{R}. \end{aligned}$$

Taken together, we have shown that the fundamental function s and the new masks P and $Q_j, j = 1, \cdots, r$, define the generators $\Psi_j, j = 1, \cdots, r$, and the refinable function Φ of an MRA tight frame of $L^2(\mathbb{R})$.

Finally we want to show that $\Psi_j = \mathcal{H}\psi_j, j = 1, \cdots, r$. From the two-scale relation of generators we have for each $j \in \{1, \cdots, r\}$,

$$\begin{aligned} \hat{\Psi}_j(\xi) &= Q_j(\xi/2)\hat{\Phi}(\xi/2) \\ &= q_j(\xi/2)e^{i\theta(\xi/2-\pi)}\hat{\phi}(\xi/2)e^{-i\sum_{k=2}^{\infty}\theta(\xi/2^k)} \\ &= \hat{\psi}_j(\xi)e^{i[\theta(\xi/2-\pi)-\sum_{k=2}^{\infty}\theta(\xi/2^k)]}, \quad a.e.\ \xi \in \mathbb{R}. \end{aligned} \tag{4.16}$$

It is clear that $\Psi_j \in L^2(\mathbb{R})$ from $|\hat{\Psi}_j| = |\hat{\psi}_j|$ and the function

$$e^{i[\theta(\xi/2-\pi)-\sum_{k=2}^{N}\theta(\xi/2^k)]}$$

converges pointwise to $-i\text{sgn}(\xi)$ as $N \to \infty$ (see [**26**] and Figure 4.2). We have consequently

$$\Psi_j = \mathcal{H}\psi_j, \ j = 1, \cdots, r. \qquad \square$$

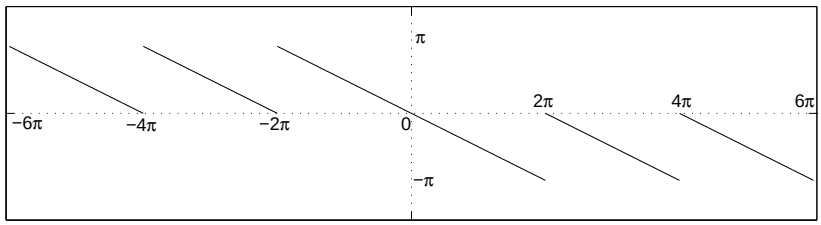

FIGURE 4.1. $-\sum_{k=1}^{\infty}\theta(\xi/2^k)$.

Remark 4.9. *1. The approximation order of the refinable function Φ is a matter of interest. It is known that $\phi \in L^2(\mathbb{R}^d)$ provides approximation order m if and only if the function*

$$\Lambda_\phi := \left(1 - \frac{|\hat{\phi}|^2}{[\hat{\phi}, \hat{\phi}]}\right)^{1/2} \tag{4.17}$$

*has a zero of order m at the origin ([**1**]). When, especially, ϕ has compact support and $\hat{\phi}(0) \neq 0$, the condition (4.17) is equivalent to the Strang-Fix (SF) condition,*

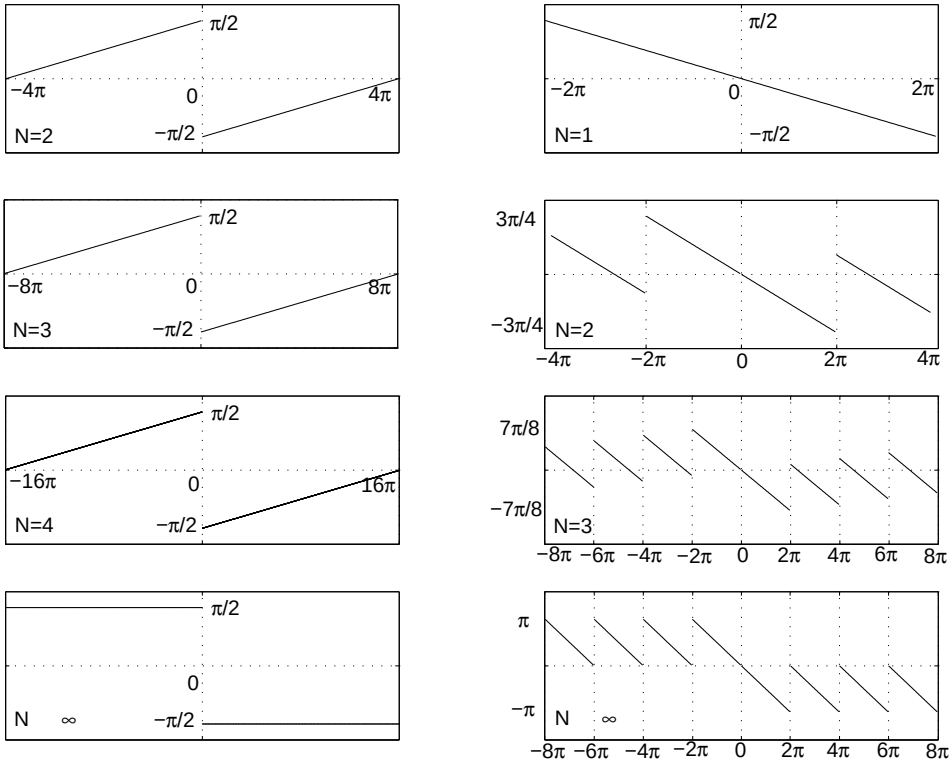

FIGURE 4.2. Left: $\theta(\xi/2 - \pi) - \sum_{k=2}^{N} \theta(\xi/2^k)$, *for* $N = 2, 3, 4$, *and* $N \to \infty$, Right: $-\sum_{k=1}^{N} \theta(\xi/2^k)$, *for* $N = 1, 2, 3$, *and* $N \to \infty$.

namely, $\hat{\phi}$ *has a zero of order* m *at each point in* $2\pi\mathbb{Z}^d \backslash \{0\}$. *When the given refinable function* ϕ *in Theorem 4.8 provides approximation order* m, *then* Φ *has the same approximation order, since*

$$\Lambda_\Phi = \left(1 - \frac{|\hat{\Phi}|^2}{[\hat{\Phi}, \hat{\Phi}]}\right)^{1/2} = \left(1 - \frac{|\hat{\phi}|^2}{[\hat{\phi}, \hat{\phi}]}\right)^{1/2} = \Lambda_\phi.$$

2. The generators $\Psi_j, j = 1, \cdots, r$, *and refinable function* Φ *do not have compact support, in general, even if the given generators* $\psi_j, j = 1, \cdots, r$, *and the refinable function* ϕ *do. In other words, from (2.4) we have*

$$\Psi_j = \mathcal{H}\psi_j = \frac{1}{\pi}\left(\frac{1}{x} * \psi_j\right), \quad j = 1, \cdots, r.$$

Hence, each Ψ_j *is the convolution with the globally supported function* $\frac{1}{\pi x}$. *The refinable function* Φ, *in the next place, is acquired by (4.15), in which the factor*

$e^{-i\sum_{k=1}^{\infty}\theta(\xi/2^k)}$ has jumps at $2\pi k, k \in \mathbb{Z}\setminus\{0\}$, see Figure 4.1. In other words, Φ is obtained by the convolution of ϕ and a globally supported function (this function will be exactly described in Proposition 4.10) obtained by the inverse Fourier transform of $e^{-i\sum_{k=1}^{\infty}\theta(\xi/2^k)}$ in the distributional sense. Hence, Φ has a global support in the time domain as well. However, if ϕ has compact support and $\hat{\phi}$ has a zero of order m at each point in $2\pi\mathbb{Z}\backslash\{0\}$ (SF-condition), then $\hat{\Phi} \in C^{m-1}$ around $2\pi\mathbb{Z}\backslash\{0\}$. Thus, $\hat{\Phi} \in C^{m-1}$ globally. Consequently, Φ decays at a certain rate in the time domain.
3. Now we consider the masks P and $Q_j, j = 1, \cdots, r$. It is clear from (4.14) that they have jumps, which implies that they are not trigonometric polynomials any more, even though p and $q_j, j = 1, \cdots, r$, may be trigonometric polynomials. But, Q_j has the same order of root at $\xi = 0$, which means that the generators $\Psi_j,\ j = 1, \cdots, r$, have the same order of vanishing moments as $\psi_j,\ j = 1, \cdots, r$.
4. The result of Theorem 4.8 reveals an interesting aspect of the equations (4.4) and (4.5). That is, when the given s, p, and $q_j, j = 1, \cdots, r$, satisfy the two equations then s, P, and $Q_j, j = 1, \cdots, r$, do as well. This can be rephrased from another point of view, i.e. when the fundamental function s is given, $p, q_j, j = 1, \cdots, r$, and $P, Q_j, j = 1, \cdots, r$, are different solutions of the two equations which generate a Hilbert transform pair of tight frames with the same order of vanishing moments.

Now we want to find out what is the meaning of (4.15) in the time domain. It is clear that Φ is the convolution of ϕ and a certain function or distribution as pointed out above.

Proposition 4.10. *The relation (4.15) is equivalent to*

$$\Phi(x) = \left(\phi * \frac{\cot(\pi\cdot)}{\pi(\cdot + 1/2)}\right)(x)$$

Proof.

The Fourier series of the 2π-periodic function $e^{-i\theta(\xi)}$ on $[-\pi, \pi]$ is

$$e^{-i\theta(\xi)} = \frac{1}{\pi}\sum_{k\in\mathbb{Z}} \frac{(-1)^k}{k + 1/2} e^{ik\xi},\ \xi \in [-\pi, \pi].$$

If we use $\hat{\delta}(\xi - k) = e^{ik\xi}$, in the distributional sense, then we have

$$e^{-i\theta(\xi)} = \left(\frac{1}{\pi}\sum_{k\in\mathbb{Z}} \frac{(-1)^k}{k + 1/2}\delta(x - k)\right)^{\wedge}(\xi).$$

Furthermore, the scaling and translation in frequency domain yields,

$$e^{-i\theta(\xi/2-\pi)} = \left(\frac{2}{\pi}\sum_{k\in\mathbb{Z}}\frac{(-1)^k}{k+1/2}e^{2\pi ix}\delta(2x-k)\right)^{\wedge}(\xi),\ a.e.\ \xi\in\mathbb{R}.$$

Now we recall

$$e^{i[\theta(\xi/2-\pi)-\sum_{\ell=2}^{\infty}\theta(2^{-\ell}\theta)]} = \left(\frac{1}{\pi x}\right)^{\wedge}(\xi),\ a.e.\ \xi\in\mathbb{R},$$

which implies

$$\begin{aligned} e^{-i\sum_{\ell=2}^{\infty}\theta(2^{-\ell}\xi)} &= \left(\frac{1}{\pi x}\right)^{\wedge}(\xi)e^{-i\theta(\xi/2-\pi)} \\ &= \left(\frac{2}{\pi^2 x} * \left[\sum_{k\in\mathbb{Z}}\frac{(-1)^k}{k+1/2}e^{2\pi ix}\delta(2x-k)\right]\right)^{\wedge}(\xi),\ a.e.\ \xi\in\mathbb{R}. \end{aligned}$$

The scaling $\xi\to 2\xi$, in the end, results in,

$$e^{-i\sum_{k=1}^{\infty}\theta(2^{-k}\xi)} = \left(\frac{1}{\pi^2 x} * \left[\sum_{k\in\mathbb{Z}}\frac{(-1)^k}{k+1/2}e^{\pi ix}\delta(x-k)\right]\right)^{\wedge}(\xi),\ a.e.\ \xi\in\mathbb{R}.$$

The convolution can be simplified as follows,

$$\begin{aligned} &\left(\frac{1}{\pi^2 x} * \left[\sum_{k\in\mathbb{Z}}\frac{(-1)^k}{k+1/2}e^{\pi ix}\delta(x-k)\right]\right)(y) \\ =\ &\int_{\mathbb{R}}\frac{1}{\pi^2 t}\sum_{k\in\mathbb{Z}}\frac{(-1)^k}{k+1/2}e^{\pi i(y-t)}\delta(y-t-k)dt \\ =\ &\frac{1}{\pi^2}\sum_{k\in\mathbb{Z}}\frac{1}{(y-k)(k+1/2)}. \end{aligned}$$

Now the sum $\sum_{k\in\mathbb{Z}}\frac{1}{(y-k)(k+1/2)}$ converges for all $y\in\mathbb{R}\backslash\mathbb{Z}$ and is equal to the partial fraction decomposition of $\frac{\pi\cot(\pi y)}{y+1/2}$, i.e.

$$\frac{1}{\pi^2}\sum_{k\in\mathbb{Z}}\frac{1}{(y-k)(k+1/2)} = \frac{\cot(\pi y)}{\pi(y+1/2)}.$$

The refinable function Φ can be obtained by convolution of ϕ and $\frac{\cot(\pi y)}{\pi(y+1/2)}$, whose sketch is given in Figure 4.3. It behaves much like $\frac{1}{\pi y}$ near 0, but has additional poles in $\mathbb{Z}$. $\square$

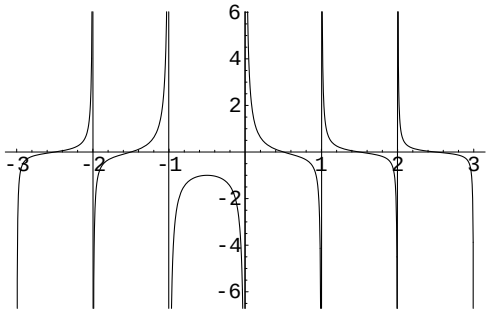

FIGURE 4.3. $\frac{\cot(\pi x)}{\pi(x+1/2)}$ on $[-3,3]$.

Remark 4.11. *The formulation* $\Phi = \phi * \frac{\cot(\pi\cdot)}{\pi(\cdot+1/2)}$ *presents us another aspect of the fact that* Φ *is a half-sample delayed version of* ϕ*, which was pointed out by Selesnick (*[**26, 27**]*).*

4.3. Another closed form of the Hilbert transform of MRA tight frames

The closed form of each $\mathcal{H}\psi_j, j = 1, \ldots, r$, and the associated refinable function Φ were given in (4.15)-(4.16). They were described by the function $e^{i\theta(\xi)}$, so were the associated symbols $P, Q_j, j = 1, \ldots, r$. Now we present simpler forms which are more suitable in the context of spline MRA tight frames. Recall that $\hat{N}_m(\xi) = \left(\frac{1-e^{-i\xi}}{i\xi}\right)^m$ is the Fourier transform of the cardinal B-spline of order m.

Theorem 4.12. *Let two-scale symbols be given by*

$$p(\xi) = \left(\frac{1+e^{i\xi}}{2}\right)^m p_0(\xi) = p_m(\xi)p_0(\xi), \quad m \geq 1, \tag{4.18}$$

$$q_j(\xi) = \left(\frac{1-e^{-i\xi}}{2}\right)^{m_j} q_0^j(\xi), \quad m_j \geq 1, \tag{4.19}$$

such that they are subjected to the assumptions of Proposition 4.5, i.e. they generate an MRA tight frame $\{\psi_{j,k,\ell},\ 1 \leq j \leq r, k, \ell \in \mathbb{Z}\}$ *and the refinable function* ϕ*. The refinable function is, as a result, described by* $\hat{\phi}(\xi) = \hat{N}_m(\xi)R(\xi)$, $R(\xi) := \prod_{k=1}^{\infty} p_0(2^{-k}\xi)$ *and the generators are* $\hat{\psi}_j(\xi) = q_j(\xi/2)\hat{\phi}(\xi/2)$*. Then the refinable function* Φ *in (4.15) and the generators* $\Psi_j = \mathcal{H}\psi_j, j = 1, \ldots, r$*, in (4.16) are given*

by

$$\hat{\Phi}(\xi) = M(\xi)\frac{1-e^{-i\xi}}{i\xi}\hat{\phi}(\xi) = M(\xi)R(\xi)\hat{N}_{m+1}(\xi), \tag{4.20}$$

$$M(\xi) := \left|\frac{\xi/2}{\sin\xi/2}\right| = \frac{|\xi|}{|1-e^{-i\xi}|},$$

$$\hat{\Psi}_j(\xi) = N(\xi/2)\frac{1-e^{-i\xi/2}}{i\xi/2}\hat{\psi}_j(\xi)$$

$$= \frac{N(\xi/2)}{M(\xi/2)}q_j(\xi/2)\hat{\Phi}(\xi/2) = N(\xi/2)q_j(\xi/2)R(\xi/2)\hat{N}_{m+1}(\xi/2), \tag{4.21}$$

$$N(\xi) := \frac{|\xi|}{1-e^{-i\xi}} = -ie^{i\xi/2}\frac{|\xi|/2}{\sin\xi/2}.$$

Thus the symbols P and $Q_j, j = 1, \ldots, r$, are equal to

$$P(\xi) = \frac{M(2\xi)}{M(\xi)}\frac{1+e^{-i\xi}}{2}p(\xi) = \frac{1+e^{-i\xi}}{|1+e^{-i\xi}|}p(\xi), \tag{4.22}$$

$$Q_j(\xi) = \frac{N(\xi)}{M(\xi)}q_j(\xi) = \frac{|1-e^{-i\xi}|}{1-e^{-i\xi}}q_j(\xi). \tag{4.23}$$

Proof.

We study the exponential function $e^{-i\sum_{k=1}^{\infty}\theta(2^{-k}\xi)}$ in (4.15) first. The exponent is neither periodic nor continuous, as we noted in Figure 4.1. But its phase can be described by

$$-\sum_{k=1}^{\infty}\theta(2^{-k}\xi) = g(\xi) + h(\xi), \tag{4.24}$$

where

$$g(\xi) := -\xi/2 \text{ on } [-2\pi, 2\pi] \text{ and } 4\pi - \text{periodic},$$

and h is piecewise constant as in Figure 4.4 (compare with Figure 4.2).

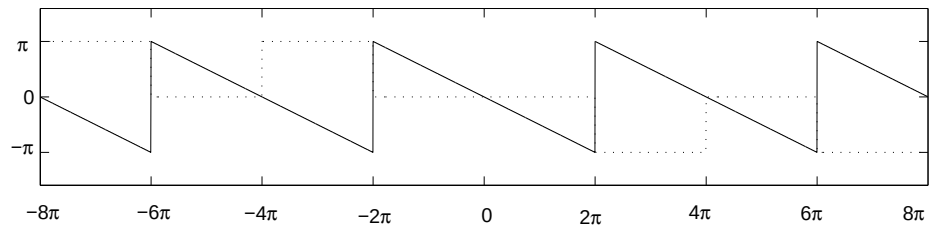

FIGURE 4.4. g (solid) and h (dotted).

Hence, (4.24) gives

$$e^{-i\sum_{k=1}^{\infty}\theta(2^{-k}\xi)} = e^{ig(\xi)}e^{ih(\xi)} = e^{-i\xi/2}A(\xi),\ A(\xi) := e^{ih(\xi)}. \tag{4.25}$$

Note that we have $e^{ig(\xi)} = e^{-i\xi/2}$ for $\xi \in \mathbb{R}$ by the periodicity of $e^{ig(\xi)}$. The function A is piecewise constant with range $\{-1, 1\}$ (see Figure 4.5). Now we show (4.20).

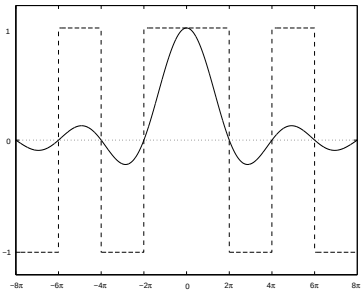

FIGURE 4.5. $\frac{\sin(\xi/2)}{\xi/2}$ (solid) and A (dashed).

If we insert (4.25) into (4.15), we have

$$\begin{aligned}
\hat{\Phi}(\xi) &= e^{-i\sum_{k=1}^{\infty}\theta(2^{-k}\xi)}\hat{\phi}(\xi) = e^{-i\xi/2}A(\xi)\hat{N}_m(\xi)R(\xi) \\
&= e^{-i\xi/2}A(\xi)\frac{i\xi}{1-e^{-i\xi}}\left(\frac{1-e^{-i\xi}}{i\xi}\right)^{m+1}R(\xi) \\
&= A(\xi)\frac{\xi/2}{\sin(\xi/2)}R(\xi)\hat{N}_{m+1}(\xi) \\
&= \left|\frac{\xi/2}{\sin(\xi/2)}\right|R(\xi)\hat{N}_{m+1}(\xi) = M(\xi)R(\xi)\hat{N}_{m+1}(\xi), \qquad (4.26)
\end{aligned}$$

where N_{m+1} is the B-spline of order $m+1$. Note that the identity

$$A(\xi)\frac{\xi/2}{\sin(\xi/2)} = \left|\frac{\xi/2}{\sin(\xi/2)}\right|$$

is due to the same behavior of signs of A and $\frac{\xi/2}{\sin(\xi/2)}$ (see Figure 4.5).
From (4.26) we show (4.22) next. The two-scale relation and (4.26) result in

$$\begin{aligned}
P(\xi) &= \frac{\hat{\Phi}(2\xi)}{\hat{\Phi}(\xi)} = \frac{M(2\xi)R(2\xi)\hat{N}_{m+1}(2\xi)}{M(\xi)R(\xi)\hat{N}_{m+1}(\xi)} = \frac{M(2\xi)}{M(\xi)}\frac{1+e^{-i\xi}}{2}p(\xi) \\
&= \frac{2}{|1+e^{-i\xi}|}p_{m+1}(\xi)p_0(\xi) = \frac{1+e^{-i\xi}}{|1+e^{-i\xi}|}p(\xi). \qquad (4.27)
\end{aligned}$$

Finally, note that

$$\hat{\Psi}_j(\xi) = -i\mathrm{sgn}(\xi)\hat{\psi}_j(\xi) = N(\xi/2)\frac{1-e^{-i\xi/2}}{i\xi/2}\hat{\psi}_j(\xi),$$

where $N(\xi) = \frac{|\xi|}{1-e^{-i\xi}}$. From the two-scale relation of ψ_j and (4.20) we have

$$\begin{aligned}\hat{\Psi}_j(\xi) &= N(\xi/2)\frac{1-e^{-i\xi/2}}{i\xi/2}q_j(\xi/2)\hat{\phi}(\xi/2)\\ &= N(\xi/2)\frac{1-e^{-i\xi/2}}{i\xi/2}q_j(\xi/2)\frac{1}{M(\xi/2)}\frac{i\xi/2}{1-e^{-i\xi/2}}\hat{\Phi}(\xi/2)\\ &= \frac{N(\xi/2)}{M(\xi/2)}q_j(\xi/2)\hat{\Phi}(\xi/2).\end{aligned}$$

Thus, we have $Q_j(\xi) = \frac{N(\xi)}{M(\xi)}q_j(\xi)$. If we insert (4.26) into the last formula, we have

$$\hat{\Psi}_j(\xi) = N(\xi/2)q_j(\xi/2)R(\xi/2)\hat{N}_{m+1}(\xi/2). \qquad \square$$

Remark 4.13. *1. Comparing (4.14) with (4.22)-(4.23) results in*

$$e^{-i\theta(\xi)} = \frac{1+e^{-i\xi}}{|1+e^{-i\xi}|} = \frac{M(2\xi)}{M(\xi)}\frac{1+e^{-i\xi}}{2}, \tag{4.28}$$

$$e^{i\theta(\xi-\pi)} = \frac{1-e^{i\xi}}{|1-e^{i\xi}|} = \frac{|1-e^{-i\xi}|}{1-e^{-i\xi}} = \frac{N(\xi)}{M(\xi)}. \tag{4.29}$$

2. Note that the identity (4.28) is also contained in Zhao's work ([**30**, p.356]*). Namely,*

$$e^{-i\theta(\xi)} = e^{-i\xi/2}\mathrm{sgn}(\cos(\xi/2)), \quad e^{i\theta(\xi-\pi)} = e^{i(\xi-\pi)/2}\mathrm{sgn}(\sin(\xi/2)).$$

3. Now we look at the Strang-Fix condition from the point of view of Theorem 4.12. M has simple poles at $2\pi\mathbb{Z}\setminus\{0\}$. But, the term $R(\xi)\hat{N}_{m+1}(\xi)$ has one more zero at $2\pi\mathbb{Z}\setminus\{0\}$ than $\hat{\phi}(\xi) = R(\xi)\hat{N}_m(\xi)$. Taken together, $\hat{\Phi}$ has the same number of zeros at $2\pi\mathbb{Z}\setminus\{0\}$ as $\hat{\phi}$ does. On this account, the Strang-Fix condition holds for Φ and ϕ with the same order of zeros at $2\pi\mathbb{Z}\setminus\{0\}$.

4. We have $M = |N|$. Namely, the refinable function $\hat{\Phi}$ is described by the amplitude factor M multiplied by $R(\xi)\hat{N}_{m+1}(\xi)$. Note, however, that the function $R(\xi)\hat{N}_{m+1}(\xi)$ (or $\phi * N_1$ in the time domain) generates a different MRA, since M is not a trigonometric polynomial, i.e. $\Phi \notin \overline{span\{\phi * N_1(\cdot - k), k \in \mathbb{Z}\}}$.

5. For the MRA tight frames $\{\psi^{m,L}_{j,k,\ell}, 1 \le j \le r, k, \ell \in \mathbb{Z}\}$ which appeared in section 3.3 and the appendix, the formulations of their Hilbert transforms become much

simpler. Recall that the refinable function is $\phi = N_m$, i.e. $R \equiv 1$ a.e., and the associated two-scale symbol is p_m, i.e. $p_0 \equiv 1$ a.e..

4.4. General method generating an MRA tight frame from a given one

We have, hitherto, examined how one can obtain an MRA tight frame of $L^2(\mathbb{R})$ that is the Hilbert transform of a given MRA tight frame of $L^2(\mathbb{R})$. Furthermore, we showed in Theorem 4.8 that these pairs of MRA tight frames have a common fundamental function. Now, we want to generalize this result to the generation of a pair of MRA tight frames of $L^2(\mathbb{R})$ that has the same fundamental function.

Theorem 4.14. *Let two-scale symbols $p, q_j, j = 1, \cdots, r$, and a fundamental function s satisfy the characterization of Proposition 4.5 which provides the generators $\{\psi_j, j = 1, \cdots, r\}$ of an MRA tight frame of $L^2(\mathbb{R})$. Now, suppose that*

$$P(\xi) = \alpha(\xi)p(\xi),\ Q_j(\xi) = \beta_j(\xi)q_j(\xi), \quad j = 1, \cdots, r,$$

where α and $\beta_j,\ j = 1, \ldots, r$, are subjected to the following conditions:

(i) *$\alpha,\ \beta_j$, are 2π-periodic and measurable.*

(ii) *α is continuous at 0, $\alpha(0) = 1$, and $\gamma(\xi) := \prod_{k=1}^{\infty} \alpha(2^{-k}\xi)$ exist a.e. $\xi \in \mathbb{R}$ with $\lim_{\xi \to 0} \gamma(\xi) = 1$.*

(iii) *$|\alpha(\xi)| = |\beta_j(\xi)| = 1$, a.e. $\xi \in \mathbb{R}$.*

(iv) *$\alpha(\xi)\overline{\alpha(\xi + \pi)} = \beta_j(\xi)\overline{\beta_j(\xi + \pi)}$, for $1 \le j \le r$.*

Then $\{\Psi_j, j = 1, \ldots, r\}$ are the generators of an MRA tight frame of $L^2(\mathbb{R})$ with the refinable function Φ, where $\Psi_j = T\psi_j$, $(T\psi_j)\hat{}(\xi) = \beta_j(\xi/2)\gamma(\xi/2)\hat{\psi}_j(\xi)$ and $\hat{\Phi}(\xi) = \gamma(\xi)\hat{\phi}(\xi)$. Furhtermore, $\Psi_j, j = 1, \ldots, r$, and Φ are generated by the two-scale symbols $P,\ Q_j, j = 1, \cdots, r$, and have the same fundamental function s.

Proof.

The proof is similar to that of Theorem 4.8, i.e. we employ Proposition 4.5 for the proof. First, we check the assumptions on the two-scale symbols $P,\ Q_j, j = 1, \ldots, r$, and refinable function. P and Q_j are bounded and measurable, by the assumptions on p, q_j, α, and β_j. The refinable function Φ is defined by the infinite product

$$\hat{\Phi}(\xi) = \prod_{j=1}^{\infty} P(2^{-j}\xi) = \prod_{k=1}^{\infty} \alpha(2^{-k}\xi) \prod_{j=1}^{\infty} p(2^{-j}\xi) = \gamma(\xi)\hat{\phi}(\xi),$$

where $\gamma(\xi) := \prod_{k=1}^{\infty} \alpha(2^{-k}\xi)$ is well-defined by (ii). The generator Ψ_j is obtained by

$$\begin{aligned}\hat{\Psi}_j(\xi) &= Q_j(\xi/2)\hat{\Phi}(\xi/2) = \beta_j(\xi/2)\gamma(\xi/2)q_j(\xi/2)\hat{\phi}(\xi/2) \\ &= \beta_j(\xi/2)\gamma(\xi/2)\hat{\psi}_j(\xi).\end{aligned}$$

Furthermore, we have $|\hat{\Phi}| = |\hat{\phi}|$ and $|\hat{\Psi}| = |\hat{\psi}|$ from (iii) and, thus, $\Phi, \Psi_j \in L^2(\mathbb{R})$. Note that from $|\hat{\Phi}| = |\hat{\phi}|$ the associated spectrums $\sigma(V_0)$ and $\sigma(v_0)$ are identical. On the other hand, the condition $\lim_{\xi\to 0} \hat{\Phi}(\xi) = 1$ follows from (ii).

It remains to show that (b1) and (b2) of Proposition 4.5 hold. We have $|P| = |p|$ and $|Q_j| = |q_j|$ from (iii), which implies the same fundamental function $S = s$. Thus, condition (b1) holds trivially. Condition (b2) is satisfied by (iv)

$$\begin{aligned}& s(2\xi)P(\xi)\overline{P(\xi+\pi)} + \sum_{j=1}^{r} Q_j(\xi)\overline{Q_j(\xi+\pi)} \\ =\ & s(2\xi)p(\xi)\overline{p(\xi+\pi)}\alpha(\xi)\overline{\alpha(\xi+\pi)} + \sum_{j=1}^{r} q_j(\xi)\overline{q_j(\xi+\pi)}\beta_j(\xi)\overline{\beta_j(\xi+\pi)} \\ =\ & \alpha(\xi)\overline{\alpha(\xi+\pi)}\left(s(2\xi)p(\xi)\overline{p(\xi+\pi)} + \sum_{j=1}^{r} q_j(\xi)\overline{q_j(\xi+\pi)}\right) = 0, \quad \text{for a.e } \xi \in \mathbb{R}.\end{aligned}$$

By Proposition 4.5, $\{\Psi_j, j = 1, \cdots, r\}$ generates an MRA tight frame of $L^2(\mathbb{R})$. □

Remark 4.15. *It is easy to check that the form of P and Q_j in Theorem 4.8 is a special case of Theorem 4.14. We set*

$$\alpha(\xi) = \frac{1+e^{-i\xi}}{|1+e^{-i\xi}|},\ \beta_j(\xi) = \frac{1-e^{i\xi}}{|1-e^{i\xi}|}, \quad j = 1, \ldots, r.$$

Then (i) α and β_j are 2π-periodic and measurable, (ii) α is continuous at 0 and $\alpha(0) = 1$. Furthermore, the infinite product converges pointwise,

$$\prod_{k=1}^{\infty} \alpha(2^{-k}\xi) = \prod_{k=1}^{\infty} \frac{1+e^{-i2^{-k}\xi}}{|1+e^{-i2^{-k}\xi}|} = e^{-i\xi/2}\frac{\cos\xi/2}{|\cos\xi/2|}(-i\mathrm{sgn}(\xi/2)),$$

where $\frac{\cos\xi/2}{|\cos\xi/2|}$ is an alternative form of the function A in (4.25), i.e. $A(\xi) = \frac{\cos\xi/2}{|\cos\xi/2|}$. Finally, (iii) holds trivially and (iv) does as well by

$$\alpha(\xi)\overline{\alpha(\xi+\pi)} = \frac{1+e^{-i\xi}}{|1+e^{-i\xi}|}\frac{1-e^{i\xi}}{|1-e^{i\xi}|} = \beta_j(\xi)\overline{\beta_j(\xi+\pi)}, \quad j = 1, \ldots, r.$$

CHAPTER 5

Approximate Hilbert transforms of MRA tight frames: general case

We already pointed out the drawbacks of the conventional approaches ([**15, 16, 18, 26, 27, 28**]) for the construction of (approximate) Hilbert transform pairs, i.e. the absence of the analytical form of the refinable function Φ and the symmetry of the associated wavelets (or frame generators). In order to overcome these shortcomings, we propose a new method getting approximate Hilbert transform pairs of MRA tight frames. Unlike the conventional approaches, we begin with an MRA tight frame $\{\psi_{j,k,\ell}, 1 \le j \le r, k, \ell \in \mathbb{Z}\}$ of $L^2(\mathbb{R})$ and then find its approximate Hilbert transform $\{\tilde{\Psi}_{j,k,\ell}, 1 \le j \le r, k, \ell \in \mathbb{Z}\}$ such that $\tilde{\Psi}_j \approx \mathcal{H}\psi_j$. For the design of the approximations we recall Theorem 4.12 and suggest the approximations of the functions M, N in (4.20)-(4.21). These approximations lead to the desired approximate Hilbert transform. At the end of this chapter, some examples will be given for spline MRA tight frames of $L^2(\mathbb{R})$ whose generators are given in section 3.3.

5.1. Approximate MRA tight frames

We suppose that the refinable function ϕ, the associated symbols p, q_j, and the fundamental function s of the given MRA tight frame satisfy the characterization of Proposition 4.5. In addition, we suppose that p and q_j are subjected to (4.18)-(4.19). Now we take a close look at Theorem 4.12. Note that $\Psi_j = \mathcal{H}\psi_j$ has the following properties:

- Ψ_j is the exact Hilbert transform of ψ_j.
- $\Psi_j,\ j = 1, \ldots, r$, constitute a tight frame,
- the two-scale symbols P and Q_j are not trigonometric polynomials nor rational functions.

These properties will only be recovered approximately by our construction, i.e. our approximation procedure of Ψ_j will result in $\tilde{\Psi}_j$ such that

- $\tilde{\Psi}_j$ is an approximate Hilbert transform of ψ_j,
- $\tilde{\Psi}_j, j = 1, \dots, r$, generate an approximate tight frame,
- two-scale symbols, say $\tilde{P}, \tilde{Q}_j$, are trigonometric polynomials.

It is clear that $\{\tilde{\Psi}_j,\ j = 1, \dots, r\}$ might well not satisfy the characterization of Proposition 4.5, since we substitute simple (trigonometric polynomial) symbols for the complicated symbols in (4.22)-(4.23). Thus, in all cases which we consider Proposition 4.5 does not hold exactly. Moreover, although the associated fundamental function of the approximations $\tilde{\Psi}_j, j = 1, \dots, r$, and $\tilde{\Phi}$ is essentially bounded, it does not satisfy (b1) of Proposition 4.5. On this account we introduce the notion of *approximate MRA tight frames.*

Definition 5.1. *If an extended mask vector $\tau := (\tilde{P}, \tilde{Q}_1, \dots, \tilde{Q}_r)$ and the associated fundamental function $\tilde{S}$ satisfy Assumption 4.4 as well as*

(i)
$$\overline{\lim_{j \to -\infty}} \left| \tilde{S}(2^j \xi) - 1 \right| \le \delta_1,$$
for some $0 \le \delta_1 \ll 1$ and a.e. $\xi \in \mathbb{R}$,

(ii)
$$\left| \tilde{S}(2\xi) \tilde{P}(\xi) \overline{\tilde{P}(\xi + \pi)} + \sum_{j=1}^{r} \tilde{Q}_j(\xi) \overline{\tilde{Q}_j(\xi + \pi)} \right| \le \delta_2$$
for some $0 \le \delta_2 \ll 1$ and a.e. $\xi \in \mathbb{R}$,

then we call the system $\{\tilde{\Psi}_{j,k,\ell}, 1 \le j \le r, k, \ell \in \mathbb{Z}\}$ generated by the mask vector τ an approximate MRA tight frame.

Depending on the features of the given MRA tight frame we can add some more properties that $\tilde{\Psi}_j$ should have. For example, $\tilde{\Psi}_j$ are required to have almost the same regularity in the sense of (d) of Proposition 2.2. Furthermore, from the basic property (v) of the Hilbert transform, $\tilde{\Psi}_j$ should be symmetric (resp. antisymmetric) if ψ_j is antisymmetric (resp. symmetric). $\tilde{\Psi}_j$ is obliged to keep the order of vanishing moments of ψ_j in effect. Taken together, we impose the following constraints on $\tilde{\Psi}_j,\ j = 1, \dots, r$, and $\tilde{\Phi}$.

Constraint A

(i) $\tilde{\Psi}_j$ and $\tilde{\Phi}$ are real and finite linear combinations of a compactly supported function. Namely, the associated two-scale symbols are trigonometric polynomials with real coefficients and $\tilde{\Psi}_j$ and $\tilde{\Phi}$ have compact supports.

(ii) $\tilde{\Psi}_j$ has almost the same regularity as ψ_j does.

(iii) $\tilde{\Psi}_j$ has the same order of vanishing moments as ψ_j.

(iv) $\tilde{\Psi}_j$ is nearly symmetric (resp. antisymmetric) if ψ_j is antisymmetric (resp. symmetric).

(v) $\widehat{\tilde{\Psi}}_j(\xi) + i\hat{\psi}_j(\xi)$ is approximately zero for all $\xi < 0$ and all $1 \le j \le r$.

(vi) $\{\tilde{\Psi}_{j,k,\ell}\}$ is an approximate tight frame in the sense of Definition 5.1.

For the construction of the approximations, we propose the representations

$$\widehat{\tilde{\Phi}}(\xi) := \tilde{M}(\xi)R(\xi)\hat{N}_{m+1}(\xi), \tag{5.1}$$

$$\widehat{\tilde{\Psi}}_j(\xi) := \frac{\tilde{N}(\xi/2)}{\tilde{M}(\xi/2)} q_j(\xi/2)\widehat{\tilde{\Phi}}(\xi/2) \tag{5.2}$$

$$= \tilde{N}(\xi/2)q_j(\xi/2)R(\xi/2)\hat{N}_{m+1}(\xi/2), \tag{5.3}$$

where $\tilde{M}$ and $\tilde{N}$ were substituted for the original M and N from the closed forms of Theorem 4.12. The two-scale symbols are

$$\tilde{P}(\xi) := \frac{\widehat{\tilde{\Phi}}(2\xi)}{\widehat{\tilde{\Phi}}(\xi)} = \frac{\tilde{M}(2\xi)}{\tilde{M}(\xi)} p_{m+1}(\xi)p_0(\xi), \tag{5.4}$$

$$\tilde{Q}_j(\xi) := \frac{\tilde{N}(\xi)}{\tilde{M}(\xi)} q_j(\xi). \tag{5.5}$$

The associated fundamental function $\tilde{S}$ is, by (4.9),

$$\tilde{S}(\xi) = \sum_{k=0}^{\infty}\sum_{j=1}^{r} |\tilde{Q}_j(2^k\xi)|^2 \prod_{m=0}^{k-1} |\tilde{P}(2^m\xi)|^2. \tag{5.6}$$

In the light of Constraint A and the suggested formulations (5.1)-(5.5), we impose the following constraints on $\tilde{M}$ and $\tilde{N}$.

Constraint B

(i) $\tilde{M}$ and $\tilde{N}$ are trigonometric polynomials.

(ii) $\frac{\tilde{N}(\xi)}{\tilde{M}(\xi)} \approx \frac{N(\xi)}{M(\xi)} = \frac{|1-e^{-i\xi}|}{1-e^{-i\xi}}$.

(iii) $\tilde{M}$ is real, symmetric, and $\tilde{M}(\xi) \approx M(\xi) = \frac{|\xi/2|}{|\sin \xi/2|} = \frac{|\xi|}{|1-e^{-i\xi}|}$.

(iv) $\tilde{N}(\xi) \approx N(\xi) = \frac{|\xi|}{1-e^{-i\xi}}$.

(v) $\tilde{M}(\xi) = |\tilde{N}(\xi)| \in [1-\varepsilon, \pi/2+\varepsilon]$ for some $0 < \varepsilon \ll 1$ and $\forall\ \xi \in [-\pi, \pi]$ and $\tilde{M}(0) = |\tilde{N}(0)| = 1$.

Remark 5.2. *1. Constraint B(i) will guarantee that the functions $\tilde{\Phi}$ and $\tilde{\Psi}_j$ are finite linear combinations of $\phi * N_1$ due to $R(\xi)\hat{N}_{m+1}(\xi) = \hat{\phi}(\xi)\hat{N}_1(\xi)$. If ϕ has compact support, e.g. $\phi = N_m$, then Constraint B(i) implies Constraint A(i). Constraints B(ii)-(iv) are natural requirements in comparison with the exact Hilbert transform in Theorem 4.12. In particular, constraint B(ii) is most important for the design of a Hilbert transform pair of the given MRA tight frame, since a good approximation would result in $\tilde{\Psi}_j$ satisfying Constraint A(v). Constraint B(iii) and Constraint B(v) are natural in the sense that the original M is real, symmetric, and satisfies $M(\xi) \in [1, \pi/2]$ for $\xi \in [-\pi, \pi]$ and $M(\xi) = |N(\xi)|$. Furthermore, the last constraint is related to the condition $\lim_{\xi\to 0} \hat{\tilde{\Phi}}(\xi) = 1$.*

2. Note that the constructions of $\tilde{M}$ and $\tilde{N}$ do not depend on the given MRA tight frames, i.e. they are universal for the approximation.

3. We take a closer look at the symbols $\tilde{P}$ and $\tilde{Q}_j, j = 1, \ldots, r$, in (5.4)-(5.5). In general, they are not trigonometric polynomials but rational trigonometric functions. On that account we consider another refinable function in order to get FIR filters. A good clue for an alternative refinable function is based on the fact that both $\tilde{\Phi}$ and $\tilde{\Psi}_j, j = 1, \ldots, r$, are linear combinations of the function $\phi * N_1$.

Based on the last observation, we show in the next theorem that $\{\tilde{\Psi}_{j,k,\ell}, 1 \le j \le r, k, \ell \in \mathbb{Z}\}$ is an approximate MRA tight frame with the refinable function $\tilde{\Phi}$ if and only if $\{\tilde{\Psi}_{j,k,\ell}, 1 \le j \le r, k, \ell \in \mathbb{Z}\}$ is an approximate MRA tight frame with the refinable function $\phi * N_1$. Note that the associated two-scale symbols of the latter are trigonometric polynomials. The fact that the MRA itself does not determine the associated scaling function and its mask uniquely, was already pointed out by Daubechies et al. ([**13**, p.4]).

If we have another refinable function, the associated fundamental function changes as well, since the fundamental function depends on the symbols. We show that

the new fundamental function is just $\tilde{S}\tilde{M}^2$. We suppose that Constraint B holds a priori. We will obtain such an $\tilde{M}$ and $\tilde{N}$ in the next section.

Theorem 5.3. *The family* $\{\tilde{\Psi}_{j,k,\ell}, 1 \le j \le r, k, \ell \in \mathbb{Z}\}$ *in (5.2) is an approximate MRA tight frame with respect to the refinable function* $\tilde{\Phi}$ *in (5.1) if and only if it is an approximate MRA tight frame with respect to the refinable function* $\phi * N_1$.

Proof.

Let $\tau_1 := (\tilde{P}, \tilde{Q}_1, \ldots, \tilde{Q}_r)$ and $\tau_2 := (\tilde{p}, \tilde{q}_1, \ldots, \tilde{q}_r)$ be the mask vectors with respect to the refinable functions $\tilde{\Phi}$ and $\phi * N_1$, respectively. Furthermore, we let $\tilde{S}_{\tau_1}$ and $\tilde{S}_{\tau_2}$ denote the respective associated fundamental functions. Note that $\tilde{Q}_j, j = 1, \ldots, r$, $\tilde{P}$ are given in (5.4)-(5.5), and $\tilde{S}_{\tau_1}$ corresponds to $\tilde{S}$ in (5.6). On the other hand, $\tilde{q}_j, j = 1, \ldots, r$, are from (5.3)

$$\tilde{q}_j(\xi) = \tilde{N}(\xi) q_j(\xi),\ j = 1, \ldots, r,$$

and $\tilde{p}(\xi) = p_{m+1}(\xi) p_0(\xi)$ is from $\hat{\phi}(\xi)\hat{N}_1(\xi) = R(\xi)\hat{N}_{m+1}(\xi)$, where $p_{m+1}(\xi) = \left(\frac{1+e^{-i\xi}}{2}\right)^{m+1}$.

We start with the verification of Assumption 4.4. Firstly, the mask vectors τ_2 are measurable and essentially bounded, since p_{m+1}, p_0, q_j, and $\tilde{N}$ are. The symbol $\tilde{P}$ in τ_1 is measurable and essentially bounded by (5.4) and (v) of Constraint B,

$$|\tilde{P}(\xi)| \le |p_{m+1}(\xi)||p_0(\xi)| \frac{\pi/2 + \varepsilon}{1 - \varepsilon} < \infty,\ \xi \in [-\pi, \pi],$$

so are the symbols $\tilde{Q}_j,\ j = 1, \ldots, r$, by the same reason

$$|\tilde{Q}_j(\xi)| \le \frac{\pi/2 + \varepsilon}{1 - \varepsilon} |q_j(\xi)| < \infty,\ j = 1, \ldots, r,\ \xi \in [-\pi, \pi].$$

The refinable function $\phi * N_1$ clearly satisfies (b) of Assumption 4.4 since $\hat{\phi}(\xi)\hat{N}_1(\xi)$ is continuous at the origin and $\hat{\phi}(0)\hat{N}_1(0) = 1$. By $[\hat{\phi}\hat{N}_1, \hat{\phi}\hat{N}_1](\xi) \le [\hat{\phi}, \hat{\phi}](\xi)[\hat{N}_1, \hat{N}_1](\xi)$, we have the condition (c) of Assumption 4.4 as well. For the refinable function $\tilde{\Phi}$ we have the condition (b)

$$\lim_{\xi \to 0} \tilde{\Phi}(\xi) = \lim_{\xi \to 0} \hat{N}_{m+1}(\xi)\tilde{M}(\xi) = 1,$$

by Constraint B(i) and Constraint B(v) on $\tilde{M}$. Furthermore, we have by $R\hat{N}_{m+1} = \hat{\phi}\hat{N}_1$

$$[\tilde{\Phi}, \tilde{\Phi}] = \tilde{M}^2 [R\hat{N}_{m+1}, R\hat{N}_{m+1}] \le \tilde{M}^2 [\hat{\phi}, \hat{\phi}][\hat{N}_1, \hat{N}_1],$$

thus, $[\tilde{\Phi}, \tilde{\Phi}]$ is essentially bounded.

Now, we show that the fundamental function $\tilde{S}_{\tau_2}$ is $\tilde{M}^2\tilde{S}_{\tau_1}$. It follows from the definition that

$$\tilde{S}_{\tau_2}(\xi) = \sum_{k=0}^{\infty}\sum_{j=1}^{r} |\tilde{q}_j(2^k\xi)|^2 \prod_{\ell=0}^{k-1} |\tilde{p}(2^\ell\xi)|^2. \tag{5.7}$$

The relations (5.4)-(5.5) lead to

$$\begin{aligned}\tilde{S}_{\tau_2}(\xi) &= \sum_{k=0}^{\infty}\sum_{j=1}^{r} |\tilde{M}(2^k\xi)\tilde{Q}_j(2^k\xi)|^2 \prod_{\ell=0}^{k-1} \left|\frac{\tilde{M}(2^\ell\xi)}{\tilde{M}(2^{\ell+1}\xi)}\tilde{P}(2^\ell\xi)\right|^2 \\ &= \sum_{k=0}^{\infty}\sum_{j=1}^{r} |\tilde{M}(2^k\xi)\tilde{Q}_j(2^k\xi)|^2 \left|\frac{\tilde{M}(\xi)}{\tilde{M}(2^k\xi)}\right|^2 \prod_{\ell=0}^{k-1} |\tilde{P}(2^\ell\xi)|^2.\end{aligned}$$

By the fact that $\tilde{M}$ is real, we deduce that

$$\tilde{S}_{\tau_2}(\xi) = \tilde{M}^2(\xi)\tilde{S}_{\tau_1}(\xi).$$

Now we check if $\tilde{S}_{\tau_1}$ and $\tilde{S}_{\tau_2}$ are well-defined, namely if they are essentially bounded. If we show that $\tilde{S}_{\tau_1}$ is bounded, then $\tilde{S}_{\tau_2}$ is bounded as well due to the boundedness of $\tilde{M}$. From the definition, we have

$$\tilde{S}_{\tau_1}(\xi) = \sum_{k=0}^{\infty}\sum_{j=1}^{r} |\tilde{Q}_j(2^k\xi)|^2 \prod_{\ell=0}^{k-1} |\tilde{P}(2^\ell\xi)|^2.$$

By (5.4)-(5.5)

$$\begin{aligned}\tilde{S}_{\tau_1}(\xi) &= \sum_{k=0}^{\infty}\sum_{j=1}^{r} \left|\frac{\tilde{N}(2^k\xi)}{\tilde{M}(2^k\xi)}\right|^2 |q_j(2^k\xi)|^2 \prod_{\ell=0}^{k-1} \left|\frac{\tilde{M}(2^{\ell+1}\xi)}{\tilde{M}(2^\ell\xi)}\right|^2 \prod_{\ell=0}^{k-1} |p_{m+1}(2^\ell\xi)|^2 |p_0(2^\ell\xi)|^2 \\ &= \sum_{k=0}^{\infty} \left|\frac{\tilde{N}(2^k\xi)}{\tilde{M}(\xi)}\right|^2 \sum_{j=1}^{r} |q_j(2^k\xi)|^2 \prod_{\ell=0}^{k-1} |p_{m+1}(2^\ell\xi)|^2 |p_0(2^\ell\xi)|^2. \qquad (5.8)\end{aligned}$$

It is obvious from (v) of Constraint B, that

$$\left|\frac{\tilde{N}(2^j\cdot)}{\tilde{M}(\cdot)}\right| \le \frac{\pi/2+\varepsilon}{1-\varepsilon} =: C$$

independently of j. Hence,

$$\tilde{S}_{\tau_1}(\xi) \le C^2 \sum_{k=0}^{\infty}\sum_{j=1}^{r} |q_j(2^k\xi)|^2 \prod_{\ell=0}^{k-1} |p_{m+1}(2^\ell\xi)|^2 |p_0(2^\ell\xi)|^2.$$

Now, if we use the simple inequality $|p_{m+1}(\xi)| = \left|\frac{1+e^{-i\xi}}{2}\right| |p_m(\xi)| \le |p_m(\xi)|$, we have

$$\tilde{S}_{\tau_1}(\xi) \le C^2 \sum_{k=0}^{\infty} \sum_{j=1}^{r} |q_j(2^k\xi)|^2 \prod_{\ell=0}^{k-1} |p(2^\ell\xi)|^2 = C^2 s(\xi),$$

where s is the fundamental function of the tight frame generated by the mask vector $\tau = (p, q_1, \ldots, q_r)$, which was assumed to be essentially bounded at the beginning of this section. Hence, the boundedness of $\tilde{S}_{\tau_1}$ follows from that of s. Finally we put $(\tau_1, \tilde{S}_{\tau_1})$ and $(\tau_2, \tilde{S}_{\tau_2})$ to the test of (i) and (ii) of Definition 5.1. Firstly, (i) holds for $\tilde{S}_{\tau_1}$ if and only if it holds for $\tilde{S}_{\tau_2}$ due to $\lim_{j\to-\infty} \tilde{M}^2(2^j\xi) = \tilde{M}^2(0) = 1$. Furthermore, for (ii) we observe

$$\begin{aligned} E_{\tau_1}(\xi) &:= \tilde{S}_{\tau_1}(2\xi)\tilde{P}(\xi)\overline{\tilde{P}(\xi+\pi)} + \sum_{j=1}^{r} \tilde{Q}_j(\xi)\overline{\tilde{Q}_j(\xi+\pi)} \\ &= \tilde{S}_{\tau_1}(2\xi)\frac{\tilde{M}(2\xi)\overline{\tilde{M}(2\xi+2\pi)}}{\tilde{M}(\xi)\overline{\tilde{M}(\xi+\pi)}} p_{m+1}(\xi)\overline{p_{m+1}(\xi+\pi)}p_0(\xi)\overline{p_0(\xi+\pi)} \\ &\quad + \sum_{j=1}^{r} \frac{\tilde{N}(\xi)\overline{\tilde{N}(\xi+\pi)}}{\tilde{M}(\xi)\overline{\tilde{M}(\xi+\pi)}} q_j(\xi)\overline{q_j(\xi+\pi)}, \end{aligned} \tag{5.9}$$

and owing to the fact that $\tilde{M}$ is 2π-periodic and real, we have further

$$\begin{aligned} E_{\tau_1}(\xi) &= \frac{1}{\tilde{M}(\xi)\overline{\tilde{M}(\xi+\pi)}}[\tilde{S}_{\tau_1}(2\xi)\tilde{M}^2(2\xi)\tilde{p}(\xi)\overline{\tilde{p}(\xi+\pi)} + \sum_{j=1}^{r} \tilde{q}_j(\xi)\overline{\tilde{q}_j(\xi+\pi)}] \\ &= \frac{1}{\tilde{M}(\xi)\overline{\tilde{M}(\xi+\pi)}} E_{\tau_2}(\xi). \end{aligned}$$

Hence, we have

$$E_{\tau_2}(\xi) = \tilde{M}(\xi)\overline{\tilde{M}(\xi+\pi)}E_{\tau_1}(\xi). \tag{5.10}$$

For this reason if one of E_{τ_1} and E_{τ_2} satisfies (ii) of Definition 5.1, then the other does equivalently by (v) of Constraint B. □

Remark 5.4. *Note that from the choice of* $(\tilde{p}, \tilde{q}_1, \ldots, \tilde{q}_r)$ *we have trigonometric two-scale symbols and the error bound in (5.10) does not increase much, since* $1 + \varepsilon_1 < \tilde{M}(\cdot)\tilde{M}(\cdot+\pi) < 1 + \varepsilon_2$ *on* $[-\pi, \pi]$*, where* $0 < \varepsilon_1 < \varepsilon_2 \ll 1$ *(e.g. see Figure 5.3).*

5.2. Design of $\tilde{M}$ and $\tilde{N}$ by use of Thiran Allpass Filters

Now we study the approximations in (5.1)-(5.2). We find them through the constructions of the trigonometric polynomials $\tilde{M}$ and $\tilde{N}$ satisfying Constraint B. In order to take the three approximations in (ii)-(iv) of Constraint B into account at the same time, it is sufficient to get two of the approximations. Among them, the approximation in (ii) is most important, as we pointed out before, and for the approximation we employ the approach that was adopted by Gopinath ([**15, 16**]) and Selesnick ([**27, 28**]). Their method is based on the so-called *Thiran allpass filters*. We recall some basic facts which are necessary for the design of the approximation in (ii) of constraint B.

The *Jth-order Thiran allpass filter* for delay $0 < \lambda < 1$ is given by

$$A_J(z) := \frac{z^{-J} D_J(z^{-1})}{D_J(z)},$$

where

$$D_J(z) := \sum_{k=0}^{J} d(k) z^{-k}, \tag{5.11}$$

with

$$d(k) := (-1)^k \begin{pmatrix} J \\ k \end{pmatrix} \frac{(\lambda - J)_k}{(\lambda + 1)_k}, \ k = 0, 1, \ldots, J. \tag{5.12}$$

Here, $(x)_k$ represents the rising factorial (or Pochhammer symbol)

$$(x)_k := (x)(x+1)\cdots(x+k-1).$$

For convenience, we use the notations $A_J(\xi), D_J(\xi)$, for $z = e^{i\xi}$, $\xi \in \mathbb{R}$. Note that $A_J(z)$ is an allpass filter and approximates the delay by λ samples, i.e.

$$A_J(z) \approx z^{-\lambda} \text{ around } z = 1. \tag{5.13}$$

The bigger J is, the better is the above approximation.

For the design of the Hilbert transform pair, we will use the case $\lambda = 1/2$ and choose either $J = 1$ or $J = 2$. The corresponding coefficients are

$$d = [1, 1/3] \text{ for } J = 1,$$

$$d = [1, 2, 1/5] \text{ for } J = 2. \tag{5.14}$$

Notice that, for all $0 < \lambda < 1$, the Laurent polynomial D_J has J real negative J roots $\{r_1, \ldots, r_J\}$ none of which lies on the unit circle and $r_k \neq \frac{1}{r_\ell}$ for all k, ℓ (see [**15**, Appendix B]). Therefore, $D_J(z)$ and $D_J(z^{-1})$ do not have common zeros. That is, the rational function A_J is irreducible. Table 5.1 shows the roots of $D_J(z)$ and $D_J(z^{-1})$ for $\lambda = 1/2$ and $J = 1, 2, 3, 4$.

J	roots of $D_J(z)$	roots of $D_J(z^{-1})$
1	$-1/3$	-3
2	$-1.8944, -0.1056$	$-9.4721, -0.5279$
3	$-4.3119, -0.6360, -0.0521$	$-19.1957, -1.5724, -0.2319$
4	$-7.5486, -1.4203, -1/3, -0.0311$	$-32.1634, -3, -0.7041, -0.1325$

TABLE 5.1. Roots of the Laurent polynomials $D_J(z)$ and $D_J(z^{-1})$.

Note that for $\lambda = 1/2$ it follows from (5.13) and (4.29) that

$$A_J(\xi) \approx \frac{1 + e^{-i\xi}}{|1 + e^{-i\xi}|} = \frac{\overline{N(\xi + \pi)}}{\overline{M(\xi + \pi)}} \text{ around } \xi = 0, \tag{5.15}$$

since $\frac{\overline{N(\xi+\pi)}}{\overline{M(\xi+\pi)}} = e^{-i\xi/2}\mathrm{sgn}(\cos\xi/2)$, and therefore $\frac{\overline{N(\xi+\pi)}}{\overline{M(\xi+\pi)}} = e^{-i\xi/2}$ for $\xi \in [-\pi, \pi]$. Namely, the trigonometric rational function $A_J(\xi)$ provides a good approximation to $\frac{\overline{N(\xi+\pi)}}{\overline{M(\xi+\pi)}}$. This fact provides a good clue to the approximation in (ii) of Constraint B. Namely, we have

$$\overline{A_J(\xi - \pi)} \approx \frac{N(\xi)}{M(\xi)} \text{ around } \xi = \pi.$$

The phase of the 2π-periodic function $\frac{N(\xi)}{M(\xi)} = e^{i(\xi-\pi)/2}\mathrm{sgn}(\sin\xi/2)$ is depicted in Figure 5.1, and the approximations by $\overline{A_J(\xi - \pi)}$ for $J = 1, \ldots, 6$, are in Figure 5.2. In Figure 5.2, one can see the approximation on $[-\pi, \pi]$ of the discontinuous phase of $\frac{N(\xi)}{M(\xi)}$ by the continuous phase of $\overline{A_J(\xi - \pi)}$.

Thus, we take the trigonometric rational function $\overline{A_J(\xi - \pi)}$ as the desired approximation in (ii) of Constraint B, that is,

$$\frac{\tilde{N}(\xi)}{\tilde{M}(\xi)} = \overline{A_J(\xi - \pi)} = \frac{(-e^{i\xi})^J D_J(\xi - \pi)}{\overline{D_J(\xi - \pi)}} \approx \frac{N(\xi)}{M(\xi)}. \tag{5.16}$$

From (5.16) it is clear that if we have an approximation $\tilde{M}$ then we have automatically $\tilde{N}$, and vice versa. In other words, we have two choices. One is getting $\tilde{M}$

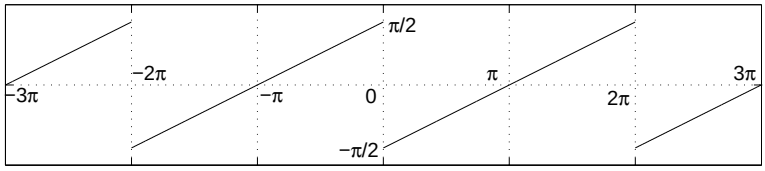

FIGURE 5.1. Phase of $\frac{N(\xi)}{M(\xi)}$ on $[-3\pi, 3\pi]$.

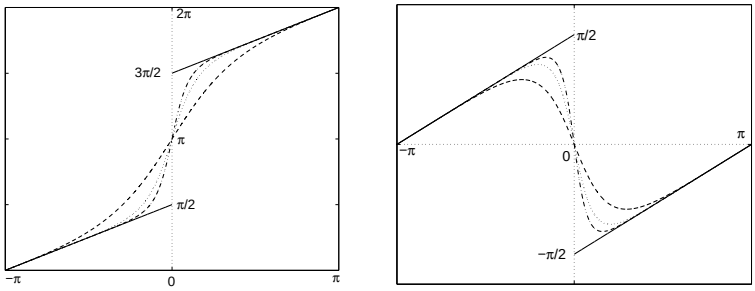

FIGURE 5.2. Phases of $\overline{A_J(\xi-\pi)}$, $\xi \in [-\pi, \pi]$, for $J = 1, 3, 5$, (left) and for $J = 2, 4, 6$ (right).

first, and then $\tilde{N}$ by

$$\tilde{N}(\xi) = \overline{A_J(\xi-\pi)}\tilde{M}(\xi) = \frac{(-e^{i\xi})^J D_J(\xi-\pi)}{\overline{D_J(\xi-\pi)}}\tilde{M}(\xi), \tag{5.17}$$

the other is getting $\tilde{N}$ first, and then $\tilde{M}$. We choose, for convenience, the former, since $M(\xi) = \frac{|\xi/2|}{|\sin \xi/2|}$ is real. In addition, the symmetry of M makes it possible to save computational costs in the approximation. In summary, we will find an approximation $\tilde{M}$ and then obtain $\tilde{N}$ using (5.17).

For the study of the approximation $\tilde{M}$, we recall Constraint B. The second constraint is satisfied by the choice in (5.16). To satisfy the first constraint, we should have,

$$\tilde{M}(\xi) = \overline{D_J(\xi-\pi)}F(\xi), \tag{5.18}$$

where F is a trigonometric polynomial, since $\tilde{N}$ in (5.17) would not be a trigonometric polynomial otherwise. If we take the third constraint into account, we have

$$\begin{aligned} \tilde{M}(\xi) &= \overline{D_J(\xi-\pi)}F(\xi) \\ &= \overline{D_J(\xi-\pi)}D_J(\xi-\pi)F_0(\xi) = |D_J(\xi-\pi)|^2 F_0(\xi), \end{aligned} \tag{5.19}$$

where F_0 is a real and even trigonometric polynomial, i.e. a cosine polynomial. Moreover, we require $F_0(0) = 1/|D_J(-\pi)|^2$ for $\tilde{M}(0) = 1$. Constraint Constraint B(iv) will be automatically satisfied from the approximations of Constraint B(ii) and (iii), i.e. we have from (5.17) and (5.19)

$$\begin{aligned} \tilde{N}(\xi) &= \frac{(-e^{i\xi})^J D_J(\xi-\pi)}{\overline{D_J(\xi-\pi)}} \tilde{M}(\xi) \\ &= (-e^{i\xi})^J (D_J(\xi-\pi))^2 F_0(\xi). \end{aligned} \tag{5.20}$$

Constraint B(v) will be easily satisfied, if we find a reasonable approximation $\tilde{M}$ due to $M(\xi) \in [1, \pi/2]$, $\forall\ \xi \in [-\pi, \pi]$. Now it is obvious from (5.19) and (5.20) that the construction of the cosine polynomial F_0 results in $\tilde{M}$ and $\tilde{N}$.
As the next step, we want to find

$$F_0(\xi) = \sum_{k=0}^{K_0} a_k \cos k\xi, \tag{5.21}$$

so that $\tilde{M}(\xi)$ gives a good approximation to M, i.e.

$$\tilde{M}(\xi) = |D_J(\xi-\pi)|^2 F_0(\xi) \approx M(\xi) = \frac{|\xi/2|}{|\sin \xi/2|} \text{ on } [-\pi, \pi]. \tag{5.22}$$

This is equivalent to

$$F_0(\xi) \approx B_J(\xi) := \frac{\xi/2}{\sin \xi/2\ |D_J(\xi-\pi)|^2} \text{ on } [-\pi, \pi]. \tag{5.23}$$

Based on the given observation we present the following lemma.

Lemma 5.5. *Let the trigonometric polynomials $\tilde{M}$ and $\tilde{N}$ be given by*

$$\tilde{M}(\xi) := |D_J(\xi-\pi)|^2 F_0(\xi),\ \tilde{N}(\xi) := (-e^{i\xi})^J (D_J(\xi-\pi))^2 F_0(\xi),$$

where F_0 is a cosine polynomial satisfying the approximation in (5.23) with $F_0(0) = 1/|D_J(-\pi)|^2$. Then $\tilde{M}$ and $\tilde{N}$ satisfy Constraint B.

We know that the function B_J is continuous at $\xi = 0$, since the function $|D_J(\xi-\pi)|^2$ has no roots on the unit circle. The function B_J is apparently not periodic and we approximate it by 2π-periodic F_0 on $[-\pi, \pi]$. For this approximation we employ Hermite Interpolation at the Chebyshev nodes on $[-\pi, \pi]$. We choose one node at the origin, so that the last constraint $\tilde{M}(0) = 1$ holds automatically. We present the results in the next section through several examples.

5.3. Some examples

In this section, we give some examples of approximate Hilbert transforms of MRA tight frames. We take the spline MRA tight frames of section 3.3 and then find their approximate Hilbert transform pairs which are approximate MRA tight frames. In other words, for a given spline MRA tight frame $\{\psi^{m,L}_{j,k,\ell}, 1 \le j \le r, k, \ell \in \mathbb{Z}\}$ of order m and L vanishing moments, we find an approximate MRA tight frame $\{\tilde{\Psi}_{j,k,\ell}, 1 \le j \le r, k, \ell \in \mathbb{Z}\}$ using the method introduced in the previous section. Recall from Remark 4.13 that spline MRA tight frames have simpler formulations since $p_0 = R = 1$. Namely, the refinable function is $\phi = N_m$ with the symbol $p = p_m$. For convenience, we take only $J = 1, 2$, for the computation of the Jth-order Thiran allpass filter (5.16). Firstly, for $J = 1$ we have from (5.11)

$$D_1(\xi) = 1 + \frac{1}{3}e^{-i\xi},\ D_1(\xi - \pi) = 1 - \frac{1}{3}e^{-i\xi}$$
$$|D_1(\xi - \pi)|^2 = \frac{10}{9} - \frac{2}{3}\cos\xi.$$

If we find an approximation

$$F_0(\xi) = \sum_{k=0}^{K_0} a_k \cos k\xi \ \approx\ B_1(\xi) = \frac{\xi/2}{\sin\xi/2\ |D_1(\xi - \pi)|^2} \text{ on } [-\pi, \pi], \tag{5.24}$$

then by (5.20)-(5.23) we have

$$\tilde{M}(\xi) = |D_1(\xi - \pi)|^2 F_0(\xi), \tag{5.25}$$
$$\tilde{N}(\xi) = -e^{i\xi}(D_1(\xi - \pi))^2 F_0(\xi). \tag{5.26}$$

We give an approximation F_0 by its coefficients a_k which are obtained by Hermite interpolation. Namely, for $J = 1$, we take 11 Chebyshev nodes on $[-\pi, \pi]$,

$$\omega_k := \pi \cos\left(\frac{\pi}{2}\frac{2k-1}{11}\right),\ k = 1, \ldots, 11,$$

and Hermite interpolation conditions

$$\frac{d^\ell}{d\xi^\ell}F_0(\xi)|_{\xi=\omega_k} = \frac{d^\ell}{d\xi^\ell}B_1(\xi)|_{\xi=\omega_k},\ \ell = 0, \ldots, \zeta_k,\ k = 1, \ldots, 11, \tag{5.27}$$

of orders $(\zeta_k) = (0, 0, 1, 2, 0, 4, 0, 2, 1, 0, 0)$ at each node ω_k. The resulting F_0 is given by

$$
\begin{aligned}
(5.28) \qquad F_0(\xi) &= 1.23976790776388 + 0.63350413697975\cos\xi \\
&+0.26789403554534\cos 2\xi + 0.05812502671878\cos 3\xi + 0.03945332896836\cos 4\xi \\
&+0.00468789622758\cos 5\xi + 0.01086970558701\cos 6\xi - 0.00508016557257\cos 7\xi \\
&+0.00243735166848\cos 8\xi - 0.00412602131519\cos 9\xi + 0.00246679742858\cos 10\xi.
\end{aligned}
$$

It will be used for the case $J = 1$ in the following examples. In Figure 5.3 we see that, F_0 and $\tilde{M}$ approximate B_1 and M well. Notice that Constraint B is satisfied

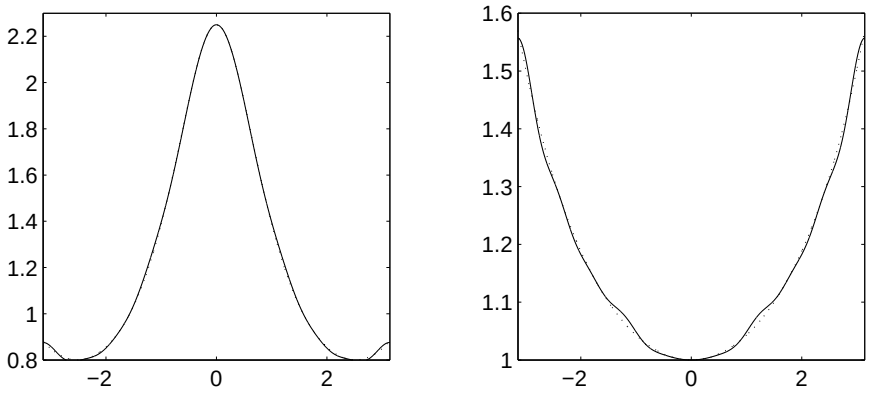

FIGURE 5.3. Left: Approximation F_0 (solid) to B_1 (dotted), Right: Approximation $\tilde{M}$ (solid) to M (dotted).

by (5.25)-(5.26) and our choice of F_0 (see Figure 5.3). The errors of approximation for F_0 and $\tilde{M}$ with respect to the maximum norm are

$$
\begin{aligned}
\|F_0 - B_1\|_\infty &\doteq 0.0153, \\
\|\tilde{M} - M\|_\infty &\doteq 0.0180.
\end{aligned}
$$

(see Figure 5.4.) On the other hand, N is not real and discontinuous at $\xi = 0$, in contrast to M. Thus, we show the approximation $\tilde{N}$ to N by closed curves in the complex plane. The parametric curve for N begins at $N(-\pi) = \frac{\pi}{2}$ on the positive real axis and goes counterclockwise to $N(0-) = i$. Then it jumps to $N(0+) = -i$ and goes counterclockwise to $N(\pi) = \frac{\pi}{2}$. The trigonometric polynomial $\tilde{N}$ is a continuous approximation of N. Figure 5.5 shows the values of $N(\xi_j)$ (marked by $\circ$) and $\tilde{N}(\xi_j)$ (marked by $*$), where ξ_j is equally spaced on $[-\pi, \pi]$. Note that $\tilde{N}$ accelerates near

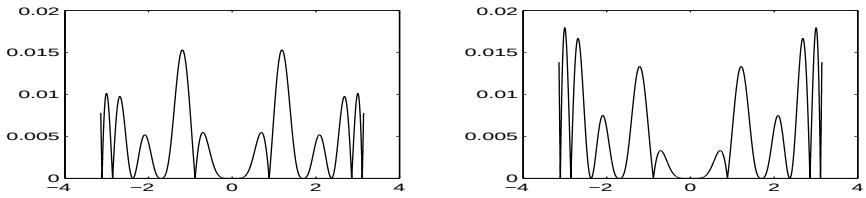

FIGURE 5.4. Left: $|F_0(\xi) - B_1(\xi)|,\ \xi \in [-\pi, \pi]$, Right: $|M(\xi) - \tilde{M}(\xi)|,\ \xi \in [-\pi, \pi]$

zero in order to approximate the jump of N at $\xi = 0$. For the case $J = 2$, from

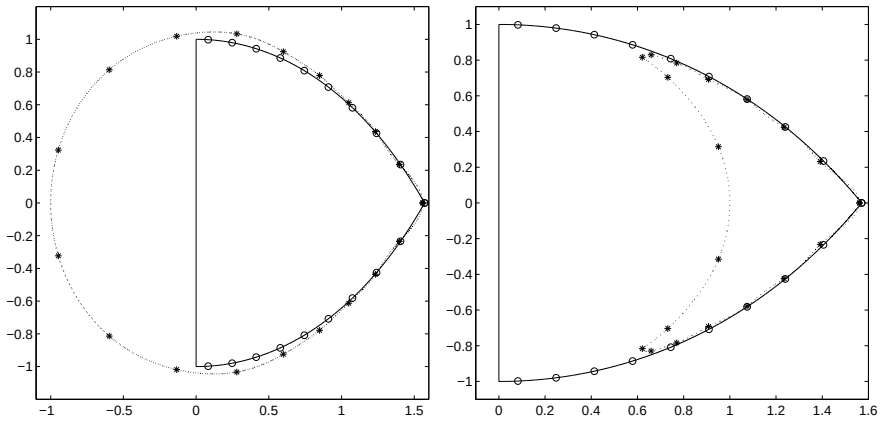

FIGURE 5.5. Approximation of $\tilde{N}$ (dotted) to N(solid) for $J = 1$ (left) and $J = 2$ (right). The values of $N(\xi_j)$ are marked by $\circ$ and $\tilde{N}(\xi_j)$ by $*$, where ξ_j's are equally spaced on $[-\pi, \pi]$.

(5.14) we have

$$D_2(\xi) = 1 + 2e^{-i\xi} + \frac{1}{5}e^{-2i\xi},\ D_2(\xi - \pi) = 1 - 2e^{-i\xi} + \frac{1}{5}e^{-2i\xi},$$
$$|D_2(\xi - \pi)|^2 = \frac{126}{25} - \frac{24}{5}\cos\xi + \frac{2}{5}\cos 2\xi.$$

Furthermore, $\tilde{M}$ and $\tilde{N}$ are set by

$$\tilde{M}(\xi) = |D_2(\xi - \pi)|^2 F_0(\xi), \tag{5.29}$$

$$\tilde{N}(\xi) = e^{2i\xi}(D_2(\xi - \pi))^2 F_0(\xi), \tag{5.30}$$

and a trigonometric polynomial F_0 approximating B_2 should be obtained, namely,

$$F_0(\xi) \approx B_2(\xi) = \frac{\xi/2}{\sin\xi/2\ |D_2(\xi - \pi)|^2} \text{ on } [-\pi, \pi].$$

We propose the following Hermite Interpolation. With 13 Chebyshev nodes on $[-\pi, \pi]$,

$$\omega_k := \pi \cos\left(\frac{\pi}{2}\frac{2k-1}{13}\right),\ k = 1, \ldots, 13,$$

and $(\zeta_k) = (0, 0, 1, 1, 2, 1, 4, 1, 2, 1, 1, 0, 0)$ at each node ω_k we find F_0 satisfying

$$\frac{d^\ell}{d\xi^\ell} F_0(\xi)|_{\xi=\omega_k} = \frac{d^\ell}{d\xi^\ell} B_2(\xi)|_{\xi=\omega_k} \tag{5.31}$$

for $\ell = 0, \ldots, \zeta_k$, and $k = 1, \ldots, 13$. As a result we obtain

$$\begin{aligned} F_0(\xi) &= 0.46109148979134 + 0.50701763950757\cos\xi \\ &+ 0.28466184491444\cos 2\xi + 0.14481523187640\cos 3\xi + 0.07977219294095\cos 4\xi \\ &+ 0.03956874890536\cos 5\xi + 0.02185794683537\cos 6\xi + 0.00971199048350\cos 7\xi \\ &+ 0.00607199386946\cos 8\xi + 0.00301301634923\cos 9\xi + 0.00261247054575\cos 10\xi \\ &+ 0.000910841241721\cos 11\xi + 0.00139459273892\cos 12\xi. \end{aligned} \tag{5.32}$$

As in the case $J = 1$, it is obvious that $\tilde{M}$ and $\tilde{N}$ in (5.29)-(5.30) satisfy Constraint B as well. The errors of approximation of F_0 and $\tilde{M}$ with respect to the maximum norm are

$$\begin{aligned} \|F_0 - B_2\|_\infty &\doteq 0.0047, \\ \|\tilde{M} - M\|_\infty &\doteq 0.0144. \end{aligned}$$

The trigonometric polynomial $\tilde{N}$ for $J = 2$ is shown in Figure 5.5. Note that $\tilde{N}$ approximates the function N better than $\tilde{N}$ for $J = 1$.

5.3.1. Approximate Hilbert transform pairs of spline MRA tight frame $\{\psi^{5,5}_{j,k,\ell}, j = 1, 2, 3, k, \ell \in \mathbb{Z}\}$.

We begin with the MRA tight frame $\{\psi^{5,5}_{j,k,\ell}, j = 1, 2, 3, k, \ell \in \mathbb{Z}\}$ whose generators $\psi^{5,5}_j$, $j = 1, 2, 3$, are given in section 3.3.2 (see Figure 3.4 and Table 3.4). We demonstrate their approximate Hilbert transform pairs for $J = 1, 2$.

Example 5.6. *We consider the case $J = 1$ in this example. From F_0 in (5.28) we get $\tilde{M}$ and $\tilde{N}$ using (5.25)-(5.26). Moreover, we get the approximations (5.1)-(5.3)*

by means of $\tilde{M}$ and $\tilde{N}$. They are given by

$$\begin{aligned}
\widehat{\tilde{\Phi}}(\xi) &= \tilde{M}(\xi)\hat{N}_6(\xi) = \left(\frac{10}{9} - \frac{2}{3}\cos\xi\right) F_0(\xi)\hat{N}_6(\xi), \\
\widehat{\tilde{\Psi}}_j(\xi) &= \frac{\tilde{N}(\xi/2)}{\tilde{M}(\xi/2)} q_j^{5,5}(\xi/2)\widehat{\tilde{\Phi}}(\xi/2) \\
&= -e^{i\xi/2}\left(1 - \frac{1}{3}e^{-i\xi/2}\right)^2 F_0(\xi/2)q_j^{5,5}(\xi/2)\hat{N}_6(\xi/2) \\
&= -2^5 e^{i\xi/2}\left(1 - \frac{1}{3}e^{-i\xi/2}\right)^2 F_0(\xi/2)\hat{q}_j^{5,5}(\xi/2)(1 - e^{-i\xi/2})^5\hat{N}_6(\xi/2). \qquad (5.33)
\end{aligned}$$

We compare the $\tilde{\Psi}_j,\ j = 1, 2, 3,$ to the exact Hilbert transforms $\Psi_j,\ j = 1, 2, 3,$ in (4.21). The magnitudes of $\hat{\Psi}_j$ and $\widehat{\tilde{\Psi}}_j$ and their errors are shown in Figure 5.6 and Figure 5.7.

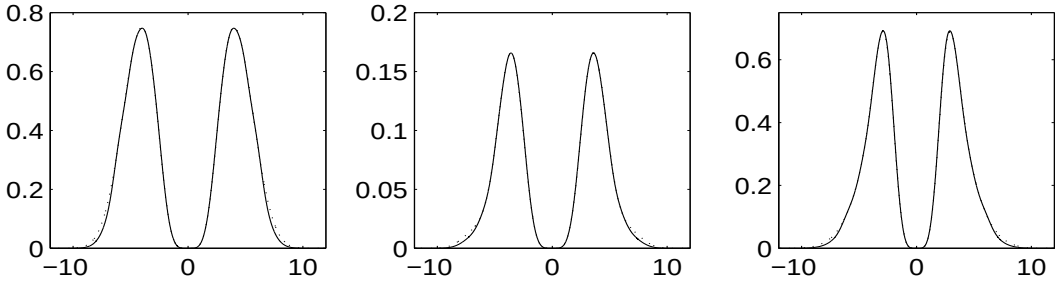

FIGURE 5.6. Magnitudes of $\hat{\Psi}_j$ (solid) and $\widehat{\tilde{\Psi}}_j$ (dotted) for $j = 1$ (left), $j = 2$ (middle), and $j = 3$ (right) for $J = 1$.

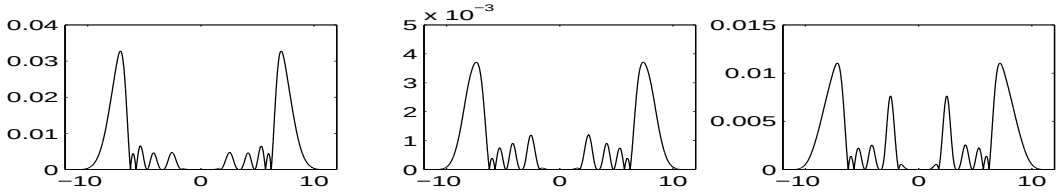

FIGURE 5.7. Error of $|\ \hat{\Psi}_j - \widehat{\tilde{\Psi}}_j\ |$ for $j = 1$ (left), $j = 2$ (middle), and $j = 3$ (right) for $J = 1$.

As we mentioned in Theorem 5.3, however, we take N_6 as the refinable function of the approximate MRA tight frame $\{\tilde{\Psi}_{j,k,\ell}, j = 1, 2, 3, k, \ell \in \mathbb{Z}\}$. The two-scale

symbols of the generators $\tilde{\Psi}_j,\ j = 1, 2, 3,$ *and the refinable function* N_6 *are described by (5.33) and the notations of Theorem 5.3*

$$\tilde{p}(\xi) = p_6(\xi) = \left(\frac{1 + e^{-i\xi}}{2}\right)^6,$$
$$\tilde{q}_j(\xi) = -2^5 e^{i\xi}\left(1 - \frac{1}{3}e^{-i\xi}\right)^2 F_0(\xi)\hat{q}_j^{5,5}(\xi)(1 - e^{-i\xi})^5.$$

Now we show that $\tilde{\Psi}_j,\ j = 1, 2, 3,$ *satisfy Constraint A. We check Constraint A(v) first. It is clear that the symbols* $\tilde{p} = p_6$ *and* $\tilde{q}_j,\ j = 1, 2, 3,$ *are trigonometric polynomials and thus they satisfy the Assumption 4.4, so does the refinable function* N_6*. Furthermore,* $\hat{N}_6$ *is continuous at the origin and* $\hat{N}_6(0) = 1$*. Next, we compute the fundamental function* $\tilde{S}_{\tau_2}$ *numerically by (5.7). Figure 5.8 shows that (i) of Definition 5.1 holds, i.e. the* 2π*-periodic function* $\tilde{S}_{\tau_2}$ *is positive, bounded, and*

$$\overline{\lim_{j\to-\infty}}|\tilde{S}_{\tau_2}(2^j\xi) - 1| \le \delta_1$$

for $0 < \delta_1 < 0.02$*. In order to check (ii) of Definition 5.1 we compute numerically*

$$E_{\tau_2}(\xi) = \tilde{S}_{\tau_2}(2\xi)p_6(\xi)\overline{p_6(\xi + \pi)} + \sum_{j=1}^{3}\tilde{q}_j(\xi)\overline{\tilde{q}_j(\xi + \pi)}. \tag{5.34}$$

It is clear that the function E_{τ_2} *is* 2π*-periodic and its magnitude* $|E_{\tau_2}|$ *is* π*-periodic. A numerical computation asserts that* $0 \le |E_{\tau_2}| \le \delta_2,\ \delta_2 \doteq 0.104$*, see Figure 5.8.*

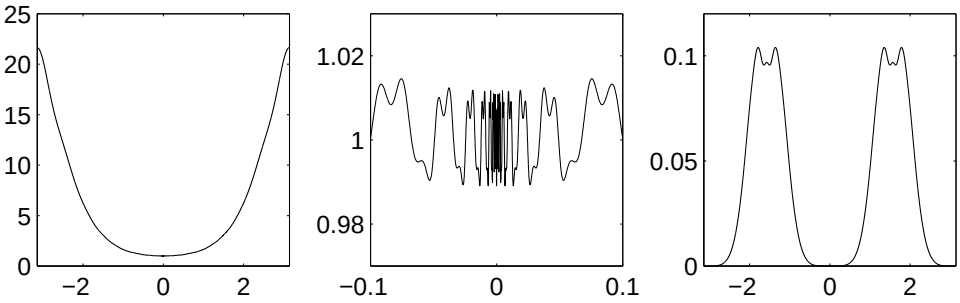

FIGURE 5.8. $\tilde{S}_{\tau_2}$ on $[-\pi, \pi]$ (left), on $[-0.1, 0.1]$ (middle), and $|E_{\tau_2}|$ (right) for $J = 1$.

It is apparent that each of $\tilde{\Psi}_j,\ j = 1, 2, 3,$ *has compact support, in fact,* $\mathrm{supp}\tilde{\Psi}_1 = [-6, 13.5],\ \mathrm{supp}\tilde{\Psi}_2 = [-5, 13.5],\ \mathrm{supp}\tilde{\Psi}_3 = [-6, 14.5]$*, and* 5 *vanishing moments from (5.33), just like the given generators* $\psi_j^{m,L}$*, i.e. we have Constraint A(i) and*

Constraint A (iii). From the associated refinable function N_6 we have $\tilde{\Psi}_j \in C^4$ (Constraint A(ii)). Now, we look at the generators in the time domain so that we

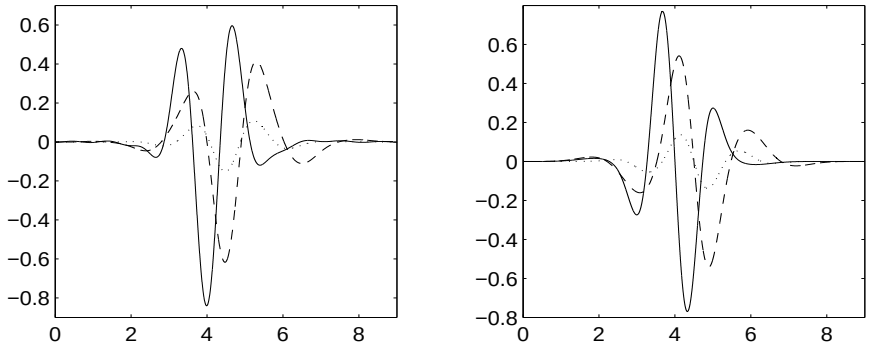

FIGURE 5.9. $\tilde{\Psi}_j$ (left) and $\psi_j^{5,5}$ (right) for $j = 1$ (solid), $j = 2$ (dotted), and $j = 3$ (dashed) for $J = 1$.

examine Constraint A(iv) (see Figure 5.9). Note that each $\psi_j^{5,5}$ is antisymmetric and each $\tilde{\Psi}_j$ should be symmetric as an approximate Hilbert transform of $\psi_j^{5,5}$. But, Figure 5.9 shows that this is not true due to the non-symmetric coefficient vector of $(D_J(\xi+\pi))^2$ in (5.20). This effect is still pronounced for $J = 1$. For a higher value of J, we expect that this effect is reduced. Finally, we make sure if

$$|\widehat{\tilde{\Psi}}_j(\xi) + i\hat{\psi}_j^{5,5}(\xi)| \approx 0, \text{ for } j = 1, 2, 3, \ \xi \in \mathbb{R}^-.$$

For a good approximation $\tilde{\Psi}_j$, $|\widehat{\tilde{\Psi}}_j(\xi) + i\hat{\psi}_j^{5,5}(\xi)|$ should vanish on $\mathbb{R}^-$ due to (2.7). Figure 5.10 shows that $|\widehat{\tilde{\Psi}}_j(\xi) + i\hat{\psi}_j^{5,5}(\xi)|$ approximately vanishes for $\xi < 0$ already for $J = 1$.

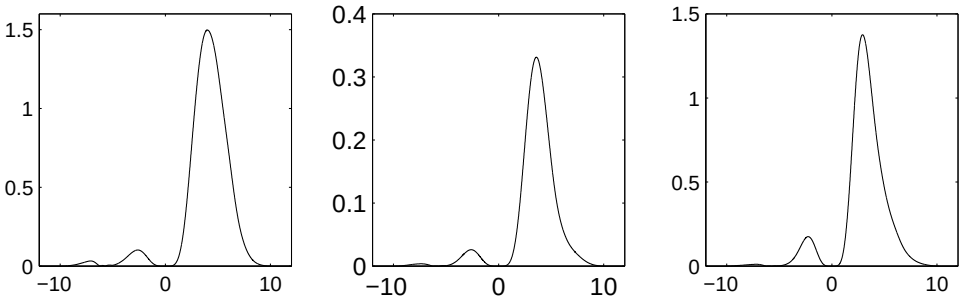

FIGURE 5.10. $|\widehat{\tilde{\Psi}}_j(\xi) + i\hat{\psi}_j^{5,5}(\xi)|$ for $j = 1$ (left), $j = 2$ (middle), and $j = 3$ (right) for $J = 1$.

Example 5.7. *Now we apply the results of the case $J = 2$. As in the previous example, we start with F_0 in (5.32) and insert it into (5.29)-(5.30) to obtain $\tilde{M}$ and $\tilde{N}$. The corresponding refinable function is N_6, and the frame generators are*

$$\begin{aligned}\widehat{\tilde{\Psi}}_j(\xi) &= e^{i\xi}\left(1-2e^{-i\xi/2}+\frac{1}{5}e^{-i\xi}\right)^2 F_0(\xi/2)q_j^{5,5}(\xi/2)\hat{N}_6(\xi/2)\\ &= 2^5 e^{i\xi}\left(1-2e^{-i\xi/2}+\frac{1}{5}e^{-i\xi}\right)^2 (1-e^{-i\xi/2})^5 F_0(\xi/2)\hat{q}_j^{5,5}(\xi/2)\hat{N}_6(\xi/2).\end{aligned}$$

The associated two-scale symbols are $\tilde{p} = p_6$ and

$$\tilde{q}_j(\xi) = 2^5 e^{2i\xi}\left(1-2e^{-i\xi}+\frac{1}{5}e^{-2i\xi}\right)^2 (1-e^{-i\xi})^5 F_0(\xi)\hat{q}_j^{5,5}(\xi),\ j=1,2,3.$$

Note that the symbols and the refinable function satisfy Assumption 4.4 trivially. If

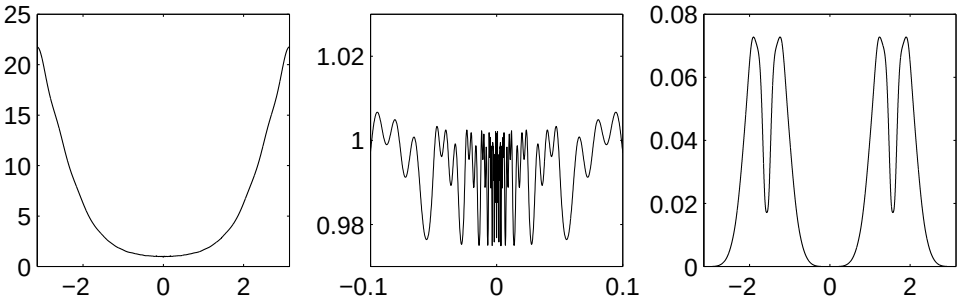

FIGURE 5.11. $\tilde{S}_{\tau_2}$ on $[-\pi,\pi]$ (left), on $[-0.1,0.1]$ (middle), and $|E_{\tau_2}|$ (right) for $J = 2$.

we compute the associated fundamental function $\tilde{S}_{\tau_2}$ using the same method of the previous example, it shows that (i) of Definition 5.1 is also valid (see Figure 5.11). The second condition (ii) of Definition 5.1 is tested by the numerical computation of the function E_{τ_2} as in (5.34). Figure 5.11 indicates that (ii) holds for the associated symbols and fundamental function as well. The 3 generators are shown in Figure 5.12. Each of them has also 5 vanishing moments, compact support, in fact, $\mathrm{supp}\tilde{\Psi}_1 = [-7.5, 15],\ \mathrm{supp}\tilde{\Psi}_2 = [-6.5, 15],\ \mathrm{supp}\tilde{\Psi}_3 = [-7.5, 16]$, *and is again in C^4. Furthermore, they are closer to being symmetric than those for $J = 1$ (compare with Figure 5.9).*

Finally Figure 5.13 shows that $|\widehat{\tilde{\Psi}}_j(\xi) + i\hat{\psi}_j^{5,5}(\xi)|$ almost vanishes for $\xi < 0$, and the size is much smaller than the case $J = 1$ (compare with Figure 5.10). From Figure 5.12 and Figure 5.13 we can conclude that for $J = 2$ we have better

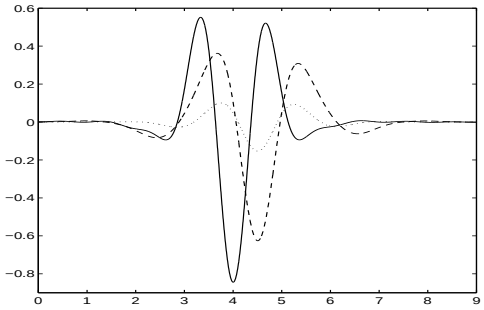

FIGURE 5.12. $\tilde{\Psi}_j$, $j = 1$ (solid), $j = 2$ (dotted), and $j = 3$ (dashed) for $J = 2$.

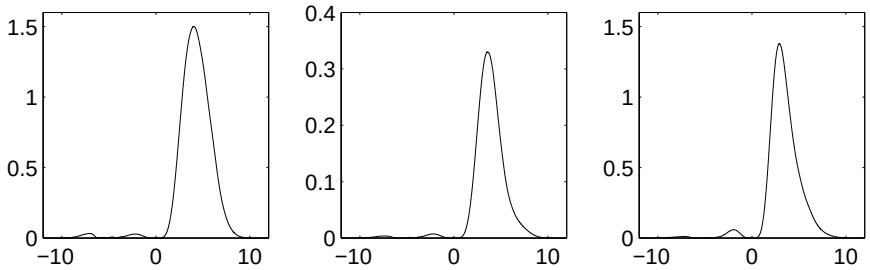

FIGURE 5.13. $|\widehat{\tilde{\Psi}}_j(\xi) + i\hat{\psi}_j^{5,5}(\xi)|$, $j = 1$ (left), $j = 2$ (middle), and $j = 3$ (right) for $J = 2$.

approximations $\tilde{\Psi}_j$ *to* $\mathcal{H}\psi_j^{5,5}$ *for* $j = 1, 2, 3$.

5.3.2. Approximate Hilbert transform pairs of spline MRA tight frame $\{\psi_{j,k,\ell}^{4,4}, j = 1, 2, 3, k, \ell \in \mathbb{Z}\}$.

The construction of the previous examples does not depend on the order of the B-splines. Thus, we get approximate Hilbert transform pairs of the spline MRA tight frame $\{\psi_{j,k,\ell}^{4,4}, j = 1, 2, 3, k, \ell \in \mathbb{Z}\}$ using the results of the cases $J = 1, 2$. Notice that the generators $\psi_j^{4,4}$, $j = 1, 2, 3$, are symmetric and finite linear combinations of N_4 (their coefficients $\hat{q}_{j,k}^{4,4}$ are given in [**8**, p.183]).

Example 5.8. *We set* $J = 1$. *The functions* F_0, $\tilde{M}$, *and* $\tilde{N}$ *are the same as those of the case* $J = 1$ *in Example 5.6. Thus we have the refinable function* N_5 *and generators*

$$\widehat{\tilde{\Psi}}_j(\xi) = -2^4 e^{i\xi/2}\left(1 - \frac{1}{3}e^{-i\xi/2}\right)^2 (1 - e^{-i\xi/2})^4 F_0(\xi/2)\hat{q}_j^{4,4}(\xi/2)\hat{N}_5(\xi/2), \tag{5.35}$$

and the two-scale symbols are $\tilde{p} = p_5$ *and*

$$\tilde{q}_j(\xi) = -2^4 e^{i\xi}\left(1 - \frac{1}{3}e^{-i\xi}\right)^2 (1 - e^{-i\xi})^4 F_0(\xi)\hat{q}_j^{4,4}(\xi),\ j = 1, 2, 3.$$

Now we examine if $\tilde{\Psi}_j,\ j = 1, 2, 3,$ *and* N_5 *constitute an approximate MRA tight frame. It is trivial to check Assumption 4.4 for the symbols and the refinable function. Thus, we compute the associated fundamental function* $\tilde{S}_{\tau_2}$ *and observe its behavior around the origin. Figure 5.14 shows that (i) of Definition 5.1 is satisfied. Moreover, a numerical computation of the function* E_{τ_2} *in (5.34) asserts that (ii) of*

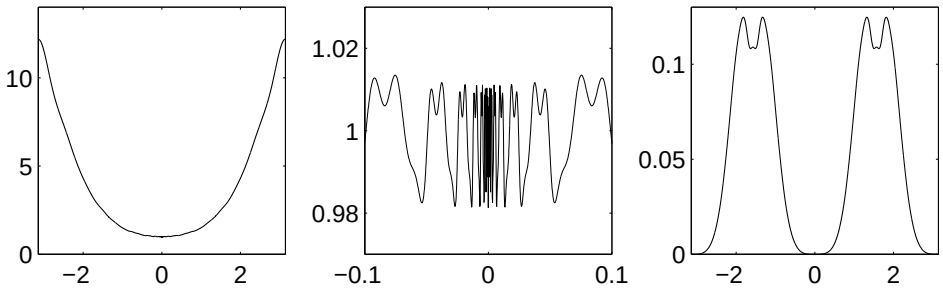

FIGURE 5.14. $\tilde{S}_{\tau_2}$ on $[-\pi, \pi]$ (left), on $[-0.1, 0.1]$ (middle), and $|E_{\tau_2}|$ (right) for $J = 1$.

Definition 5.1 holds as well. We have, therefore, an approximate MRA tight frame. From (5.35) it is obvious that the generators $\tilde{\Psi}_j,\ j = 1, 2, 3,$ *are compactly supported (*$\mathrm{supp}\tilde{\Psi}_1 = [-6, 11.5],\ \mathrm{supp}\tilde{\Psi}_2 = [-5, 11.5],\ \mathrm{supp}\tilde{\Psi}_3 = [-6, 12.5]$*) and are in* C^3*. The* 3 *generators are shown in Figure 5.15 and they are nearly antisymmetric, while* $\psi_j^{4,4},\ j = 1, 2, 3,$ *are symmetric. Finally, Figure 5.16 shows that* $|\widehat{\tilde{\Psi}}_j(\xi) + i\hat{\psi}_j^{4,4}(\xi)|$

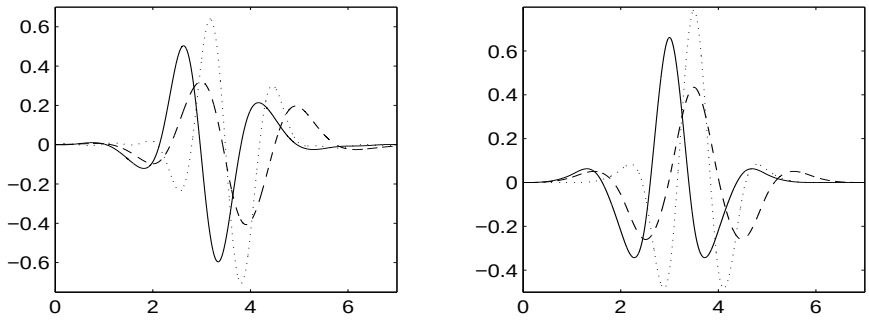

FIGURE 5.15. $\tilde{\Psi}_j$ (left) and $\psi_j^{4,4}$ (right), $j = 1$ (solid), $j = 2$ (dotted), and $j = 3$ (dashed) for $J = 1$.

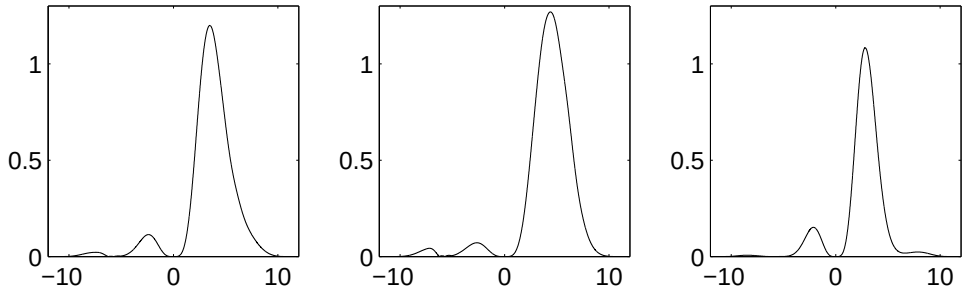

FIGURE 5.16. $|\widehat{\tilde{\Psi}}_j(\xi) + i\hat{\psi}_j^{4,4}(\xi)|$, $j = 1$ (left), $j = 2$ (middle), and $j = 3$ (right) for $J = 1$.

nearly vanishes for $\xi < 0$ for each j.

Example 5.9. *For $J = 2$ the functions F_0, $\tilde{M}$, and $\tilde{N}$ are identical with those of the case $J = 2$ in Example 5.7. Therefore, we have the refinable function N_5 and generators*

$$\widehat{\tilde{\Psi}}_j(\xi) \;=\; 2^4 e^{i\xi}\left(1 - 2e^{-i\xi/2} + \frac{1}{5}e^{-i\xi}\right)^2 (1 - e^{-i\xi/2})^4 F_0(\xi/2)\hat{q}_j^{4,4}(\xi/2)\hat{N}_5(\xi/2),$$

and the two-scale symbols are p_5 and

$$\tilde{Q}_j(\xi) = 2^4 e^{2i\xi}\left(1 - 2e^{-i\xi} + \frac{1}{5}e^{-2i\xi}\right)^2 (1 - e^{-i\xi})^4 F_0(\xi)\hat{q}_j^{4,4}(\xi),\ j = 1, 2, 3.$$

If we compute the associated fundamental function $\tilde{S}_{\tau_2}$ as in the previous examples, we can examine (i) and (ii) of Definition 5.1. Figure 5.17 displays that both (i) and (ii) hold. The 3 generators are shown in Figure 5.18. It is clear that they are

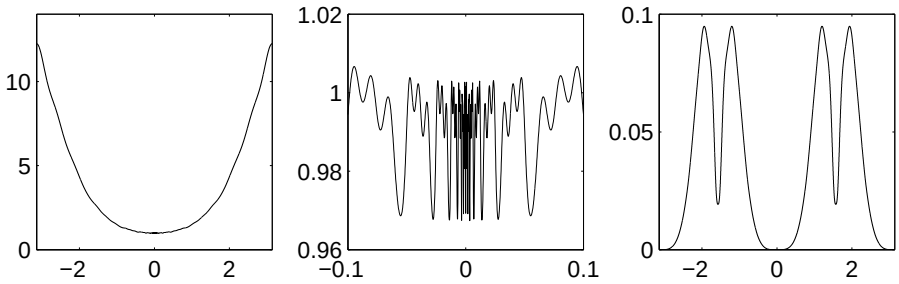

FIGURE 5.17. $\tilde{S}_{\tau_2}$ on $[-\pi, \pi]$ (left), on $[-0.1, 0.1]$ (middle), and $|E_{\tau_2}|$ (right) for $J = 2$.

compactly supported ($\mathrm{supp}\tilde{\Psi}_1 = [-7, 13],\ \mathrm{supp}\tilde{\Psi}_2 = [-6, 13],\ \mathrm{supp}\tilde{\Psi}_3 = [-7, 14]$*)*

and they are closer to being antisymmetric than those of the case $J = 1$ (compare with Figure 5.15). Finally Figure 5.19 shows that $|\widehat{\tilde{\Psi}}_j(\xi) + i\hat{\psi}_j^{4,4}(\xi)|$ almost vanishes

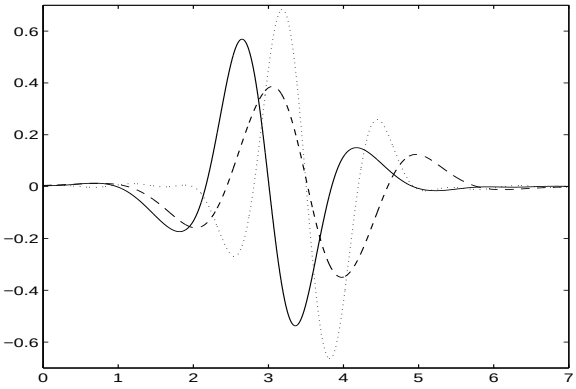

FIGURE 5.18. $\tilde{\Psi}_j$, $j = 1$ (solid), $j = 2$ (dotted), and $j = 3$ (dashed) for $J = 2$.

for $\xi < 0$, and the size is much smaller than for $J = 1$ (compare with Figure 5.16). Hence, $\tilde{\Psi}_j$ of the case $J = 2$ approximates $\mathcal{H}\psi_j^{4,4}$ better than that of the case $J = 1$ for each j.

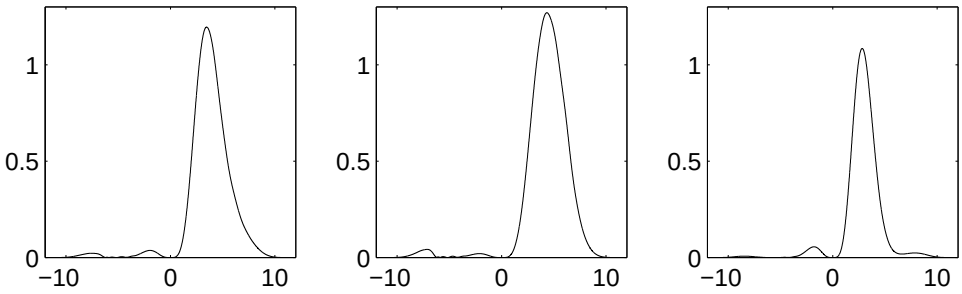

FIGURE 5.19. $|\widehat{\tilde{\Psi}}_j(\xi) + i\hat{\psi}_j^{4,4}(\xi)|$, $j = 1$ (left), $j = 2$ (middle), and $j = 3$ (right) for $J = 2$.

Remark 5.10. *1. If we are given a spline MRA tight frame $\{\psi_{j,k,\ell}^{m,L}\}$, our approach provides an approximate MRA tight frame $\{\tilde{\Psi}_{j,k,\ell}\}$ such that $\tilde{\Psi}_j \in C^{m-1} \cap L^2(\mathbb{R})$ with the associated refinable function N_{m+1}. Each generator $\tilde{\Psi}_j$ has compact support and vanishing moments of order L. Furthermore, we can expect that each generator $\tilde{\Psi}_j$ is nearly symmetric (resp. antisymmetric) if $\psi_j^{m,L}$ is antisymmetric (resp. symmetric). In other words, if the given MRA tight frame has good properties such as regularity,*

vanishing moments, symmetry, then the approximate Hilbert transform inherits the properties. Furthermore, if we once store $\tilde{M}$ and $\tilde{N}$, we obtain our approximations automatically regarding to the given MRA tight frames. Namely, in order to get approximate Hilbert transform pairs of MRA tight frames that have good properties, we only need to choose an MRA tight frame of good properties. The conventional approaches ([**15, 16, 18, 26, 27, 28**]*), however, construct both parts of the Hilbert transform pair at the same time. Thus the computational complexity will naturally increase if one requires "good" frames. This is another difference between our and the fore-existing approaches.*

2. It follows from [**10**] *that the approximate MRA tight frames are Bessel systems. We believe that they are frames of $L^2(\mathbb{R})$ as well. A complete proof is, however, still missing. We conjecture that one can prove the existence of their duals which are Bessel systems.*

In the next section, we will develop pairs of MRA tight frames which are approximate Hilbert transform pairs in the sense of (v) of Constraint A.

CHAPTER 6

Approximate Hilbert transform pairs of spline MRA tight frames

The examples in the previous section indicate that it is not possible to get an approximate Hilbert transform pair of a given spline MRA tight frame where the approximation itself is a spline MRA tight frame. Namely, although our examples are good approximate Hilbert transforms, they satisfy the characterization of tight frames, i.e. (i) and (ii) of Proposition 4.5, only approximately. Hence, they are not MRA tight frames in the strict sense, but *approximate MRA tight frames*.
In contrast to the approach of chapter 5, we want to stick to the tightness. In this chapter, we give priority to the tightness, i.e. we start with an MRA tight frame and find another MRA tight frame whose generators are approximate Hilbert transforms of the given generators. What we can expect is that the approximations would be worse than those in the previous chapter since we lose many degrees of freedom due to the tightness.
For the search for those MRA tight frame pairs, we revisit the definition of the Hilbert transform in the frequency domain and characterize a pair of functions which are Hilbert transforms of each other. Using the characterization we search for the pairs of spline MRA tight frames among the examples which are given in section 3.3, the appendix, and [**8**].

6.1. Characterization of Hilbert transform pairs in $L^2(\mathbb{R})$

If two functions η and ψ in $L^2(\mathbb{R})$ are a Hilbert transform pair, i.e. $\eta = \mathcal{H}\psi$, we have equivalently from (2.5)

$$|\hat{\eta}(\xi)| = |\hat{\psi}(\xi)|, \ a.e.\ \xi \in \mathbb{R}, \tag{6.1}$$

$$\rho_{\hat{\eta}}(\xi) = \rho_{\hat{\psi}}(\xi) - \frac{\pi}{2}\mathrm{sgn}(\xi) + 2\pi\ell, \ a.e.\ \xi \in \mathbb{R}, \ell \in \mathbb{Z}, \tag{6.2}$$

where $\rho_{\hat{\eta}}$ and $\rho_{\hat{\psi}}$ are the phases of $\hat{\eta}$ and $\hat{\psi}$. We make use of (6.1) and (6.2) in our search for approximate Hilbert transform pairs of spline MRA tight frames. Namely, for a spline MRA tight frame $\{\psi_{j,k,\ell}, 1 \le j \le r,\ k,\ell \in \mathbb{Z}\}$, we search for another spline MRA tight frame $\{\eta_{j,k,\ell}, 1 \le j \le r,\ k,\ell \in \mathbb{Z}\}$ with

$$|\hat{\eta}_j(\xi)| \approx |\hat{\psi}_j(\xi)|,\ a.e.\ \xi \in \mathbb{R} \tag{6.3}$$

$$\rho_{\hat{\eta}_j}(\xi) \approx \rho_{\hat{\psi}_j}(\xi) - \frac{\pi}{2}\mathrm{sgn}(\xi) + 2\pi\ell,\ a.e.\ \xi \in \mathbb{R}, \ell \in \mathbb{Z}, \tag{6.4}$$

for each $j = 1, \ldots, r$. For the sake of the construction of approximate Hilbert transform pairs, we require that (6.3) and (6.4) hold. In the next section we present examples of such pairs.

6.2. Examples

We begin with $\{\psi^{5,5}_{j,k,\ell}, j = 1,2,3,\ k,\ell \in \mathbb{Z}\}$ and find its approximate Hilbert transform pair. In fact, Theorem 4.12 and Remark 4.13 give us a good hint, since the exact Hilbert transform of each generator $\psi^{5,5}_j$ is described by N_6. In other words, the candidates are MRA tight frames with refinable function N_6, i.e. $\psi^{6,L}_j$ for some L. Furthermore, the ideal pair should be symmetric since $\psi^{5,5}_j$ is antisymmetric for each $j = 1,2,3$. Our examples in section 3.3 and the appendix show that each $\psi^{6,L}_j,\ j = 1,2,3$, is symmetric for even L (the example of the case $L = 2$ is not given in this thesis for the sake of saving space). Among the candidates of the generators $\{\psi^{6,L}_j, j = 1,2,3\}$, for $L = 2,4,6$, we recall that each of the two-scale symbols of $\psi^{6,4}_j$ is given by

$$q^{6,4}_j(\xi) = 2^4 \hat{q}^{6,4}_j(\xi)(1 - e^{-i\xi})^4,$$

and each $\hat{q}^{6,4}_j$ has the same number of coefficients as $\hat{q}^{5,5}_j$, where

$$q^{5,5}_j(\xi) = 2^5 \hat{q}^{5,5}_j(\xi)(1 - e^{-i\xi})^5.$$

We show that this fact is crucial for the condition (6.4). We demonstrate, furthermore, that (6.3) holds for $\psi^{5,5}_j$ and $\psi^{6,4}_j$. After that we extend the result to the pairs $(\psi^{4,4}_j, \psi^{5,3}_j)$ and $(\psi^{3,3}_j, \psi^{4,2}_j)$.

Example 6.1. *For each $j \in \{1,2,3\}$, we show that $\psi^{5,5}_j$ and $\psi^{6,4}_j$ satisfy (6.3) and (6.4). In other words, $\psi^{5,5}_j$ and $\psi^{6,4}_j, j = 1,2,3$, generate an approximate Hilbert*

transform pair of spline MRA tight frames.

We begin with the Fourier transforms of $\psi_j^{5,5}$ *and* $\psi_j^{6,4}$,

$$\begin{aligned}\hat{\psi}_j^{5,5}(\xi) &= 2^5 \hat{q}_j^{5,5}(\xi/2)\left(1-e^{-i\xi/2}\right)^5 \hat{N}_5(\xi/2),\\ \hat{\psi}_j^{6,4}(\xi) &= 2^4 \hat{q}_j^{6,4}(\xi/2)\left(1-e^{-i\xi/2}\right)^4 \hat{N}_6(\xi/2).\end{aligned}$$

The coefficients $\hat{q}_{j,k}^{5,5}$ *and* $\hat{q}_{j,k}^{6,4}$ *are given in Table 3.4 and Table 3.6. Note that the coefficient vectors* $(\hat{q}_{j,k}^{5,5})$ *and* $(\hat{q}_{j,k}^{6,4})$ *have the same length for each* j. *In addition, we*

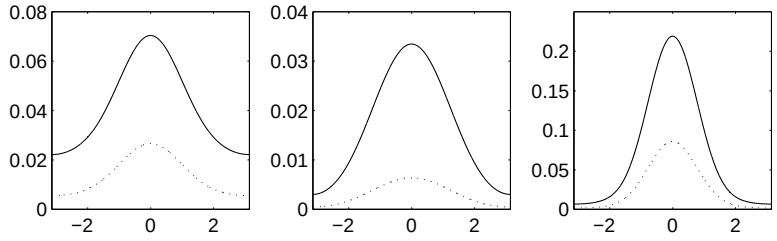

FIGURE 6.1. $e^{3i\xi}\hat{q}_1^{5,5}(\xi)$ (left, dotted) and $e^{3i\xi}\hat{q}_1^{6,4}(\xi)$ (left, solid), $e^{4i\xi}\hat{q}_j^{5,5}(\xi)$ (dotted) and $e^{4i\xi}\hat{q}_j^{6,4}(\xi)$ (solid) for $j=2$ (middle) and $j=3$ (right).

have (see Figure 6.1)

$$\begin{aligned}&\hat{q}_1^{5,5}(\xi) = e^{-3i\xi}|\hat{q}_1^{5,5}(\xi)|,\ \hat{q}_1^{6,4}(\xi) = e^{-3i\xi}|\hat{q}_1^{6,4}(\xi)|,\\ &\hat{q}_2^{5,5}(\xi) = e^{-4i\xi}|\hat{q}_2^{5,5}(\xi)|,\ \hat{q}_2^{6,4}(\xi) = e^{-4i\xi}|\hat{q}_2^{6,4}(\xi)|,\\ &\hat{q}_3^{5,5}(\xi) = e^{-4i\xi}|\hat{q}_3^{5,5}(\xi)|,\ \hat{q}_3^{6,4}(\xi) = e^{-4i\xi}|\hat{q}_3^{6,4}(\xi)|,\ \xi\in\mathbb{R}.\end{aligned}$$

Namely, the phases of $\hat{q}_j^{5,5}$ *and* $\hat{q}_j^{6,4}$ *are identical for each* j. *Now we compare the phases of* $\hat{\psi}_j^{5,5}$ *and* $\hat{\psi}_j^{6,4}$. *For the comparison we describe* $\hat{\psi}_j^{5,5}$ *in a different way as*

$$\begin{aligned}\hat{\psi}_j^{5,5}(\xi) &= 2^5 \hat{q}_j^{5,5}(\xi/2)\left(1-e^{-i\xi/2}\right)^4 (i\xi/2)\hat{N}_6(\xi/2)\\ &= 2^4 i\xi \hat{q}_j^{5,5}(\xi/2)\left(1-e^{-i\xi/2}\right)^4 \hat{N}_6(\xi/2)\\ &= 2^4 i\mathrm{sgn}(\xi)|\xi|\hat{q}_j^{5,5}(\xi/2)\left(1-e^{-i\xi/2}\right)^4 \hat{N}_6(\xi/2).\end{aligned}$$

Note that $\hat{\psi}_j^{5,5}$ *and* $\hat{\psi}_j^{6,4}$ *have the common factor* $\left(1-e^{-i\cdot/2}\right)^4\hat{N}_6$. *In addition, owing to* $\rho_{\hat{q}_j^{5,5}} = \rho_{\hat{q}_j^{6,4}}$, $j=1,2,3$, *the difference of the phases arises only from the factor* $i\mathrm{sgn}(\xi)$ *whose phase corresponds to* $\frac{\pi}{2}\mathrm{sgn}(\xi)$. *Therefore, we have*

$$\rho_{\hat{\psi}_j^{5,5}}(\xi) = \rho_{\hat{\psi}_j^{6,4}}(\xi) + \frac{\pi}{2}\mathrm{sgn}(\xi) + 2\pi\ell,\ \ell\in\mathbb{Z}\ a.e.\ \xi\in\mathbb{R}, \tag{6.5}$$

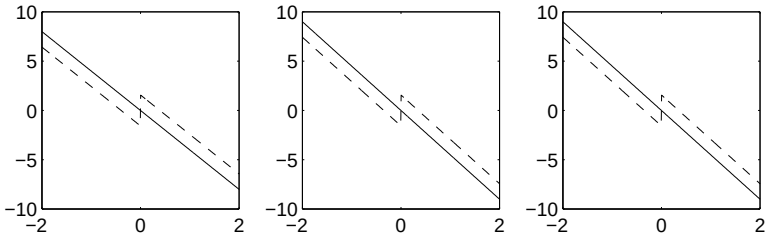

FIGURE 6.2. $\rho_{\hat{\psi}_j^{5,5}}$ (dashed) and $\rho_{\hat{\psi}_j^{6,4}}$ (solid), for $j = 1$ (left), $j = 2$ (middle), and $j = 3$ (right).

which satisfies the requirement (6.4) perfectly (see Figure 6.2). The linear phase of $\hat{\psi}_j^{6,4}$ *is*

$$\rho_{\hat{\psi}_j^{6,4}}(\xi) = (\rho_j - 5)\xi/2 + 2\pi\ell, \quad \ell \in \mathbb{Z}$$

from

$$\hat{\psi}_j^{6,4}(\xi) \;=\; 2^3|\hat{q}_j^{6,4}(\xi/2)||2\sin\xi/4|^4|\hat{N}_6(\xi/2)|e^{i(\rho_j-5)\xi/2},$$

where $\rho_j\xi$ *is the phase of* $\hat{q}_j^{6,4}(\xi)$ *and* $\rho_1 = -3, \rho_2 = \rho_3 = -4$.
If we compare the magnitudes of $\hat{\psi}_j^{5,5}$ *and* $\hat{\psi}_j^{6,4}$*, we have (see Figure 6.3)*

$$|\hat{\psi}_j^{5,5}| \approx |\hat{\psi}_j^{6,4}|, \text{ for } j = 1, 2, 3.$$

Figure 6.4 shows that $|\hat{\psi}_j^{5,5}(\xi) + i\hat{\psi}_j^{6,4}(\xi)|$ *vanishes approximately for* $\xi < 0$.

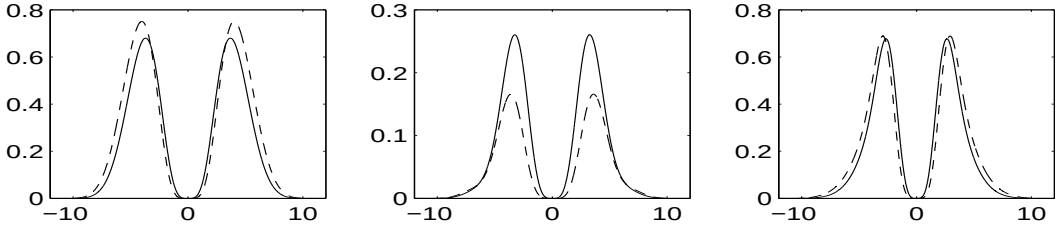

FIGURE 6.3. $|\hat{\psi}_j^{5,5}|$ (dashed) and $|\hat{\psi}_j^{6,4}|$ (solid), for $j = 1$ (left), $j = 2$ (middle), and $j = 3$ (right) .

Remark 6.2. *1. If we give priority to the approximation of the Hilbert transform of* $\psi_j^{5,5}$ *for* $j = 1, 2, 3$*, we obtain better approximations of the magnitudes of* $\hat{\psi}_j^{5,5}$ *through* $c_j\psi_j^{6,4}$*, where* $c_1 \doteq 1.1042$*,* $c_2 \doteq 0.6370$*, and* $c_3 \doteq 1.0177$*. Hence* $|\hat{\psi}_j^{5,5}(\xi) + ic_j\hat{\psi}_j^{6,4}(\xi)|$ *is smaller for* $\xi < 0$ *(see Figure 6.4). Note that* $\{c_j\psi_{j,k,\ell}^{6,4}, j = 1, 2, 3, k, \ell \in \mathbb{Z}\}$ *is not a tight frame anymore, but a frame with frame bounds*

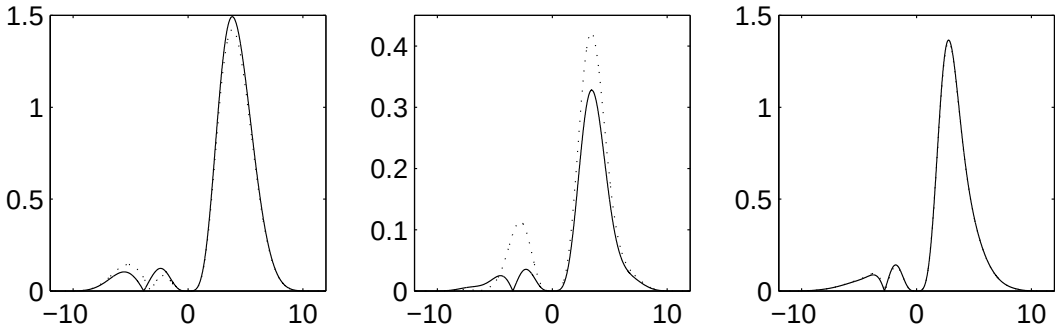

FIGURE 6.4. $|\hat{\psi}_j^{5,5} + i\hat{\psi}_j^{6,4}|$ (dotted) and $|\hat{\psi}_j^{5,5} + ic_j\hat{\psi}_j^{6,4}|$ (solid) for $j = 1$ (left), $j = 2$ (middle), and $j = 3$ (right).

$A \doteq 0.6370^2$ *and* $B \doteq 1.1042^2$.

2. Note that the generators $\psi_j^{5,5}$ *and* $\psi_j^{6,4}$ *for* $j = 1, 2, 3$, *are antisymmetric and symmetric, respectively (see Figure 3.4 and Figure 3.6). Furthermore, they have compact supports, high vanishing moments, and enough smoothness.*

3. It is apparent that (6.5) follows from the fact that the trigonometric polynomials $\hat{q}_j^{5,5}(\xi)$ *and* $\hat{q}_j^{6,4}(\xi)$ *have the same number of coefficients and, moreover, the phases are the same for each* j. *If these properties hold generally for the trigonometric polynomials* $\hat{q}_j^{m,m}(\xi)$ *and* $\hat{q}_j^{m+1,m-1}(\xi)$, *we have automatically (6.5) for the pair* $(\psi_j^{m,m}, \psi_j^{m+1,m-1})$, $j = 1, 2, 3$. *In addition, we expect that the magnitudes of* $\psi_j^{m,m}$ *and* $\psi_j^{m+1,m-1}$, $j = 1, \ldots, r$, *are approximately the same as those in Example 6.1. Therefore we conjecture that* $(\psi_j^{m,m}, \psi_j^{m+1,m-1})$, $j = 1, \ldots, r, m \geq 3$, *generate approximate Hilbert transform pairs of MRA tight frames in the sense of (6.3) and (6.4).*

Now we recall that $\hat{q}_j^{m,m}(\xi)$ and $\hat{q}_j^{m+1,m-1}(\xi)$ have the same number of coefficients for $m = 3, 4$. Using it we address that $(\psi_j^{4,2}, \psi_j^{3,3})$ and $(\psi_j^{4,4}, \psi_j^{5,3})$, $j = 1, 2, 3$, are approximate Hilbert transform pairs as well.

Example 6.3. *For the pairs* $(\psi_j^{3,3}, \psi_j^{4,2})$, $j = 1, 2, 3$, *we have*

$$\begin{aligned}
\hat{\psi}_j^{3,3}(\xi) &= 2^3 \hat{q}_j^{3,3}(\xi/2) \left(1 - e^{-i\xi/2}\right)^3 \hat{N}_3(\xi/2), \\
\hat{\psi}_j^{4,2}(\xi) &= 2^2 \hat{q}_j^{4,2}(\xi/2) \left(1 - e^{-i\xi/2}\right)^2 \hat{N}_4(\xi/2),
\end{aligned}$$

where the coefficients of the trigonometric polynomials are given in Table 3.2 and Table A.3, respectively. As in the previous example, Figure 6.5 shows that $|\hat{\psi}_j^{3,3}(\xi) + i\hat{\psi}_j^{4,2}(\xi)|$ *vanishes approximately for* $\xi < 0$.

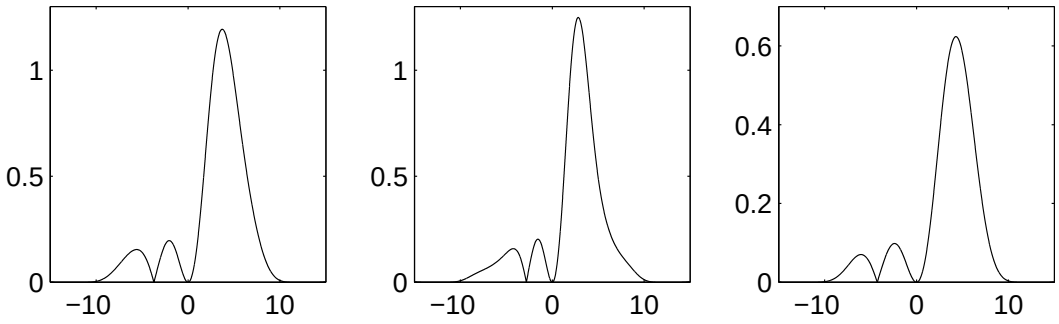

FIGURE 6.5. $|\hat{\psi}_j^{3,3} + i\hat{\psi}_j^{4,2}|$ for $j = 1$ (left), $j = 2$ (middle), and $j = 3$ (right).

Example 6.4. *The pairs* $(\psi_j^{4,4}, \psi_j^{5,3}), j = 1, 2, 3$, *have the Fourier transforms*

$$\begin{aligned} \hat{\psi}_j^{4,4}(\xi) &= 2^4 \hat{q}_j^{4,4}(\xi/2) \left(1 - e^{-i\xi/2}\right)^4 \hat{N}_4(\xi/2), \\ \hat{\psi}_j^{5,3}(\xi) &= 2^3 \hat{q}_j^{5,3}(\xi/2) \left(1 - e^{-i\xi/2}\right)^3 \hat{N}_5(\xi/2), \end{aligned}$$

where the coefficients of $\hat{q}_j^{4,4}$ *and* $\hat{q}_j^{5,3}$ *are given in (*[**8**]*) and Table A.5. Figure 6.6 indicates that* $|\hat{\psi}_j^{4,4}(\xi) + i\hat{\psi}_j^{5,3}(\xi)|$ *vanishes approximately for* $\xi < 0$.

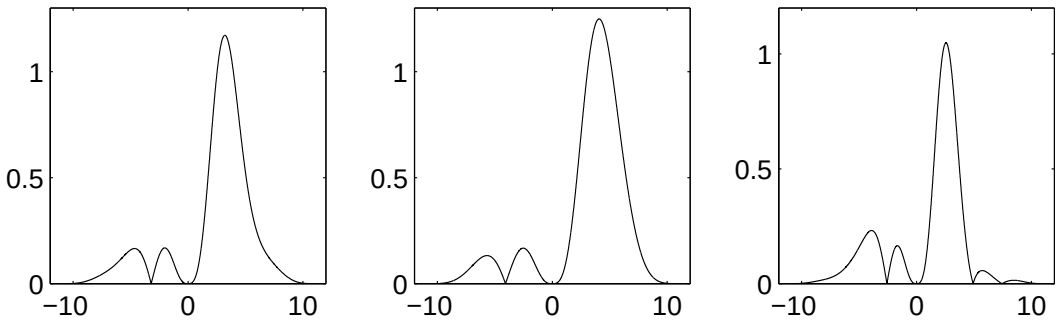

FIGURE 6.6. $|\hat{\psi}_j^{4,4} + i\hat{\psi}_j^{5,3}|$ for $j = 1$ (left), $j = 2$ (middle), and $j = 3$ (right).

CHAPTER 7

Generating new MRA bi-frames from given MRA bi-frames

From an MRA bi-frame, we find a way to produce an MRA bi-frame $(\{T\psi_{j,k,\ell}\}, \{T^{-1}\psi_{j,k,\ell}\})$, where T is a linear (possibly unbounded) operator. Our construction is based on the characterization of MRA bi-frames of [**13**] which we present in Section 7.1. As some concrete examples for T, we study the differentiation $T = \mathcal{D}$ in Section 7.2 and the operator $\Lambda = \mathcal{H}\mathcal{D}$ in Section 7.3. The connection of $\mathcal{D}$ with the "commutation" of wavelets is explored. Section 7.4 provides much more general method. Our Theorem 7.9 is an extension of the result by Zhao ([**30**]) to MRA bi-frames. Finally, in Section 7.5 we develop an analogue of the "Lifting Scheme" by Sweldens ([**29**]) for MRA bi-frames.

7.1. Characterization of MRA bi-frames

The characterization of MRA bi-frames are based on the *mixed fundamental function*. Let $\{\psi_{j,k,\ell}, 1 \le j \le r, k, \ell \in \mathbb{Z}\}$ and $\{\tilde{\psi}_{j,k,\ell}, 1 \le j \le r, k, \ell \in \mathbb{Z}\}$ be two MRA-based families in $L^2(\mathbb{R})$, with two-scale symbols q_j and $\tilde{q}_j, j = 1, \dots, r$, respectively, and ϕ, $\tilde{\phi}$, be the corresponding refinable functions with two-scale symbols p and $\tilde{p}$, respectively. The following function is called *the mixed fundamental function* for dyadic scaling:

$$S_M(\xi) := \sum_{k=0}^{\infty} \sum_{j=1}^{r} q_j(2^k\xi)\overline{\tilde{q}_j(2^k\xi)} \prod_{m=0}^{k-1} p(2^m\xi)\overline{\tilde{p}(2^m\xi)}. \tag{7.1}$$

The function S_M is well-defined, and essentially bounded, if each of the two families $\{\psi_{j,k,\ell}\}$ and $\{\tilde{\psi}_{j,k,\ell}\}$ is a Bessel system ([**13**]), since the inequality

$$S_M \le \sqrt{S\widetilde{S}}$$

holds, where S and $\widetilde{S}$ are the fundamental functions (4.9) of the two families. In addition, it follows from the definition, as in (4.10), that

$$S_M(\xi) \;=\; S_M(2\xi)p(\xi)\overline{\tilde{p}(\xi)} + \sum_{j=1}^{r} q_j(\xi)\overline{\tilde{q}_j(\xi)},\ a.e.\ \xi \in \mathbb{R} \tag{7.2}$$

Now we give the characterization of MRA bi-frames for the one-dimensional and dyadic case. This is a special case of [**13**, Proposition 5.2].

Proposition 7.1. [**13**, Proposition 5.2] *Assume that the combined MRA masks $\tau = (p, q_1, \dots, q_r)$ and $\tilde{\tau} = (\tilde{p}, \tilde{q}_1, \dots, \tilde{q}_r)$ are bounded. Assume also that $\hat{\phi}$ and $\hat{\tilde{\phi}}$ are continuous at the origin and $\hat{\phi}(0) = \hat{\tilde{\phi}}(0) = 1$, and that the corresponding wavelet systems $\{\psi_{j,k,\ell}, 1 \le j \le r, k, \ell \in \mathbb{Z}\}$ and $\{\tilde{\psi}_{j,k,\ell}, 1 \le j \le r, k, \ell \in \mathbb{Z}\}$ are Bessel systems. Then the following conditions are equivalent:*
(a) The pair $\Big(\{\psi_{j,k,\ell}, 1 \le j \le r, k, \ell \in \mathbb{Z}\}, \{\tilde{\psi}_{j,k,\ell}, 1 \le j \le r, k, \ell \in \mathbb{Z}\}\Big)$ is an MRA bi-frame.
(b) For all $\xi \in \sigma(V_0) \cap \sigma(\tilde{V}_0)$, the mixed fundamental function S_M satisfies:
(b1) $\lim_{j\to-\infty} S_M(2^j\xi) = 1$,
(b2) If $\xi + \pi \in \sigma(V_0) \cap \sigma(\tilde{V}_0)$, we have

$$S_M(2\xi)p(\xi)\overline{\tilde{p}(\xi+\pi)} + \sum_{j=1}^{r} q_j(\xi)\overline{\tilde{q}_j(\xi+\pi)} = 0. \tag{7.3}$$

This result leads to the following sufficient condition for the construction of an MRA bi-frame, which allows us to adopt a simple 2π-periodic function instead of the mixed fundamental function.

Proposition 7.2. [**13**, Corollary 5.3] *(The mixed oblique extension principle (MOEP)) Let $\tau := (p, q_1, \dots, q_r)$ and $\tilde{\tau} = (\tilde{p}, \tilde{q}_1, \dots, \tilde{q}_r)$ be the combined masks of the wavelet systems $\{\psi_{j,k,\ell}, 1 \le j \le r, k, \ell \in \mathbb{Z}\}$ and $\{\tilde{\psi}_{j,k,\ell}, 1 \le j \le r, k, \ell \in \mathbb{Z}\}$, respectively. Assume that Assumption 4.4 is satisfied by each system and that both are Bessel systems. Suppose that there exists a 2π-periodic function S_M that satisfies the following:*
(i) S_M is essentially bounded, continuous at the origin, and $S_M(0) = 1$.

(ii) If $\xi, \xi+\pi \in \sigma(V_0) \cap \sigma(\tilde{V}_0)$, *then*

$$S_M(2\xi)p(\xi)\overline{\tilde{p}(\xi+\nu)} + \sum_{j=1}^{r} q_j(\xi)\overline{\tilde{q}_j(\xi+\nu)} = \begin{cases} S_M(\xi), & \text{if } \nu = 0, \\ 0, & \text{if } \nu = \pi. \end{cases} \tag{7.4}$$

Then $\Big(\{\psi_{j,k,\ell}, 1 \le j \le r, k, \ell \in \mathbb{Z}\}, \{\tilde{\psi}_{j,k,\ell}, 1 \le j \le r, k, \ell \in \mathbb{Z}\}\Big)$ *is an MRA bi-frame.*

7.2. Commutation of MRA bi-frames

First, we recall the commutation of biorthogonal wavelets ([**12**]). Our aim is to show that the same approach works for MRA bi-frames.

Let $\{\psi, \tilde{\psi}\}$ be a biorthogonal wavelet with corresponding scaling functions ϕ and $\tilde{\phi}$. Furthermore, let $q, \tilde{q}$, and $p, \tilde{p}$, be the respective two-scale symbols. Commutation constructs a new pair $P, \tilde{P}$, by means of

$$P(\xi) = 2p(\xi)/(1+e^{i\xi}),\ \tilde{P}(\xi) = \frac{1}{2}\tilde{p}(\xi)(1+e^{-i\xi}). \tag{7.5}$$

They result in a new pair of scaling functions Φ and $\tilde{\Phi}$, which are related to ϕ and $\tilde{\phi}$ by differentiation/integration, that is to say:

$$\hat{\phi}(\xi) = \hat{\Phi}(\xi)\frac{e^{i\xi}-1}{i\xi} \quad \Leftrightarrow \quad \frac{d}{dx}\phi(x) = \Phi(x+1) - \Phi(x), \tag{7.6}$$

$$\hat{\tilde{\Phi}}(\xi) = \hat{\tilde{\phi}}(\xi)\frac{1-e^{-i\xi}}{i\xi} \quad \Leftrightarrow \quad \frac{d}{dx}\tilde{\Phi}(x) = \tilde{\phi}(x) - \tilde{\phi}(x-1). \tag{7.7}$$

The other two-scale symbols Q and $\tilde{Q}$ are given by (1.11)

$$Q(\xi) = q(\xi)(1-e^{i\xi})/2,\ \tilde{Q}(\xi) = 2\tilde{q}(\xi)/(1-e^{-i\xi}). \tag{7.8}$$

As a result, we have

$$\Psi = -\frac{1}{4}\frac{d\psi}{dx},\ \tilde{\psi} = \frac{1}{4}\frac{d\tilde{\Psi}}{dx}, \tag{7.9}$$

and $\{\Psi, \tilde{\Psi}\}$ is a biorthogonal wavelet with scaling functions $\{\Phi, \tilde{\Phi}\}$.

In Theorem 7.4 we reveal that there exists commutation for MRA bi-frames as well. Lemma 7.3 ([**10**, Theorem 1]) provides a sufficient condition for a Bessel system and will be used in the remaining sections.

Lemma 7.3. [**10**, Theorem 1] *Let* ψ *be piecewise* Lip α, $0 < \alpha \le 1$, *and* $|\psi(x)| \le C(1+|x|)^{-1-\varepsilon}$ *for some* $\varepsilon > 0$, $0 < C < \infty$. *If* $\int \psi(x)dx = 0$, *then* $\{a^{j/2}\psi(a^j x - kb), k, \ell \in \mathbb{Z}\}$ *is a Bessel system for arbitrary* $a > 1, b > 0$.

Note that if $\{\psi_{j_0,k,\ell}, k,\ell \in \mathbb{Z}\}$ is a Bessel system for each $j_0 \in \{1,\dots,r\}$, then $\{\psi_{j,k,\ell}, 1 \le j \le r, k,\ell \in \mathbb{Z}\}$ is also a Bessel system.

Theorem 7.4. *Let $\hat{\phi}$ and $\hat{\tilde{\phi}}$ be continuous at the origin and $\hat{\phi}(0) = \hat{\tilde{\phi}}(0) = 1$. Furthermore, let the corresponding wavelet system pair*

$$\Big(\{\psi_{j,k,\ell}, 1 \le j \le r, k,\ell \in \mathbb{Z}\}, \{\tilde{\psi}_{j,k,\ell}, 1 \le j \le r, k,\ell \in \mathbb{Z}\}\Big)$$

be an MRA bi-frame, in which each generator satisfies the following regularity and decay conditions: $\psi_j' \in$ Lip α, $\int_{-\infty}^x \tilde{\psi}_j(y)dy \in$ Lip $\tilde{\alpha}$, for some $\alpha, \tilde{\alpha} > 0$, and $\psi_j'(x) = O((1+|x|)^{-1-\varepsilon})$, $\int_{-\infty}^x \tilde{\psi}_j(y)dy = O((1+|x|)^{-1-\tilde{\varepsilon}})$, for some $\varepsilon, \tilde{\varepsilon} > 0$. Assume also that the symbols satisfy:

$$(7.10) \qquad (i)\ p(\xi) = \left(\frac{1+e^{-i\xi}}{2}\right)^m p_0(\xi),\ \tilde{p}(\xi) = \left(\frac{1+e^{-i\xi}}{2}\right)^{\tilde{m}} \tilde{p}_0(\xi),$$

where $m \ge 2, \tilde{m} \ge 1$, and $p_0(\pi), \tilde{p}_0(\pi) \ne 0$, and $p_0, \tilde{p}_0$, are bounded.

$$(7.11) \qquad (ii)\ q_j(\xi) = \left(\frac{1-e^{-i\xi}}{2}\right)^{m_j} q_0^j(\xi),\ \tilde{q}_j(\xi) = \left(\frac{1-e^{-i\xi}}{2}\right)^{\tilde{m}_j} \tilde{q}_0^j(\xi),$$

where $m_j \ge 1, \tilde{m}_j \ge 2$, and $q_0^j(0), \tilde{q}_0^j(0) \ne 0$, and $q_0^j, \tilde{q}_0^j$, are bounded. Namely, ψ_j and $\tilde{\psi}_j$ have m_j and $\tilde{m}_j$ vanishing moments, respectively. The associated mixed fundamental function is denoted by s_M.
If we define new symbols for j=1,...,r,

$$(7.12) \qquad P(\xi) = 2p(\xi)/(1+e^{i\xi}), \qquad \tilde{P}(\xi) = \tilde{p}(\xi)(1+e^{-i\xi})/2,$$

$$(7.13) \qquad Q_j(\xi) = q_j(\xi)(1-e^{i\xi})/2, \qquad \tilde{Q}_j(\xi) = 2\tilde{q}_j(\xi)/(1-e^{-i\xi}),$$

then the associated pair of systems

$$\Big(\{\Psi_{j,k,\ell}, 1 \le j \le r, k,\ell \in \mathbb{Z}\}, \{\tilde{\Psi}_{j,k,\ell}, 1 \le j \le r, k,\ell \in \mathbb{Z}\}\Big)$$

is again an MRA bi-frame with the same mixed fundamental function s_M. Moreover, the generators $\Psi_j, \tilde{\Psi}_j,\ j = 1,\dots,r$, and scaling functions $\Phi, \tilde{\Phi}$, are related to $\psi_j, \tilde{\psi}_j,\ j = 1,\dots,r$, and $\phi, \tilde{\phi}$, by differentiation/integration.

Proof.

We make use of Proposition 7.1 for the proof. First, the boundedness of the two-scale symbols should be examined. By (7.10) and (7.12), we have

$$P(\xi) = e^{-i\xi}\left(\frac{1+e^{-i\xi}}{2}\right)^{m-1} p_0(\xi), \quad m \geq 1.$$

Hence, P is bounded due to the boundedness of p_0. From (7.11) and (7.13) we have

$$\tilde{Q}_j(\xi) = \left(\frac{1-e^{-i\xi}}{2}\right)^{\tilde{m}_j-1} \tilde{q}_0^j(\xi), \quad \tilde{m}_j \geq 2,$$

and $\tilde{Q}_j$ is bounded as well by the boundedness of $\tilde{q}_0^j$. The other symbols $\tilde{P}$ and Q_j are also bounded since $\tilde{p}$ and q_j are.

Now we check the continuity of $\hat{\Phi}$ and $\hat{\tilde{\Phi}}$ at the origin. By (7.6) and the continuity of $\hat{\phi}$ at the origin, we have

$$\lim_{\xi\to 0}\hat{\Phi}(\xi) = \lim_{\xi\to 0}\hat{\phi}(\xi)\frac{i\xi}{e^{i\xi}-1} = \hat{\phi}(0)\cdot 1 = 1.$$

Analogously, it follows that

$$\lim_{\xi\to 0}\hat{\tilde{\Phi}}(\xi) = 1.$$

Next, we show that each system $\{\Psi_{j,k,\ell}, 1 \leq j \leq r, k, \ell \in \mathbb{Z}\}$ and $\{\tilde{\Psi}_{j,k,\ell}, 1 \leq j \leq r, k, \ell \in \mathbb{Z}\}$ is a Bessel system, which is generated from the masks Q_j and $\tilde{Q}_j, j = 1, \ldots, r$, respectively. For the proof we apply Lemma 7.3. From (7.9) we get wavelets Ψ_j and $\tilde{\Psi}_j$ such that

$$\Psi_j(x) = -\frac{1}{4}\psi_j'(x), \;\; \tilde{\Psi}_j(x) = 4\int_{-\infty}^{x}\tilde{\psi}_j(y)dy, \;\; for\; j = 1, \ldots, r.$$

By assumptions on ψ_j and $\tilde{\psi}_j$, we have $\Psi_j \in \text{Lip}\,\alpha, \tilde{\Psi}_j \in \text{Lip}\,\tilde{\alpha}$ for some $\alpha > 0, \tilde{\alpha} > 0$, and $\Psi_j = O((1+|x|)^{-1-\varepsilon}$ and $\tilde{\Psi}_j = O((1+|x|)^{-1-\tilde{\varepsilon}}$. In addition, $\hat{\Psi}_j(0) = 0$ and $\hat{\tilde{\Psi}}_j(0) = 0$ from (7.11) and (7.13). Consequently, both families $\{\Psi_{j,k,\ell}\}$ and $\{\tilde{\Psi}_{j,k,\ell}\}$ are Bessel systems.

Next, we show that the mixed fundamental function for $P, \tilde{P}, Q_j, \tilde{Q}_j, j = 1, \ldots, r$, is identical to that of $p, \tilde{p}, q_j, \tilde{q}_j, j = 1, \ldots, r$. From (7.12) and (7.13), we have

$$\begin{aligned} P(\xi)\overline{\tilde{P}(\xi)} &= p(\xi)(2/(1+e^{i\xi}))\;\overline{\tilde{p}(\xi)}((1+e^{i\xi})/2) = p(\xi)\overline{\tilde{p}(\xi)}, \\ Q_j(\xi)\overline{\tilde{Q}_j(\xi)} &= q_j(\xi)((1-e^{i\xi})/2)\;\overline{\tilde{q}_j(\xi)}(2/(1-e^{i\xi})) = q_j(\xi)\overline{\tilde{q}_j(\xi)}. \end{aligned}$$

Applying these identities to (7.1) leads to

$$\begin{aligned} S_M(\xi) &= \sum_{k=0}^{\infty}\sum_{j=1}^{r} Q_j(2^k\xi)\overline{\tilde{Q}_j(2^k\xi)}\prod_{m=0}^{k-1} P(2^m\xi)\overline{\tilde{P}(2^m\xi)} \\ &= \sum_{k=0}^{\infty}\sum_{j=1}^{r} q_j(2^k\xi)\overline{\tilde{q}_j(2^k\xi)}\prod_{m=0}^{k-1} p(2^m\xi)\overline{\tilde{p}(2^m\xi)} \\ &= s_M(\xi), \quad a.e.\ \xi\in\mathbb{R}. \end{aligned} \tag{7.14}$$

Therefore, it is clear that $(b1)$ in Proposition 7.1 holds automatically.
We demonstrate, finally, that $(b2)$ holds for S_M and the symbols $P, Q_j, \tilde{P}, \tilde{Q}_j, j = 1,\dots,r$. From (7.12) and (7.13) we see that

$$\begin{aligned} & S_M(2\xi)P(\xi)\overline{\tilde{P}(\xi+\pi)} + \sum_{j=1}^{r} Q_j(\xi)\overline{\tilde{Q}_j(\xi+\pi)} \\ = \;& s_M(2\xi)p(\xi)(2/(1+e^{i\xi}))\ \overline{\tilde{p}(\xi+\pi)}((1-e^{i\xi})/2) \\ & + \sum_{j=1}^{r} q_j(\xi)((1-e^{i\xi})/2)\ \overline{\tilde{q}_j(\xi+\pi)}(2/(1+e^{i\xi})) \\ = \;& \frac{1-e^{i\xi}}{1+e^{i\xi}}\left[s_M(2\xi)p(\xi)\overline{\tilde{p}(\xi+\pi)} + \sum_{j=1}^{r} q_j(\xi)\overline{\tilde{q}_j(\xi+\pi)}\right] = 0, \quad a.e.\ \xi\in\mathbb{R}. \end{aligned} \tag{7.15}$$

□

Remark 7.5. *The expression in (7.15) is zero even for the pole $\xi\in(2\mathbb{Z}+1)\pi$ of $\frac{1-e^{i\xi}}{1+e^{i\xi}}$. Namely, we show that*

$$s_M(2\xi)p(\xi)\overline{\tilde{p}(\xi+\pi)} + \sum_{j=1}^{r} q_j(\xi)\overline{\tilde{q}_j(\xi+\pi)} = (1+e^{i\xi})^2U(\xi), \tag{7.16}$$

for some 2π-periodic bounded function U. From the conditions on the two-scale symbols (7.10)-(7.11), we have

$$\begin{aligned} & s_M(2\xi)p(\xi)\overline{\tilde{p}(\xi+\pi)} + \sum_{j=1}^{r} q_j(\xi)\overline{\tilde{q}_j(\xi+\pi)} \\ = \;& s_M(2\xi)\left(\frac{1+e^{-i\xi}}{2}\right)^m p_0(\xi)\left(\frac{1-e^{i\xi}}{2}\right)^{\tilde{m}}\overline{\tilde{p}_0(\xi+\pi)} \\ & + \sum_{j=1}^{r}\left(\frac{1-e^{-i\xi}}{2}\right)^{m_j} q_0^j(\xi)\left(\frac{1+e^{i\xi}}{2}\right)^{\tilde{m}_j}\overline{\tilde{q}_0^j(\xi+\pi)} \\ = \;& (1+e^{i\xi})^2U(\xi), \end{aligned}$$

since $m \geq 2$ *and* $\tilde{m}_j \geq 2$.

7.3. Application to Λ-operator

As an application, we show that an MRA bi-frame $(\{\Lambda\psi_{j,k,\ell}\}, \{\Lambda^{-1}\psi_{j,k,\ell}\})$ is obtained from an MRA tight frame $\{\psi_{j,k,\ell}\}$ by combining Theorem 4.12 and Theorem 7.4.

Theorem 7.6. *Let* $\psi_j, j = 1, \ldots, r$, *be generators of an MRA tight frame with refinable function* ϕ. *Furthermore, let the refinable function and symbols* p, q_j, *satisfy all assumptions of Theorem 4.12 with* $\hat{\phi}(\xi) = R(\xi)\hat{N}_m(\xi)$ *and* $p(\xi) = p_m(\xi)p_0(\xi)$. *Let* $\Psi_j,\ j = 1, \ldots, r$, *and* Φ *denote the generators and the refinable function of the MRA tight frame with masks* P, Q_j, *obtained by the result of Theorem 4.12. If we suppose that* Φ, $\Psi_j, j = 1, \ldots, r$, *and* P, Q_j, *meet all conditions of Theorem 7.4, then* $(\{\eta_{j,k,\ell} := \Lambda\psi_{j,k,\ell}\}, \{\tilde{\eta}_{j,k,\ell} := \Lambda^{-1}\psi_{j,k,\ell}\})$ *is an MRA bi-frame with refinable functions* φ *and* $\tilde{\varphi}$, *where*

$$\hat{\varphi}(\xi) = e^{-i\xi}M(\xi)\hat{\phi}(\xi) = e^{-i\xi}M(\xi)R(\xi)\hat{N}_m(\xi), \tag{7.17}$$

$$\hat{\tilde{\varphi}}(\xi) = M(\xi)\left(\frac{1-e^{-i\xi}}{i\xi}\right)^2\hat{\phi}(\xi) = M(\xi)R(\xi)\hat{N}_{m+2}(\xi). \tag{7.18}$$

Moreover, the associated symbols are given by

$$P_\varphi(\xi) = e^{-i\xi}\frac{M(2\xi)}{M(\xi)}p(\xi) = \frac{2e^{-i\xi}}{|1+e^{-i\xi}|}p(\xi), \tag{7.19}$$

$$P_{\tilde{\varphi}}(\xi) = \frac{M(2\xi)}{M(\xi)}\left(\frac{1+e^{-i\xi}}{2}\right)^2 p(\xi) = \frac{(1+e^{-i\xi})^2}{2|1+e^{-i\xi}|}p(\xi) \tag{7.20}$$

$$= \frac{M(2\xi)}{M(\xi)}p_{m+2}(\xi)p_0(\xi), \tag{7.21}$$

and

$$Q_{\eta_j}(\xi) = \frac{1-e^{i\xi}}{2}\frac{N(\xi)}{M(\xi)}q_j(\xi) = -\frac{|1-e^{-i\xi}|}{2e^{-i\xi}}q_j(\xi), \tag{7.22}$$

$$Q_{\tilde{\eta}_j}(\xi) = \frac{2}{1-e^{-i\xi}}\frac{N(\xi)}{M(\xi)}q_j(\xi) = \frac{2|1-e^{-i\xi}|}{(1-e^{-i\xi})^2}q_j(\xi). \tag{7.23}$$

As a result, the generators of the MRA bi-frame are

$$\begin{aligned}
\hat{\eta}_j(\xi) &= Q_{\eta_j}(\xi/2)\varphi(\xi/2) \\
&= -\frac{1-e^{-i\xi/2}}{2}N(\xi/2)\hat{\psi}_j(\xi) = -\frac{|\xi|}{4}\hat{\psi}_j(\xi), \qquad (7.24)\\
\hat{\tilde{\eta}}_j(\xi) &= Q_{\tilde{\eta}_j}(\xi/2)\tilde{\varphi}(\xi/2) \\
&= \frac{2}{1-e^{-i\xi/2}}N(\xi/2)q_j(\xi/2)R(\xi/2)\hat{N}_{m+2}(\xi/2) \qquad (7.25)\\
&= -8\frac{1-e^{-i\xi/2}}{\xi^2}N(\xi/2)\hat{\psi}_j(\xi) = -\frac{4}{|\xi|}\hat{\psi}_j(\xi). \qquad (7.26)
\end{aligned}$$

Proof.

Since Ψ_j, Φ, P, and Q_j fulfill all conditions of Theorem 7.4, we have an MRA bi-frame from the result of Theorem 7.4

$$(\{\eta_{j,k,\ell} = \mathcal{D}\mathcal{H}\psi_{j,k,\ell}\}, \{\tilde{\eta}_{j,k,\ell} = \mathcal{I}\mathcal{H}\psi_{j,k,\ell}\}) \qquad (7.27)$$

with refinable functions φ and $\tilde{\varphi}$. From the commutation formulations of (7.6)-(7.7), (4.20), and $\hat{\phi}(\xi) = \hat{N}_m(\xi)R(\xi)$ we have

$$\begin{aligned}
\hat{\varphi}(\xi) &= \frac{i\xi}{e^{i\xi}-1}\widehat{\Phi}(\xi) = e^{-i\xi}M(\xi)\hat{\phi}(\xi) = e^{-i\xi}M(\xi)R(\xi)\hat{N}_m(\xi), \\
\hat{\tilde{\varphi}}(\xi) &= \frac{1-e^{-i\xi}}{i\xi}\widehat{\Phi}(\xi) = \left(\frac{1-e^{-i\xi}}{i\xi}\right)^2 M(\xi)\hat{\phi}(\xi) = M(\xi)R(\xi)\widehat{N}_{m+2}(\xi).
\end{aligned}$$

Moreover, the symbols $P_\varphi, P_{\tilde{\varphi}}$, are obtained by (7.12) and (4.22)

$$\begin{aligned}
P_\varphi(\xi) &= \frac{2}{1+e^{i\xi}}P(\xi) = \frac{2}{1+e^{i\xi}}\frac{M(2\xi)}{M(\xi)}\frac{1+e^{-i\xi}}{2}p(\xi) \\
&= e^{-i\xi}\frac{M(2\xi)}{M(\xi)}p(\xi) = \frac{2e^{-i\xi}}{|1+e^{-i\xi}|}p(\xi), \\
P_{\tilde{\varphi}}(\xi) &= \frac{1+e^{-i\xi}}{2}P(\xi) = \frac{M(2\xi)}{M(\xi)}\left(\frac{1+e^{-i\xi}}{2}\right)^2 p(\xi) \\
&= \frac{(1+e^{-i\xi})^2}{2|1+e^{-i\xi}|}p(\xi) = \frac{M(2\xi)}{M(\xi)}p_{m+2}(\xi)p_0(\xi),
\end{aligned}$$

The symbols $Q_{\eta_j}, Q_{\tilde{\eta}_j}$, are computed by (7.13) and (4.23)

$$\begin{aligned} Q_{\eta_j}(\xi) &= \frac{1-e^{i\xi}}{2} Q_j(\xi) \\ &= -e^{i\xi}\frac{1-e^{-i\xi}}{2}\frac{|1-e^{-i\xi}|}{1-e^{-i\xi}} q_j(\xi) = -\frac{|1-e^{-i\xi}|}{2e^{-i\xi}} q_j(\xi), \\ Q_{\tilde{\eta}_j}(\xi) &= \frac{2}{1-e^{-i\xi}} Q_j(\xi) = \frac{2|1-e^{-i\xi}|}{(1-e^{-i\xi})^2} q_j(\xi). \end{aligned}$$

Now from the assumptions that $\Psi_j = \mathcal{H}\psi_j \in \text{Lip } \alpha$ and $\frac{d}{dx}\Psi_j = \frac{d}{dx}\mathcal{H}\psi_j = O((1+|x|)^{-1-\epsilon})$ we have $\mathcal{H}\psi_j \in AC$ and $\frac{d}{dx}\mathcal{H}\psi_j \in L^2(\mathbb{R})$. Thus, by (c) and (d) of Proposition 2.2 we can verify that

$$\mathcal{D}\mathcal{H}\mathcal{H}\psi_j = \mathcal{H}\mathcal{D}\mathcal{H}\psi_j \Leftrightarrow -\mathcal{D}\psi_j = \mathcal{H}\mathcal{D}\mathcal{H}\psi_j.$$

Moreover, if we apply $\mathcal{H}$ on both sides, we obtain by (c) of Proposition 2.2 that

$$\mathcal{H}\mathcal{D}\psi_j = \mathcal{D}\mathcal{H}\psi_j.$$

That is to say, the operators $\mathcal{H}$ and $\mathcal{D}$ in (7.27) commute, and this gives $\eta_{j,k,\ell} = \Lambda\psi_{j,k,\ell}$. Therefore, the bi-frame in (7.27) is

$$(\{\mathcal{D}\mathcal{H}\psi_{j,k,\ell}\}, \{\mathcal{I}\mathcal{H}\psi_{j,k,\ell}\}) = \left(\{\Lambda\psi_{j,k,\ell}\}, \{\Lambda^{-1}\psi_{j,k,\ell}\}\right).$$

The two-scale relations reveal (7.24)-(7.26). □

Remark 7.7. *In Theorem 7.4 we addressed that the mixed fundamental function of the parent wavelet vectors $(\varphi, \eta_1, \ldots, \eta_r)$ and $(\tilde{\varphi}, \tilde{\eta}_1, \ldots, \tilde{\eta}_r)$ is identical with the fundamental function of the MRA tight frame $\{\Psi_{j,k,\ell}, 1 \le j \le r, k, \ell \in \mathbb{Z}\}$. The fundamental function of $\{\Psi_{j,k,\ell}, 1 \le j \le r, k, \ell \in \mathbb{Z}\}$ is, again, the same as s, the fundamental function of the MRA tight frame $\{\psi_{j,k,\ell}, 1 \le j \le r, k, \ell \in \mathbb{Z}\}$. In other words, the mask vectors $\tau^1 := (P_\varphi, Q_{\eta_1}, \ldots, Q_{\eta_r})$ and $\tilde{\tau}^1 := (P_{\tilde{\varphi}}, Q_{\tilde{\eta}_1}, \ldots, Q_{\tilde{\eta}_r})$ and the mixed fundamental function s satisfy the MOEP (7.4). Furthermore, the mask vector $\tau^2 := (P, Q_1, \ldots, Q_r)$ and s fulfill the OEP (4.12). The OEP (4.12) holds, again, for $\tau^3 := (p, q_1, \ldots, q_r)$ and s. Generally speaking, the triples $(\tau^1, \tilde{\tau}^1, s)$, $(\tau^2, \tilde{\tau}^2, s)$, and $(\tau^3, \tilde{\tau}^3, s)$ are three different solutions of (7.4), where $\tilde{\tau}^2 := \tau^2$ and $\tilde{\tau}^3 := \tau^3$.*

We present an example showing that an MRA bi-frame $\left(\{\Lambda\psi^{m,L}_{j,k,\ell}\},\{\Lambda^{-1}\psi^{m,L}_{j,k,\ell}\}\right)$ can be constructed from a spline MRA tight frame $\{\psi^{m,L}_{j,k,\ell},\ 1\le j\le r, k,\ell\in\mathbb{Z}\}$.

Example 7.8. *Let $\{\psi^{5,5}_{j,k,\ell}, j=1,2,3, k,\ell\in\mathbb{Z}\}$ be the MRA tight frame with vanishing moments of order 5 and with the refinable function N_5 (B-spline of order 5). The associated two-scale symbols are denoted by $p_5(\xi)=\left(\frac{1+e^{-i\xi}}{2}\right)^5$ and $q^{5,5}_j$ such that*

$$q^{5,5}_j(\xi)=2^5\hat{q}^{5,5}_j(\xi)\left(1-e^{-i\xi}\right)^5,\quad j=1,2,3. \tag{7.28}$$

The fundamental function $s_{5,5}$ is given explicitly in [**11**, Theorem 7.2.4].
Now, we apply Theorem 4.12 to the given MRA tight frame. If we employ the notations in Theorem 4.12, we have $m=m_j=5$ and $p_0\equiv 1$, $R\equiv 1$. The refinable function N_5 has compact support and satisfies Assumption 4.1. Moreover, from (7.28) it is clear that each symbol $q^{5,5}_j$ has real coefficients and vanishes at $\xi=0$. As we already mentioned in Remark 4.3, the associated fundamental function $s_{5,5}$ is bounded and satisfies (i)-(iii) of Proposition 4.2. Thus, all conditions of Theorem 4.12 are satisfied. As a result, we have another MRA tight frame $\{\mathcal{H}\psi^{5,5}_{j,k,\ell}, j=1,2,3, k,\ell\in\mathbb{Z}\}$ with refinable function

$$\hat{\Phi}(\xi)=M(\xi)\frac{1-e^{-i\xi}}{i\xi}\hat{N}_5(\xi), \tag{7.29}$$

and symbols

$$P(\xi) = \frac{M(2\xi)}{M(\xi)}\frac{1+e^{-i\xi}}{2}p_5(\xi)=\frac{1+e^{-i\xi}}{|1+e^{-i\xi}|}p_5(\xi), \tag{7.30}$$

$$Q_j(\xi) = \frac{N(\xi)}{M(\xi)}q^{5,5}_j(\xi)=2^5\frac{|1-e^{-i\xi}|}{1-e^{-i\xi}}\hat{q}^{5,5}_j(\xi)\left(1-e^{-i\xi}\right)^5. \tag{7.31}$$

This MRA tight frame can also be considered as an MRA bi-frame

$$\left(\{\Psi_{j,k,\ell}, j=1,2,3,k,\ell\in\mathbb{Z}\},\{\tilde{\Psi}_{j,k,\ell}, j=1,2,3,k,\ell\in\mathbb{Z}\}\right),$$

where $\Psi_j=\tilde{\Psi}_j=\mathcal{H}\psi^{5,5}_j$. The corresponding refinable functions are Φ and $\tilde{\Phi}(=\Phi)$ and the two-scale symbols are $P=\tilde{P}$, $Q_j=\tilde{Q}_j$. From Theorem 4.12 it is clear that $\hat{\Phi}$ (and trivially $\widehat{\tilde{\Phi}}$) is continuous at the origin and $\hat{\Phi}(0)=1$. Now we refer to the regularity and decay of $\mathcal{H}\psi^{5,5}_j$. It is well known that $N_5\in C^3$, and, therefore, $\psi^{5,5}_j\in$

$C^3, j = 1, 2, 3$. *Since* ψ_j *has compact support,* $\frac{d^k}{dx^k}\psi_j^{5,5} \in L^2(\mathbb{R})$ *for* $k = 0, 1, 2, 3, 4$. *If we apply* (d) *of Proposition 2.2, we have*

$$\mathcal{H}\psi_j^{5,5} \in C^2 \text{ and } (\mathcal{H}\psi_j^{5,5})^{(k)} \in L^2(\mathbb{R}), \quad k = 0, 1, 2, 3, 4,$$

which is much stronger than the requirements. Finally, the conditions (i) *and* (ii) *of Thereom7.4 should be verified for the masks* P *and* Q_j *given in (7.30) and (7.31). If we employ the expressions of Thereom7.4, we have* $m = \tilde{m} = 5$ *and again* $m_j = \tilde{m}_j = 5$ *for each* j*, which is much stronger than the required conditions. The confirmation of* $\frac{1+e^{-i\xi}}{|1+e^{-i\xi}|} \neq 0$ *for* $\xi = \pi$ *and* $\frac{|1-e^{-i\xi}|}{1-e^{-i\xi}}\hat{q}_j^{5,5}(\xi) \neq 0$ *for* $\xi = 0$ *will complete the whole process of checking the requirements of Theorem7.4. They hold obviously by the fact that* $\frac{1+e^{-i\xi}}{|1+e^{-i\xi}|}$ *and* $\frac{|1-e^{-i\xi}|}{1-e^{-i\xi}}$ *lies on the unit circle and the coefficients* $\hat{q}_{j,k}$ *are positive (see Table 3.4). Consequently, Theorem 7.4 gives rise to a new MRA bi-frame*

$$\left(\{\mathcal{D}\mathcal{H}\psi_{j,k,\ell}^{5,5}\}, \{\mathcal{I}\mathcal{H}\psi_{j,k,\ell}^{5,5}\}\right) = \left(\{\mathcal{H}\mathcal{D}\psi_{j,k,\ell}^{5,5}\}, \{\mathcal{I}\mathcal{H}\psi_{j,k,\ell}^{5,5}\}\right) = \left(\{\Lambda\psi_{j,k,\ell}^{5,5}\}, \{\Lambda^{-1}\psi_{j,k,\ell}^{5,5}\}\right).$$

7.4. General method generating an MRA bi-frame from another

Theorem 7.4 and Theorem 7.6 can be understood as special methods generating an MRA bi-frame from a given MRA bi-frame. They deal with, however, only specific cases (commutation and combination of the Hilbert transform and the commutation). These results intrigue us to ask if we can find a more general method generating an MRA bi-frame from a given one. If we find any, it would be taken for a natural extension of the case of biorthogonal wavelets ([**30**, Theorem 4.1]). On the other hand, we could regard it as a generalization of Theorem 4.14 as well. In fact, using the techniques employed in both Theorem 4.14 and [**30**, Theorem 4.1], we provide a solution of our question.

Theorem 7.9. *Let an MRA bi-frame* $\left(\{\psi_{j,k,\ell}\}, \{\tilde{\psi}_{j,k,\ell}\}\right)$ *be given with refinable functions* ϕ *and* $\tilde{\phi}$ *such that* $\hat{\phi}$ *and* $\hat{\tilde{\phi}}$ *are continuous at* $\xi = 0$ *and* $\hat{\phi}(0) = \hat{\tilde{\phi}}(0) = 1$. *Furthermore, let* $p, \tilde{p}, q_j, \tilde{q}_j, j = 1, \ldots, r$*, be the associated two-scale symbols satisfying (7.10)-(7.11) with* $m, \tilde{m}, m_j, \tilde{m}_j \geq 2$. *Suppose that* s_M *denotes the associated mixed fundamental function. Now, suppose that we have new two-scale symbols*

$$P(\xi) = a(\xi)p(\xi), \; Q_j(\xi) = b_j(\xi)q_j(\xi), \tag{7.32}$$

$$\tilde{P}(\xi) = \frac{1}{\overline{a(\xi)}}\tilde{p}(\xi), \; \tilde{Q}_j(\xi) = \frac{1}{\overline{b_j(\xi)}}\tilde{q}_j(\xi), \tag{7.33}$$

such that $P, \tilde{P}, Q_j, \tilde{Q}_j$ *and* $a(\xi)$ *and* $b_j(\xi)$ *are subjected to the following conditions:*

(i) $P, \tilde{P}$, *and* $Q_j, \tilde{Q}_j$, *are bounded.*

(ii) $a(\xi)$ *and* $b_j(\xi)$ *are* 2π*-periodic, measurable, and* $\frac{a(\xi)}{a(\xi+\pi)} = \frac{b_j(\xi)}{b_j(\xi+\pi)}$.

(iii) $\prod_{k=1}^{\infty} a(2^{-k}\xi)$ *converges a.e., and its limit* $\alpha(\xi)$ *is continuous at* $\xi = 0$ *and* $\lim_{\xi\to 0} \alpha(\xi) = 1$.

Let $\Psi_j, \tilde{\Psi}_j$ *and* $\Phi, \tilde{\Phi}$ *be the functions generated by the two-scale symbols in (7.32)-(7.33) and assume that*

(iv) *they are in* $L^2(\mathbb{R})$ *and* $\{\Psi_{j,k,\ell}\}$, $\{\tilde{\Psi}_{j,k,\ell}\}$, *are Bessel systems.*

Then $\Psi_j, \tilde{\Psi}_j$, *constitute an MRA bi-frame of* $L^2(\mathbb{R})$ *with the same mixed fundamental function* s_M, *where* $\Psi_j = T\psi_j$, $\tilde{\Psi}_j = T^{-1}\tilde{\psi}_j$ *and* $(T\psi_j)^\wedge(\xi) = \alpha(\xi/2)b_j(\xi/2)\hat{\psi}_j(\xi)$, $(T^{-1}\tilde{\psi}_j)^\wedge(\xi) = \frac{1}{\overline{\alpha(\xi/2)b_j(\xi/2)}}\hat{\tilde{\psi}}_j(\xi)$.

Proof.

We apply Proposition 7.1 for the proof. From condition (i) we have the boundedness of the two-scale symbols $P, \tilde{P}$, and $Q_j, \tilde{Q}_j$. The refinable functions are obtained by

$$\hat{\Phi}(\xi) = \prod_{k=1}^{\infty} P(2^{-k}\xi) = \prod_{\ell=1}^{\infty} a(2^{-\ell}\xi) \prod_{k=1}^{\infty} p(2^{-k}\xi) = \alpha(\xi)\hat{\phi}(\xi).$$

Similarly,

$$\hat{\tilde{\Phi}}(\xi) = \frac{1}{\overline{\alpha(\xi)}}\hat{\tilde{\phi}}(\xi).$$

Hence, $\hat{\Phi}$ and $\hat{\tilde{\Phi}}$ are continuous at $\xi = 0$ and $\hat{\Phi}(0) = \hat{\tilde{\Phi}}(0) = 1$ by (iii).
On the other hand, the generators are given by

$$\begin{aligned} \hat{\Psi}_j(\xi) &= Q_j(\xi/2)\hat{\Phi}(\xi/2) = b_j(\xi/2)q_j(\xi/2)\alpha(\xi/2)\hat{\phi}(\xi/2) \\ &= \alpha(\xi/2)b_j(\xi/2)\hat{\psi}_j(\xi), \end{aligned}$$

and analogously

$$\hat{\tilde{\Psi}}_j(\xi) = \frac{1}{\overline{\alpha(\xi/2)b_j(\xi/2)}}\hat{\tilde{\psi}}_j(\xi).$$

By our assumptions, $\Psi_j, \tilde{\Psi}_j \in L^2(\mathbb{R})$ and $\{\Psi_{j,k,\ell}\}, \{\tilde{\Psi}_{j,k,\ell}\}$, are Bessel systems.
Let us compute the mixed fundamental function S_M of the new symbols. From

(7.1), we have

$$S_M(\xi) = \sum_{k=0}^{\infty} \sum_{j=1}^{r} Q_j(2^k\xi)\overline{\tilde{Q}_j(2^k\xi)} \prod_{m=0}^{k-1} P(2^m\xi)\overline{\tilde{P}(2^m\xi)}.$$

By inserting (7.32)-(7.33), we obtain

$$S_M(\xi) = \sum_{k=0}^{\infty} \sum_{j=1}^{r} q_j(2^k\xi)\overline{\tilde{q}_j(2^k\xi)} \prod_{m=0}^{k-1} p(2^m\xi)\overline{\tilde{p}(2^m\xi)} = s_M(\xi), \quad a.e.\ \xi \in \mathbb{R}.$$

Thus (b1) of Proposition 7.1 holds trivially for S_M. Finally, (b2) for $P, \tilde{P}, Q_j, \tilde{Q}_j$, and S_M is by (ii)

$$\begin{aligned} & S_M(2\xi)P(\xi)\overline{\tilde{P}(\xi+\pi)} + \sum_{j=1}^{r} Q_j(\xi)\overline{\tilde{Q}_j(\xi+\pi)} \\ = \;& s_M(2\xi)\frac{a(\xi)}{a(\xi+\pi)}p(\xi)\overline{\tilde{p}(\xi+\pi)} + \sum_{j=1}^{r} \frac{b_j(\xi)}{b_j(\xi+\pi)}q_j(\xi)\overline{\tilde{q}_j(\xi+\pi)}, \\ = \;& \frac{a(\xi)}{a(\xi+\pi)}\left[s_M(2\xi)p(\xi)\overline{\tilde{p}(\xi+\pi)} + \sum_{j=1}^{r} q_j(\xi)\overline{\tilde{q}_j(\xi+\pi)} \right] = 0, \quad a.e.\ \xi \in \mathbb{R} \qquad \square \end{aligned}$$

Remark 7.10. *1. Notice that the condition* $\frac{a(\xi)}{a(\xi+\pi)} = \frac{b(\xi)}{b(\xi+\pi)}$ *is the same as requiring that* $\frac{a(\xi)}{b(\xi)}$ *is* π*-periodic.*

2. Theorem 4.14, thus Theorem 4.8 as well, are special cases of Theorem 7.9. Let $\{\psi_{j,k,\ell}\}$ *be an MRA tight frame. The associated symbols are denoted by* $p, \tilde{p}(= p), q_j, \tilde{q}_j(= q_j)$*. If we take* $|a(\xi)| = |b_j(\xi)| = 1$ *for a.e.* $\xi \in \mathbb{R}$*, it is clear that* $\frac{a(\xi)}{a(\xi+\pi)} = a(\xi)\overline{a(\xi+\pi)}$ *and* $\frac{1}{\overline{a(\xi)}} = a(\xi)$*. Hence, (ii) and (iii) of Theorem 7.9 imply (i)-(iv) of Theorem 4.14. In addition, (i) of Theorem 7.9 holds. The two-scale symbols are*

$$P(\xi) = \tilde{P}(\xi) = a(\xi)p(\xi), \; Q_j(\xi) = \tilde{Q}_j(\xi) = b_j(\xi)q_j(\xi).$$

Thus we have another MRA tight frame. Theorem 4.8 results from $a(\xi) = e^{-i\theta(\xi)} = \frac{1+e^{-i\xi}}{|1+e^{-i\xi}|}$ *and* $b_j(\xi) = e^{i\theta(\xi-\pi)} = \frac{|1-e^{-i\xi}|}{1-e^{-i\xi}}$*.*

3. The commutation in Theorem 7.4 is also included in Theorem 7.9. Under the same hypotheses on the given MRA bi-frame and two-scale symbols, if we take $a(\xi) = \frac{2}{1+e^{i\xi}}$ *and* $b_j(\xi) = \frac{1-e^{i\xi}}{2}$*, then we obtain* $\frac{1}{\overline{a(\xi)}} = \frac{1+e^{-i\xi}}{2}$ *and* $\frac{1}{\overline{b_j(\xi)}} = \frac{2}{1-e^{-i\xi}}$*, i.e. (7.32)-(7.33) are identical with (7.12)-(7.13). From the hypotheses, the assumptions (i)-(iv) of Theorem 7.9 hold obviously. Consequently, the commutation*

gives an MRA bi-frame.

4. Theorem 7.6 results from Theorem 7.9 as well. We suppose first that an MRA tight frame $\{\psi_{j,k,\ell}, 1 \le j \le r, k, \ell \in \mathbb{Z}\}$ *is given with refinable function* ϕ*. The conditions (7.19)-(7.23) correspond to* $a(\xi) = \frac{2e^{-i\xi}}{|1+e^{-i\xi}|}$ *and* $b_j(\xi) = \frac{|1-e^{-i\xi}|}{-2e^{-i\xi}}$ *in the notion of Theorem 7.9. Under the assumptions on* p, q_j*, and* ψ_j *of Theorem 7.6, we have trivially (i) and (iv) of Theorem 7.9. Let us we check (ii) and (iii) of Theorem 7.9. It is obvious that the functions* a *and* b_j *are* 2π*-periodic and measurable. Moreover,*

$$\frac{a(\xi)}{a(\xi+\pi)} = -\frac{|1-e^{i\xi}|}{|1+e^{i\xi}|} = \frac{b_j(\xi)}{b_j(\xi+\pi)}.$$

Next, the infinite product $\prod_{k=1}^{\infty} a(2^{-k}\xi)$ *converges and is continuous at zero, with the value 1 (see the proofs of Theorem 4.12 and Theorem 7.9). As a result, we have the bi-frame*

$$\left(\{\Lambda\psi_{j,k,\ell}\}, \{\Lambda^{-1}\psi_{j,k,\ell}\}\right).$$

5. The fractional derivative/integration is realized by $a(\xi) = |\cos\xi/2|^{-\kappa}$ *and* $b(\xi) = |\sin\xi/2|^{\kappa}$ *for* $\kappa \in \mathbb{R}$*. If a given MRA bi-frame satisfies some regularity condition (if it arises from an* r*-regular MRA of* $L^2(\mathbb{R})$*), we have from Theorem 7.9 the bi-frame*

$$\left(\{\Lambda^{\kappa}\psi_{j,k,\ell}\}, \{\Lambda^{-\kappa}\psi_{j,k,\ell}\}\right),$$

where the operator Λ^{κ} *is defined on the frequency domain by* $(\Lambda^{\kappa}\psi_j)^{\wedge}(\xi) = \left(\frac{|\xi|}{4}\right)^{\kappa} \hat{\psi}_j(\xi)$.

6. Through the special cases of Theorem 7.9, we see that it generalizes the result of Zhao ([**30**, Theorem 4.1]*). The lifting scheme for MRA bi-frames, however, can not be recovered, in contrast to* [**30**, Theorem 4.1]*. In this sense we need a more general result including the lifting scheme. In the next section we prove that the lifting scheme also works for bi-frames.*

7.5. Lifting scheme of MRA bi-frames

We develop the lifting scheme for bi-frames in this section. For the construction, we make use of Proposition 7.1. A short review of the lifting scheme for biorthogonal wavelets is presented first ([**29**]). For given biorthogonal filters $\{p, \tilde{p}, q, \tilde{q}\}$, a new set of biorthogonal filters $\{P, \tilde{P}, Q, \tilde{Q}\}$ can be found as

$$P = p, \quad \tilde{P}(\xi) = \tilde{p}(\xi) + \overline{\mu(2\xi)}\tilde{q}(\xi),$$
$$Q(\xi) = q(\xi) - \mu(2\xi)p(\xi), \quad \tilde{Q} = \tilde{q}$$

where $\mu(\xi)$ is a trigonometric polynomial. If $\{\psi, \tilde{\psi}, \phi, \tilde{\phi}\}$ denotes the given biorthogonal wavelet, as a result of the lifting scheme we can have a new biorthogonal wavelet $\{\Psi, \tilde{\Psi}, \Phi, \tilde{\Phi}\}$ such that

$$\Phi = \phi, \quad \widehat{\tilde{\Phi}}(\xi) = \tilde{p}(\xi/2)\widehat{\tilde{\Phi}}(\xi/2) + \overline{\mu(\xi)}\widehat{\tilde{\Psi}}(\xi),$$
$$\hat{\Psi}(\xi) = \hat{\psi}(\xi) - \mu(\xi)\hat{\phi}(\xi), \quad \widehat{\tilde{\Psi}}(\xi) = \tilde{q}(\xi/2)\widehat{\tilde{\Phi}}(\xi/2),$$

where $\Phi = \phi$ and the trigonometric polynomial $\mu(\xi)$ satisfies $\mu(0) = 0$. Usually $\mu(\xi)$ is determined so that Q has more roots than q at the origin, i.e. Ψ has a higher order of vanishing moments than ψ. Next, we present the lifting scheme for MRA bi-frames.

Theorem 7.11. *Let an MRA bi-frame* $\left(\{\psi_{j,k,\ell}\}, \{\tilde{\psi}_{j,k,\ell}\}\right)$ *be given with refinable functions* $\phi, \tilde{\phi}$, *such that their symbols* $p, q_j, \tilde{p}, \tilde{q}_j$, $j = 1, \ldots, r$, *and the mixed fundamental function* s_M *are subjected to the assumptions of Proposition 7.1. Now, we define new symbols* $P, \tilde{P}, Q_j, \tilde{Q}_j$, *by*

$$P(\xi) = p(\xi), \quad \tilde{P}(\xi) = \tilde{p}(\xi) + \sum_{j=1}^{r} \overline{\mu_j(2\xi)}\tilde{q}_j(\xi),$$
$$Q_j(\xi) = q_j(\xi) - \mu_j(2\xi)s_M(2\xi)p(\xi), \quad \tilde{Q}_j(\xi) = \tilde{q}_j(\xi),$$

where μ_j *are measurable and bounded* 2π*-periodic functions. We suppose that Assumption 4.4 holds and* $\{\Psi_{j,k,\ell}\}$ *and* $\{\tilde{\Psi}_{j,k,\ell}\}$ *are Bessel systems. Furthermore, we assume that the spectrum of* $\tilde{V}_0$ *(with respect to* $\tilde{\Phi}$*) is a subset of that of* $\tilde{v}_0$ *(with respect to* $\tilde{\phi}$*), i.e.* $\sigma(\tilde{V}_0) \subset \sigma(\tilde{v}_0)$. *Then* $\left(\{\Psi_{j,k,\ell}\}, \{\tilde{\Psi}_{j,k,\ell}\}\right)$ *is an MRA bi-frame in the sense that Proposition 7.1 is satisfied by the symbols* $P, \tilde{P}, Q_j, \tilde{Q}_j$, *and the given fundamental function* s_M. *The generators* $\Psi_j, \tilde{\Psi}_j$, *and refinable functions* $\Phi, \tilde{\Phi}$, *are given by*

$$\Phi = \phi, \quad \widehat{\tilde{\Phi}}(\xi) = \tilde{p}(\xi/2)\widehat{\tilde{\Phi}}(\xi/2) + \sum_{j=1}^{r} \overline{\mu_j(\xi)}\widehat{\tilde{\Psi}}_j(\xi), \tag{7.34}$$

$$\hat{\Psi}_j(\xi) = \psi_j(\xi) - \mu_j(\xi)s_M(\xi)\hat{\phi}(\xi), \quad \widehat{\tilde{\Psi}}_j(\xi) = \tilde{q}_j(\xi/2)\widehat{\tilde{\Phi}}(\xi/2). \tag{7.35}$$

Proof.

For the proof we apply Proposition 7.1. The new symbols are measurable and essentially bounded since the given symbols and μ_j are. Next, we show that the mixed fundamental function S_M of the combined masks $(P, Q_1, \ldots, Q_r)$ and $(\tilde{P}, \tilde{Q}_1, \ldots, \tilde{Q}_r)$ is identical with the given mixed fundamental function s_M. First, we look at the following computation

$$\begin{aligned}
\sum_{j=1}^{r} Q_j(\xi)\overline{\tilde{Q}_j(\xi)} &= \sum_{j=1}^{r} q_j(\xi)\overline{\tilde{q}_j(\xi)} - s_M(2\xi)p(\xi)\sum_{j=1}^{r}\mu_j(2\xi)\overline{\tilde{q}_j(\xi)} \\
&= s_M(\xi) - s_M(2\xi)p(\xi)\left(\overline{\tilde{p}(\xi)} + \sum_{j=1}^{r}\mu_j(2\xi)\overline{\tilde{q}_j(\xi)}\right) \\
&= s_M(\xi) - s_M(2\xi)p(\xi)\overline{\tilde{P}(\xi)}
\end{aligned}$$

and $P\overline{\tilde{P}} = p\overline{\tilde{P}}$ by assumption. By inserting these identities we obtain the partial sum of S_M

$$\begin{aligned}
&\sum_{k=0}^{K}\sum_{j=1}^{r} Q_j(2^k\xi)\overline{\tilde{Q}_j(2^k\xi)}\prod_{m=0}^{k-1} P(2^m\xi)\overline{\tilde{P}(2^m\xi)} \\
&= \sum_{k=0}^{K}\left(s_M(2^k\xi) - s_M(2^{k+1}\xi)p(2^k\xi)\overline{\tilde{P}(2^k\xi)}\right)\prod_{m=0}^{k-1} p(2^m\xi)\overline{\tilde{P}(2^m\xi)} \\
&= \sum_{k=0}^{K}\left(s_M(2^k\xi)\prod_{m=0}^{k-1} p(2^m\xi)\overline{\tilde{P}(2^m\xi)} - s_M(2^{k+1}\xi)\prod_{m=0}^{k} p(2^m\xi)\overline{\tilde{P}(2^m\xi)}\right) \\
&= s_M(\xi) - s_M(2^{K+1}\xi)\prod_{k=0}^{K} p(2^k\xi)\prod_{k=0}^{K}\overline{\tilde{P}(2^k\xi)}, \quad a.e.\ \xi \in \mathbb{R}.
\end{aligned}$$

Thus, we have

$$\begin{aligned}
S_M(\xi) &= \lim_{K\to\infty}\left(s_M(\xi) - s_M(2^{K+1}\xi)\prod_{k=0}^{K} p(2^k\xi)\prod_{k=0}^{K}\overline{\tilde{P}(2^k\xi)}\right) \\
&= \lim_{K\to\infty}\left(s_M(\xi) - s_M(2^{K+1}\xi)\frac{\hat{\phi}(2^{K+1}\xi)}{\hat{\phi}(\xi)}\frac{\overline{\hat{\tilde{\Phi}}(2^{K+1}\xi)}}{\overline{\hat{\tilde{\Phi}}(\xi)}}\right) \quad a.e.\ \xi \in \mathbb{R}.
\end{aligned}$$

Note that from $P = p$ we have $\sigma(V_0) = \sigma(v_0)$. From the fact that s_M is bounded and ϕ and $\tilde{\Phi}$ are in $L^2(\mathbb{R})$, it follows as in Remark 4.7 that

$$\lim_{K\to\infty} s_M(2^K\xi)\frac{\hat{\phi}(2^K\xi)}{\hat{\phi}(\xi)}\frac{\overline{\hat{\tilde{\Phi}}(2^K\xi)}}{\overline{\hat{\tilde{\Phi}}(\xi)}} = 0, \quad \xi \in \sigma(V_0) \cap \sigma(\tilde{V}_0).$$

Therefore, we have $S_M = s_M$ on $\sigma(V_0) \cap \sigma(\tilde{V}_0)$ and (b1) of Proposition 7.1 follows directly. Now we put the new symbols and s_M to the test of condition (b2). By the 2π-periodicity of μ_j, we have

$$\begin{aligned} & s_M(2\xi)P(\xi)\overline{\tilde{P}(\xi+\pi)} + \sum_{j=1}^{r} Q_j(\xi)\overline{\tilde{Q}_j(\xi+\pi)} \\ = \; & s_M(2\xi)p(\xi)\left(\overline{\tilde{p}(\xi+\pi)} + \sum_{j=1}^{r} \mu_j(2\xi)\overline{\tilde{q}_j(\xi+\pi)}\right) \\ & + \sum_{j=1}^{r} \left(q_j(\xi) - p(\xi)\mu_j(2\xi)s_M(2\xi)\right)\overline{\tilde{q}_j(\xi+\pi)} \\ = \; & s_M(2\xi)p(\xi)\overline{\tilde{p}(\xi+\pi)} + \sum_{j=1}^{r} q_j(\xi)\overline{\tilde{q}_j(\xi+\pi)} = 0 \\ & \quad for\ all\ \xi, \xi+\pi \in \sigma(V_0) \cap \sigma(\tilde{V}_0) \subset \sigma(v_0) \cap \sigma(\tilde{v}_0). \qquad \square \end{aligned}$$

Example 7.12. *We want to demonstrate an example of the lifting scheme of a bi-frame. For convenience, we take a simple MRA tight frame* $\{\psi_{j,k,\ell}, j = 1, 2, k, \ell \in \mathbb{Z}\}$ *which is given in the appendix A.1. Note that the generators* ψ_1 *and* ψ_2 *have order* $m = 3$ *and* $L = 1$ *vanishing moment. The associated fundamental function is trivial, namely* $s_M \equiv 1$. *From Table A.1, the symbols are given by* $p_3(\xi) = \left(\frac{1+e^{-i\xi}}{2}\right)^3$ *and*

$$q_1(\xi) = \frac{\sqrt{3}}{4}(1 - e^{-i\xi}),\ q_2(\xi) = \frac{1}{8}(1 - e^{-i\xi})(1 + 4e^{-i\xi} + e^{-2i\xi}).$$

Now we define new symbols $\{P, Q_1, Q_2\}$ *and* $\{\tilde{P}, \tilde{Q}_1, \tilde{Q}_2\}$ *by*

$$P(\xi) = p_3(\xi), \quad \tilde{P}(\xi) = p_3(\xi) + \sum_{j=1}^{2} \overline{\mu_j(2\xi)}\tilde{q}_j(\xi),$$
$$Q_j(\xi) = q_j(\xi) - p_3(\xi)\mu_j(2\xi), \quad \tilde{Q}_j(\xi) = q_j(\xi).$$

We choose the trigonometric polynomials $\mu_j(\xi)$ *by*

$$\mu_1(\xi) = \frac{\sqrt{3}}{8} i \sin\xi,\ \mu_2(\xi) = \frac{3}{8} i \sin\xi,$$

so that the new generators Q_1, Q_2 *have a double root at the origin, i.e.* Ψ_1 *and* Ψ_2 *have at least* 2 *vanishing moments. Using these functions, we obtain the two-scale symbol* $\tilde{P}$

$$\tilde{P}(\xi) = \frac{1}{128}(1 + e^{-i\xi})\left(-(3 + 2\sqrt{3})e^{i\xi} + 10 + 4\sqrt{3} + (50 - 2\sqrt{3})e^{-i\xi} + 10e^{-2i\xi} - 3e^{-3i\xi}\right).$$

*Note that, through the analysis of the spectral radius of the transition operator of $\tilde{P}$ ([**19**]), we have the strong convergence of the cascade algorithm, i.e. $\tilde{\Phi} \in L^2(\mathbb{R})$. Furthermore, the characterization of the regularity ([**14**]) asserts that $\tilde{\Phi} \in$ Lip α, $\alpha \doteq 0.4612$. In addition, $\tilde{\Phi}$ has compact support, i.e.* $\mathrm{supp}\tilde{\Phi} = [-1, 4]$. *Hence, $\tilde{\Phi}$ satisfies (i)-(iii) of Assumption 4.4. The computation by the cascade algorithm provides $\tilde{\Phi}$ at the dyadic points (see Figure 7.1). From the fact that $\phi = \tilde{\phi} = \Phi = N_3$ and $\tilde{\Phi}$ has compact support, we have $\sigma(v_0) = \sigma(\tilde{v}_0) = \sigma(V_0) = \sigma(\tilde{V}_0) = [-\pi, \pi] \setminus \mathcal{N}$, where $\mathcal{N}$ is a null set.*
The generators $\tilde{\Psi}_1$ and $\tilde{\Psi}_2$ are given by (see also Figure 7.1)

$$\widehat{\tilde{\Psi}}_1(\xi) = q_1(\xi/2)\widehat{\tilde{\Phi}}(\xi/2),\ \widehat{\tilde{\Psi}}_2(\xi) = q_2(\xi/2)\widehat{\tilde{\Phi}}(\xi/2).$$

Notice that they have 1 vanishing moment and compact supports with $\mathrm{supp}\tilde{\Psi}_1 = [-0.5, 2.5]$, $\mathrm{supp}\tilde{\Psi}_2 = [-0.5, 4]$. *We have $\tilde{\Psi}_j \in L^2(\mathbb{R})$ and $\tilde{\Psi}_j \in$ Lip α, $\alpha \doteq 0.4612$, from the properties of $\tilde{\Phi}$. Therefore, $\{\tilde{\Psi}_{j,k,\ell}, j = 1, 2, k, \ell \in \mathbb{Z}\}$ is a Bessel system by Lemma 7.3. On the other hand, Q_1, Q_2 are*

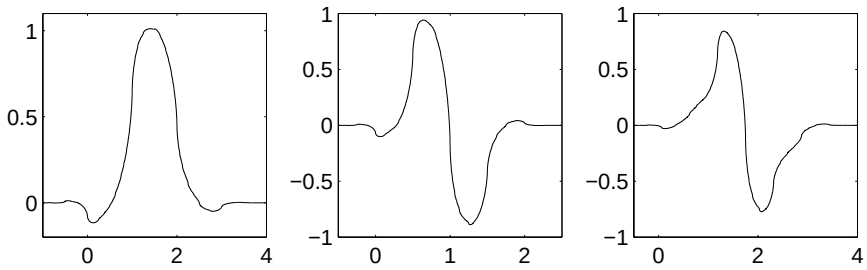

FIGURE 7.1. $\tilde{\Phi}$ (left), $\tilde{\Psi}_1$ (middle), and $\tilde{\Psi}_2$ (right).

$$Q_1(\xi) = \frac{\sqrt{3}}{128}(1 - e^{-i\xi})^2 \left(-e^{2i\xi} - 5e^{i\xi} + 20 + 12e^{-i\xi} + 5e^{-2i\xi} + e^{-3i\xi}\right),$$
$$Q_2(\xi) = -\frac{1}{128}(1 - e^{-i\xi})^3 \left(3e^{2i\xi} + 18e^{i\xi} + 38 + 18e^{-i\xi} + 3e^{-2i\xi}\right).$$

Hence, we obtain the generators Ψ_1 and Ψ_2 by

$$\hat{\Psi}_1(\xi) = Q_1(\xi/2)\hat{N}_3(\xi/2),\ \hat{\Psi}_2(\xi) = Q_2(\xi/2)\hat{N}_3(\xi/2).$$

Note that Ψ_1, Ψ_2, are in C^1 as well as in $L^2(\mathbb{R})$. Furthermore, they have compact supports and Ψ_1 has 2 vanishing moments and Ψ_2 has 3 vanishing moments (see Figure 7.2). Hence, $\{\Psi_{j,k,\ell}, j = 1, 2, k, \ell \in \mathbb{Z}\}$ is also a Bessel system by Lemma 7.3.

In summary, the new two-scale symbols $P, \tilde{P}, Q_j, \tilde{Q}_j$*, refinable functions* $\Phi, \tilde{\Phi}$*, and*

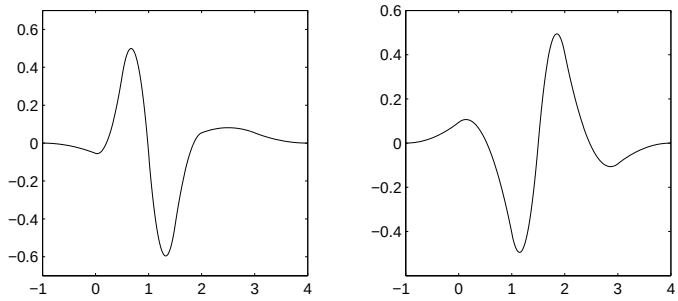

FIGURE 7.2. Ψ_1 (left) and Ψ_2 (right).

the generators $\Psi_j, \tilde{\Psi}_j$*, satisfy all conditions of Proposition 7.2. Thus, we have an MRA bi-frame* $\left(\{\Psi_{j,k,\ell}\}, \{\tilde{\Psi}_{j,k,\ell}\}\right)$ *by applying the lifting scheme to the given MRA tight frame* $\{\psi_{j,k,\ell}\}$*. The lifting scheme can be applied to other MRA tight frames, for example, spline MRA tight frames given in section 3.3 and the appendix.*

CHAPTER 8

Application of Λ-operator

We constructed MRA bi-frames $(\{\Lambda\psi_{j,k,\ell}\}, \{\Lambda^{-1}\psi_{j,k,\ell}\})$ as a result of the commutation of the tight frame $\{\Psi_{j,k,\ell}\}$ in Theorem 7.6, where $\Psi_j = \mathcal{H}\psi_j,\ j = 1, \ldots, r$. The associated two-scale symbols, however, are not easily implemented. Zhao described the symbols of biorthogonal wavelets by rational functions and truncated them to get FIR filters ([**30**]). Thus, the truncated symbols do not satisfy the conditions (1.12)-(1.13) exactly. In other words, the wavelets generated from the truncated symbols are not exactly biorthogonal.
In the same context, we introduce the notion of *approximate bi-frames* and demonstrate an approximate bi-frame approximating $(\{\Lambda\psi_{j,k,\ell}\}, \{\Lambda^{-1}\psi_{j,k,\ell}\})$ so that we have trigonometric two-scale symbols. For the search we recall the closed forms of the bi-frame $(\{\Lambda\psi_{j,k,\ell}\}, \{\Lambda^{-1}\psi_{j,k,\ell}\})$ in Theorem 7.6. At the end, we propose an approximation of the Ram-Lak filter, employed in filtered backprojection algorithms, using the two-scale symbols of the approximate MRA bi-frame.

Now, for the approximation we take a look at the closed forms of (7.17)-(7.26). In particular, the two-scale symbols are described by the functions M, N. The main difficulty of the application lies in the implementation of these functions. The term $(1 - e^{-i\xi})$ in the denominator of $Q_{\tilde{\eta}_j}$ is cancelled out by q_j owing to its vanishing moments. Recall that we constructed trigonometric polynomials $\tilde{M}$ and $\tilde{N}$ approximating M and N in section 5.1. Therefore, without any further manipulations, we can make use of the trigonometric polynomials $\tilde{M}$ and $\tilde{N}$ for the construction of the desired approximate MRA bi-frame. If we apply them to (7.17)-(7.26), we have the refinable functions and the two-scale symbols

$$\hat{\rho}(\xi) := e^{-i\xi}\tilde{M}(\xi)R(\xi)\hat{N}_m(\xi), \quad \widehat{\tilde{\rho}}(\xi) := \tilde{M}(\xi)R(\xi)\hat{N}_{m+2}(\xi), \tag{8.1}$$

$$P_\rho(\xi) := e^{-i\xi}\frac{\tilde{M}(2\xi)}{\tilde{M}(\xi)}p_m(\xi)p_0(\xi), \quad P_{\tilde{\rho}}(\xi) := \frac{\tilde{M}(2\xi)}{\tilde{M}(\xi)}p_{m+2}(\xi)p_0(\xi). \tag{8.2}$$

$$\begin{array}{ccc} \tilde{\Psi}_j & \approx & \mathcal{H}\psi_j \\ \textit{commutation} \quad \downarrow & & \downarrow \\ \{\nu_j, \tilde{\nu}_j\} & \approx & \{\Lambda\psi_j, \Lambda^{-1}\psi_j\} \end{array}$$

FIGURE 8.1. Approximate bi-frame by commutation of approximate tight frame.

The two-scale symbols of the generators are given by

$$Q_{\nu_j}(\xi) := \frac{1-e^{i\xi}}{2}\frac{\tilde{N}(\xi)}{\tilde{M}(\xi)}q_j(\xi), \quad Q_{\tilde{\nu}_j}(\xi) := \frac{2}{1-e^{-i\xi}}\frac{\tilde{N}(\xi)}{\tilde{M}(\xi)}q_j(\xi). \tag{8.3}$$

Hence, the generators are

$$\hat{\nu}_j(\xi) := Q_{\nu_j}(\xi/2)\hat{\rho}(\xi/2) = -\frac{1-e^{-i\xi/2}}{2}\tilde{N}(\xi/2)q_j(\xi/2)R(\xi/2)\hat{N}_m(\xi/2), \tag{8.4}$$

$$\widehat{\tilde{\nu}}_j(\xi) := Q_{\tilde{\nu}_j}(\xi/2)\hat{\tilde{\rho}}(\xi/2) = \frac{2}{1-e^{-i\xi/2}}\tilde{N}(\xi/2)q_j(\xi/2)R(\xi/2)\hat{N}_{m+2}(\xi/2). \tag{8.5}$$

Remark 8.1. *Note that the refinable functions, symbols, and generators are obtained from the commutation of the approximate MRA tight frame* $\{\tilde{\Psi}_{j,k,\ell}, j = 1,\dots,r, k,\ell \in \mathbb{Z}\}$ *whose generators* $\tilde{\Psi}_j,\ j = 1,\dots,r$, *with the associated refinable function* $\tilde{\Phi}$ *are given in (5.1) and (5.2) (see Figure 8.1). By a simple observation, we have*

$$\begin{aligned} P_\rho(\xi) &= 2\tilde{P}(\xi)/(1+e^{i\xi}), \qquad & \tilde{P}_\rho(\xi) &= \tilde{P}(\xi)(1+e^{-i\xi})/2, \\ Q_{\nu_j}(\xi) &= \tilde{Q}_j(\xi)(1-e^{i\xi})/2, \qquad & Q_{\nu_j}(\xi) &= 2\tilde{Q}_j(\xi)/(1-e^{-i\xi}), \end{aligned}$$

where $\tilde{P}$ *and* $\tilde{Q}_j$ *are given in (5.4)-(5.5). This setting corresponds to the commutation of* $\{\tilde{\Psi}_{j,k,\ell}\}$ *in the sense of (7.12) and (7.13).*

Analogously to the case of approximate MRA tight frames, the new symbols in (8.2)-(8.3) define a new mixed fundamental function, say $\tilde{S}_M$, and the new symbols and the mixed fundamental function $\tilde{S}_M$ do not exactly satisfy the conditions $(b1)$ and $(b2)$ of Proposition 7.1, but only approximately. That is to say, the system pair

$$(\{\nu_{j,k,\ell}, 1 \le j \le r, k,\ell \in \mathbb{Z}\}, \{\tilde{\nu}_{j,k,\ell}, 1 \le j \le r, k,\ell \in \mathbb{Z}\})$$

is not an MRA bi-frame, in general. Thus, we introduce the notion of *approximate MRA bi-frames.*

Definition 8.2. *A system pair*

$$(\{\nu_{j,k,\ell}, 1 \le j \le r, k, \ell \in \mathbb{Z}\}, \{\tilde{\nu}_{j,k,\ell}, 1 \le j \le r, k, \ell \in \mathbb{Z}\})$$

is an approximate MRA bi-frame with the refinable functions $\rho, \tilde{\rho}$, if they satisfy all hypothesis of Proposition 7.1 and

(i)

$$\overline{\lim_{j \to -\infty}} |\tilde{S}_M(2^j \xi) - 1| \le \delta_1,$$

for some $0 \le \delta_1 \ll 1$ and a.e. $\xi \in \mathbb{R}$

(ii)

$$\left| \tilde{S}_M(2\xi) P_\rho(\xi) \overline{P_{\tilde{\rho}}(\xi + \pi)} + \sum_{j=1}^{r} Q_{\nu_j}(\xi) \overline{Q_{\tilde{\nu}_j}(\xi + \pi)} \right| \le \delta_2$$

for some $0 \le \delta_2 \ll 1$ and a.e. $\xi \in \mathbb{R}$.

Remark 8.3. *1. Clearly, the notion in Definition 8.2 is an extension of the notion of approximate MRA tight frames.*
2. Let an approximate MRA tight frame $\{\tilde{\Psi}_{j,k,\ell}\}$ be given such that the associated symbols $\tilde{P}, \tilde{Q}_j, j = 1, \dots, r$, and the fundamental function $\tilde{S}$ are given in (5.4)-(5.6) with the conditions

$$\tilde{P}(\xi) = \left(\frac{1 + e^{-i\xi}}{2} \right)^m \tilde{P}_0(\xi), \quad \tilde{Q}_j(\xi) = \left(\frac{1 - e^{-i\xi}}{2} \right)^{m_j} \tilde{Q}_j^0(\xi), \tag{8.6}$$

where $m, m_j \ge 2$, and $\tilde{P}_0, \tilde{Q}_j^0$ are bounded and $\tilde{P}_0(\pi),\ \tilde{Q}_j^0(0) \ne 0$. Then, using a similar process as in the proof of Theorem 7.4, we can show that the system pair $(\{\nu_{j,k,\ell}\}, \{\tilde{\nu}_{j,k,\ell}\})$ resulting from the commutation of $\{\tilde{\Psi}_{j,k,\ell}\}$ is an approximate MRA bi-frame. Note that all assumptions on the two-scale symbols and refinable functions hold similarly to the proof of Theorem 7.4. Furthermore, from (7.14) in the proof of the Theorem 7.4, it is clear that the mixed fundamental function of the system pair is equal to the fundamental function of the approximate MRA tight frame. Therefore, (i) of Definition 8.2 is satisfied by (i) of Definition 5.1. In addition, from (7.15)

and the notations of (5.4)-(5.6), we have

$$E_M(\xi) := \tilde{S}_M(2\xi)P_\rho(\xi)\overline{P_{\tilde{\rho}}(\xi+\pi)} + \sum_{j=1}^{r} Q_{\nu_j}(\xi)\overline{Q_{\tilde{\nu}_j}(\xi+\pi)}$$

$$= \frac{1-e^{-i\xi}}{1+e^{i\xi}}\left[\tilde{S}(2\xi)\tilde{P}(\xi)\overline{\tilde{P}(\xi+\pi)} + \sum_{j=1}^{r}\tilde{Q}_j(\xi)\overline{\tilde{Q}_j(\xi+\pi)}\right] =: \frac{1-e^{-i\xi}}{1+e^{i\xi}}E(\xi), \tag{8.7}$$

where $0 \le |E(\xi)| \le \delta,\ 0 < \delta \ll 1$ *from the assumption. Similar to (7.16), we have from* $m, m_j \ge 2$, *that*

$$E(\xi) = \left(\frac{1+e^{i\xi}}{2}\right)^2 U(\xi), \tag{8.8}$$

where U *is some* 2π*-periodic and bounded function with a double root at* $\xi \in (2\mathbb{Z}+1)\pi$. *Thus, we can find* $\delta_1,\ 0 < \delta_1 \ll 1$ *such that* $|E_M(\xi)| \le \delta_1$. *Thus, (ii) of Definition 8.2 follows from (ii) of Definition 5.1 as well.*

As in the case of the approximate MRA tight frames, it is obvious that the symbols in (8.2)-(8.3) are not trigonometric polynomials. In order to get trigonometric symbols, we apply the same technique applied in Theorem 5.3. Namely, we show that $(\{\nu_{j,k,\ell}, 1 \le j \le r, k, \ell \in \mathbb{Z}\}, \{\tilde{\nu}_{j,k,\ell}, 1 \le j \le r, k, \ell \in \mathbb{Z}\})$ is an approximate MRA bi-frame with refinable functions ϕ and $\phi * N_2$ as well. The proof is similar to Theorem 5.3, so we give only a short version.

Theorem 8.4. *We suppose that the symbols in (8.2)-(8.3) are subjected to the condition (8.6). Then* ρ *and* $\tilde{\rho}$ *in (8.1) are refinable functions of the approximate MRA bi-frame* $(\{\nu_{j,k,\ell}\}, \{\tilde{\nu}_{j,k,\ell}\})$ *in (8.4) and (8.5) if and only if* ϕ *and* $\phi * N_2$ *are refinable functions of the same approximate MRA bi-frame.*

Proof.

We employ Definition 8.2 for the proof. Firstly, the assumptions of Proposition 7.1 on two-scale symbols and those of refinable functions hold trivially from the same argument of the proof of Theorem 5.3. Note that the symbols of the generators with respect to ϕ and $\phi * N_2$ are $q_{\nu_j} := e^{-i\cdot}\tilde{M}Q_{\nu_j}$ and $q_{\tilde{\nu}_j} := \tilde{M}Q_{\tilde{\nu}_j}$. Let $\tilde{S}_{M_1}$ be the mixed fundamental function of the bi-frame with refinable functions ρ and $\tilde{\rho}$ and $\tilde{S}_{M_2}$ be that of ϕ and $\phi * N_2$. First, from the definition of the mixed fundamental function

in (7.1) and (8.2)-(8.3), we have

$$\tilde{S}_{M_1}(\xi) = \frac{1}{\tilde{M}^2(\xi)}\tilde{S}_{M_2}(\xi).$$

Thus,

$$\overline{\lim_{j\to-\infty}}|\tilde{S}_{M_1}(2^j\xi) - 1| \le \delta_1 \Leftrightarrow \overline{\lim_{j\to-\infty}}|\tilde{S}_{M_2}(2^j\xi) - 1| \le \delta_1$$

due to the fact that $\tilde{M}(0) = 1$ and $\tilde{M}$ is continuous. By the same argument of the proof of Theorem 5.3 and by employing the notation

$$E_1(\xi) := \tilde{S}_{M_1}(2\xi)P_\rho(\xi)\overline{P_{\tilde{\rho}}(\xi+\pi)} + \sum_{j=1}^{r} Q_{\tilde{\nu}_j}(\xi)\overline{Q_{\tilde{\nu}_j}(\xi+\pi)},$$

(E_2 is defined similarly) we can show that $E_1(\xi) = \frac{1}{\tilde{M}(\xi)\overline{\tilde{M}(\xi+\pi)}}E_2(\xi)$. Hence, (ii) holds equivalently. $\square$

Now we present an approximate MRA bi-frame which is an approximation to the MRA bi-frame $\{\Lambda\psi^{m,L}_{j,k,\ell}, \Lambda^{-1}\psi^{m,L}_{j,k,\ell}, 1 \le j \le r, k, \ell \in \mathbb{Z}\}$ for the case $m = 5$ and $L = 5$. The approximate MRA bi-frame and the associated refinable functions depend on the functions $\tilde{M}$ and $\tilde{N}$, so do the associated symbols. Thus $\tilde{M}$ and $\tilde{N}$ are crucial for the construction. Thanks to the construction of $\tilde{M}$ and $\tilde{N}$ in section 5.1, there is no additional work needed. In order to check the quality of the approximation, we compare the magnitudes of $\hat{\nu}_j$ and $\hat{\tilde{\nu}}_j$ to those of $\widehat{\Lambda\psi_j^{5,5}}$ and $\widehat{\Lambda^{-1}\psi_j^{5,5}}$, respectively.

Example 8.5. *For the case $m = 5$ and $L = 5$, we have generators ν_j, $\tilde{\nu}_j$, $j = 1, 2, 3$, and refinable functions N_5 and N_7 from (8.1)-(8.3) and Theorem 8.4. We take $\tilde{M}$ and $\tilde{N}$ from Example 5.7 (with $J = 2$ for the Thiran allpass filter). We have from (8.4)-(8.5)*

$$\begin{aligned}
\hat{\nu}_j(\xi) &= -\frac{1-e^{-i\xi/2}}{2}\tilde{N}(\xi/2)q_j^{5,5}(\xi/2)\hat{N}_5(\xi/2) \\
&= -\frac{1-e^{-i\xi/2}}{2}\tilde{N}(\xi/2)2^5(1-e^{-i\xi/2})^5(\xi/2)\hat{q}_j^{5,5}(\xi/2)\hat{N}_5(\xi/2) \\
&= -2^4\tilde{N}(\xi/2)(1-e^{-i\xi/2})^6\hat{q}_j^{5,5}(\xi/2)\hat{N}_5(\xi/2),
\end{aligned}$$

and

$$\begin{aligned}\widehat{\tilde{\nu}}_j(\xi) &= \frac{2}{1-e^{-i\xi/2}}\tilde{N}(\xi/2)q_j^{5,5}(\xi/2)\hat{N}_7(\xi/2)\\ &= \frac{2}{1-e^{-i\xi/2}}\tilde{N}(\xi/2)2^5(1-e^{-i\xi/2})^5\hat{q}_j^{5,5}(\xi/2)\hat{N}_7(\xi/2)\\ &= 2^6\tilde{N}(\xi/2)(1-e^{-i\xi/2})^4\hat{q}_j^{5,5}(\xi/2)\hat{N}_7(\xi/2).\end{aligned}$$

*Notice that ν_j and $\tilde{\nu}_j$ have compact supports and good regularities, i.e. $\nu_j \in C^3$ and $\tilde{\nu}_j \in C^5$. Furthermore, ν_j has 6 vanishing moments and $\tilde{\nu}_j$ has 4. If we compare our result to that of Zhao ([***30***]), our generators have explicit forms described by finite linear combinations of B-splines in contrast to the biorthogonal wavelets of* [**30**, p.358]. *In addition, both of the generators ν_j and $\tilde{\nu}_j$ have good regularities which is not the case in* [**30**, FIG.1 p.358].
From the commutation we have $\nu_j(x) = -\frac{1}{4}\frac{d}{dx}\tilde{\Psi}_j(x)$ and $\tilde{\nu}_j(x) = 4\int_{-\infty}^{x}\tilde{\Psi}_j(y)dy$, where $\tilde{\Psi}_j$ is given from Example 5.7. Figure 8.2 and Figure 8.3 show ν_j and $\tilde{\nu}_j$ for $j = 1, 2, 3$.

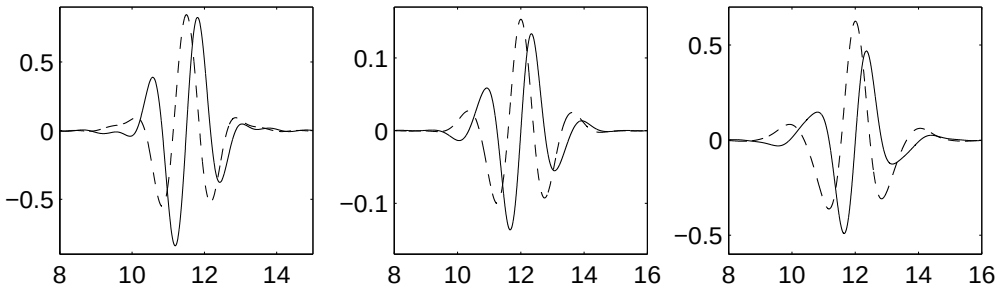

FIGURE 8.2. ν_j (solid) and $\tilde{\Psi}_j$ (dotted) for $j = 1$ (left), $j = 2$ (middle), and $j = 3$ (right).

The system pair $(\{\nu_{j,k,\ell}\}, \{\tilde{\nu}_{j,k,\ell}\})$ is an approximate MRA bi-frame in the sense of Definition 8.2. First, (i) holds trivially from the fundamental function of the approximate MRA tight frame $\{\tilde{\Psi}_{j,k,\ell}\}$ (see Figure 5.11). From (8.7) we have $E_M(\xi) = \frac{1-e^{i\xi}}{1+e^{i\xi}}E(\xi)$, where E is the expression in (ii) of Definition 5.1 and E_M is that in (ii) of Definition 8.2. Numerical computation shows that $0 \le |E_M| \le \delta,\ \delta \doteq 0.1045$ (see Figure 8.4). Next, using the relation

$$\nu_j \approx \Lambda\psi_j^{5,5},\ \tilde{\nu}_j \approx \Lambda^{-1}\psi_j^{5,5},\ j = 1, 2, 3, \tag{8.9}$$

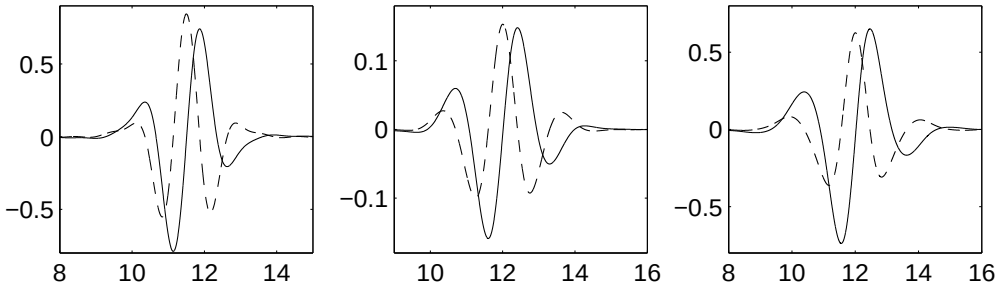

FIGURE 8.3. $\tilde{\nu}_j$ (solid) and $\tilde{\Psi}_j$ (dotted) for $j = 1$ (left), $j = 2$ (middle), and $j = 3$ (right).

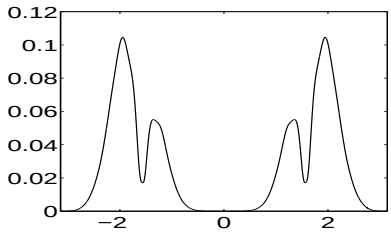

FIGURE 8.4. $|E_M(\xi)|$ in (ii) of Definition 8.2.

we compare the magnitudes of the pairs $(\hat{\nu}_j, \widehat{\Lambda\psi_j^{5,5}})$ *and* $(\hat{\tilde{\nu}}_j, \widehat{\Lambda^{-1}\psi_j^{5,5}})$. *Figure 8.5 and Figure 8.6 indicate that* ν_j *and* $\tilde{\nu}_j$ *approximate* $\Lambda\psi_j^{5,5}$ *and* $\Lambda^{-1}\psi_j^{5,5}$ *well.*

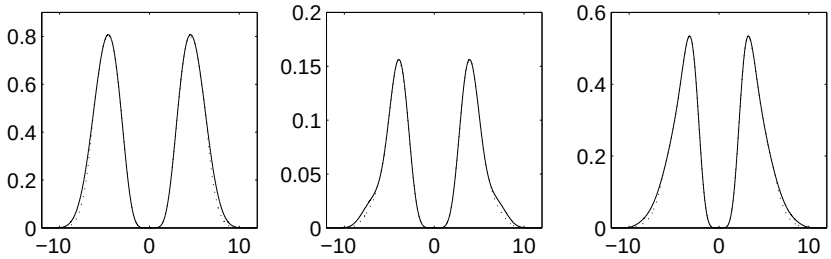

FIGURE 8.5. $|\hat{\nu}_j|$ (dotted) and $|\widehat{\Lambda\psi_j^{5,5}}|$ (solid) for $j = 1$ (left), $j = 2$ (middle), and $j = 3$ (right).

Now we want to look at the two-scale symbols of the generators. For their application in the DFRT, the symbols of ν_j *should be good approximations to the symbols of (7.24)-(7.26). We describe* $\hat{\nu}_j$ *and* $\hat{\tilde{\nu}}_j$ *with respect to* $\hat{\psi}_j^{5,5}$ *in order to compare the*

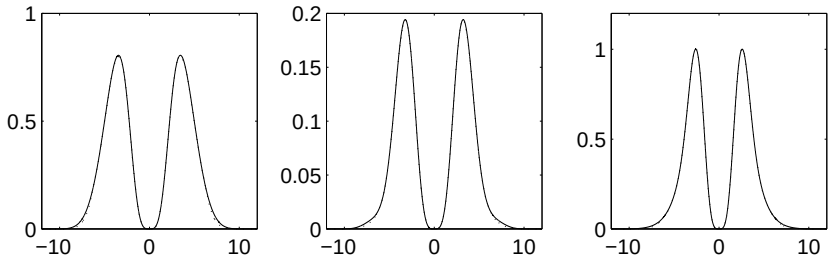

FIGURE 8.6. $|\hat{\tilde{\nu}}_j|$ (dotted) and $|\widehat{\Lambda^{-1}\psi_j^{5,5}}|$ (solid) for $j = 1$ (left), $j = 2$ (middle), and $j = 3$ (right).

symbols.

$$\begin{aligned}
\hat{\nu}_j(\xi) &= -\frac{1-e^{-i\xi/2}}{2}\tilde{N}(\xi/2)q_j^{5,5}(\xi/2)\hat{N}_5(\xi/2) \\
&= -\frac{1-e^{-i\xi/2}}{2}\tilde{N}(\xi/2)\hat{\psi}_j^{5,5}(\xi), \qquad (8.10) \\
\widehat{\tilde{\nu}}_j(\xi) &= \frac{2}{1-e^{-i\xi/2}}\tilde{N}(\xi/2)q_j^{5,5}(\xi/2)\hat{N}_7(\xi/2) \\
&= \frac{2}{1-e^{-i\xi/2}}\left(\frac{1-e^{-i\xi/2}}{i\xi/2}\right)^2\tilde{N}(\xi/2)q_j^{5,5}(\xi/2)\hat{N}_5(\xi/2) \\
&= -\frac{16}{\xi^2}\frac{1-e^{-i\xi/2}}{2}\tilde{N}(\xi/2)\hat{\psi}_j^{5,5}(\xi). \qquad (8.11)
\end{aligned}$$

In the sense of (7.24)-(7.26) we should have

$$\frac{1-e^{-i\xi/2}}{2}\tilde{N}(\xi/2) \approx \frac{|\xi|}{4}, \qquad (8.12)$$

$$\frac{16}{\xi^2}\frac{1-e^{-i\xi/2}}{2}\tilde{N}(\xi/2) \approx \frac{4}{|\xi|}. \qquad (8.13)$$

We focus on the approximation in (8.12), since a good approximation in (8.12) leads to (8.13) directly. The filter $\frac{|\xi|}{4}$ *is called the Ram-Lak filter. Note that the* 4π*-periodic trigonometric polynomial* $\tau(\xi) := \frac{1-e^{-i\xi/2}}{2}\tilde{N}(\xi/2)$ *is not real. Thus, it approximates the Ram-Lak filter* $\frac{|\xi|}{4}$ *in the complex plane. We plot the curves* $\xi \mapsto \left(\frac{|\xi|}{4}, 0\right)$ *and* $\xi \mapsto (\mathrm{Re}\tau(\xi), \mathrm{Im}\tau(\xi))$ *in order to compare them graphically (see Figure 8.7.). On the other hand, if we take the magnitude or real part of* $\frac{1-e^{-i\xi/2}}{2}\tilde{N}(\xi/2)$*, they also provide good approximations to the Ram-Lak filter (see Figure 8.8). Note that* $|\frac{1-e^{-i\xi/2}}{2}\tilde{N}(\xi/2)| = |\sin\xi/4|\tilde{M}(\xi/2)$.

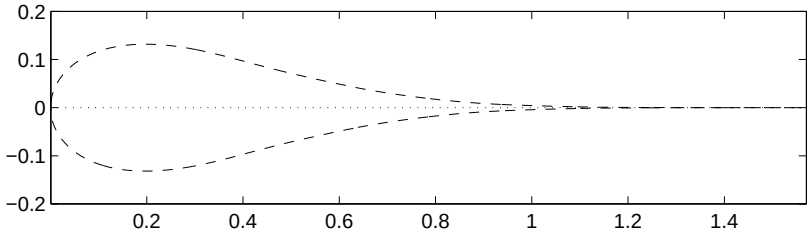

FIGURE 8.7. The Ram-Lak filter (dotted) and its approximation $\frac{1-e^{-i\xi/2}}{2}\tilde{N}(\xi/2)$ (dashed) as curves in the complex plane for $\xi \in [-2\pi, 2\pi]$.

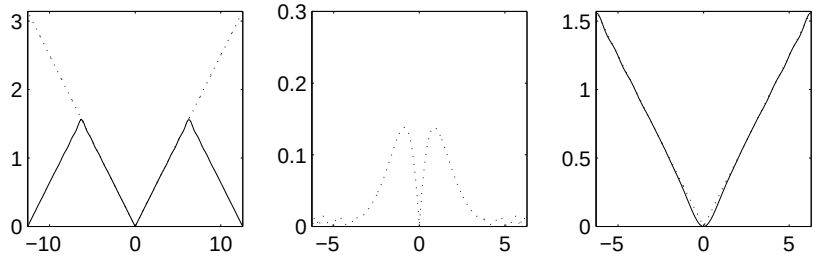

FIGURE 8.8. Left: The Ram-Lak filter (dotted) and the magnitude of $\frac{1-e^{-i\xi/2}}{2}\tilde{N}(\xi/2)$ (solid) on $[-4\pi, 4\pi]$. Middle: The error of $\left|\frac{|\xi|}{4} - \frac{1-e^{-i\xi/2}}{2}\tilde{N}(\xi/2)\right|$ on $[-2\pi, 2\pi]$. Right: The Ram-Lak filter (dotted) and the real part of $\frac{1-e^{-i\xi/2}}{2}\tilde{N}(\xi/2)$ (solid) on $[-2\pi, 2\pi]$.

Remark 8.6. *1. Note that our construction of the so-called approximate Ram-Lak filter* $\frac{1-e^{-i\xi/2}}{2}\tilde{N}(\xi/2)$ *does not depend on the order of the B-spline. Thus we can apply this approach to construct approximate MRA bi-frames approximating* $\left(\{\Lambda\psi^{m,L}_{j,k,\ell}\}, \{\Lambda^{-1}\psi^{m,L}_{j,k,\ell}\}\right)$ *for further* $m \geq 2$ *and* $L \geq 2$*. Namely, we take an MRA tight frame* $\{\psi^{m,L}_{j,k,\ell}\}$ *of splines from the examples in section 3.3 or in the appendix then find its approximate Hilbert transform using the technique in section 5.1. Then, by applying the commutation for bi-frames of Theorem 7.4 we can obtain the approximate MRA bi-frame.*

2. The construction of an approximate MRA bi-frame approximating $\{\Lambda\psi^{m,L}_{j,k,\ell}, \Lambda^{-1}\psi^{m,L}_{j,k,\ell}\}$ *allows us a good possibility of the application to the filtered backprojection algorithm of computed tomography. Namely, we can extend the algorithm for biorthogonal wavelets (see* [**30**, Section 5]*) to using an MRA tight frame* $\{\psi^{m,L}_{j,k,\ell}\}$ *and its approximate MRA bi-frame* $\{\nu_{j,k,\ell}, \tilde{\nu}_{j,k,\ell}\}$*.*

APPENDIX A

Further examples of stationary spline MRA tight frames on an interval

A.1. Construction of a quadratic spline tight frame with 1 vanishing moment ($m = 3, L = 1$)

We choose $n = 4$ in (3.13) and (3.14) for the construction. From the corresponding representation (3.15), we want to get a factorization of the 9×9 matrix Z_1. We apply the symmetric reduction to get

$$\tilde{Z}_1 = T_{9,1,-1/4} Z_1 T_{9,1,-1/4}^T.$$

Note that $\tilde{Z}_1$ is a diagonal matrix with diagonal elements

$$\left[\frac{1}{12}, \frac{1}{8}, \frac{3}{16}, \frac{1}{4}, \frac{3}{16}, \frac{1}{4}, \frac{3}{16}, \frac{1}{8}, \frac{1}{12}\right].$$

Hence, we have the factorization of $\tilde{Z}_1 = BB^T$, where B is the square root of $\tilde{Z}_1$, i.e. a possible solution of B is the diagonal matrix with diagonal elements

$$\left[\frac{\sqrt{3}}{6}, \frac{\sqrt{2}}{4}, \frac{\sqrt{3}}{4}, \frac{1}{2}, \frac{\sqrt{3}}{4}, \frac{1}{2}, \frac{\sqrt{3}}{4}, \frac{\sqrt{2}}{4}, \frac{\sqrt{3}}{6}\right].$$

As a result we have the 9×11 matrix $\hat{Q} := T_{9,1,1/4} B$. The 5 columns (3rd to 7th) of $\hat{Q}$ contain the coefficients (see Table A.1) of the interior wavelets

$$\psi_j(\cdot - k), \quad j = 1, 2, \ 0 \le k \le 1, \quad \psi_1(\cdot - 2),$$

which are given by 2 antisymmetric generators $\psi_1 := \psi_{0,3}$ and $\psi_2 := \psi_{0,4}$. The supports of $\psi_1, \ \psi_2$, are (see Figure A.1)

$$\text{supp } \psi_1 = [0, 2], \quad \text{supp } \psi_2 = [0, 3].$$

The first two columns of the matrix $\hat{Q}$ represent the coefficients (see Table A.2) of the 2 boundary wavelets for the left endpoint of the interval and Figure A.2 shows their graphs.

i	$\hat{q}_{0,2+i}$	$\hat{q}_{1,2+i}$	$\hat{q}_{2,2+i}$
1	$\frac{\sqrt{3}}{4}$		
2	$\frac{1}{8}$	$\frac{1}{2}$	$\frac{1}{8}$

TABLE A.1. Coefficients of interior wavelets $\psi_{0,2+i}, i = 1, 2$, in expansion (3.21).

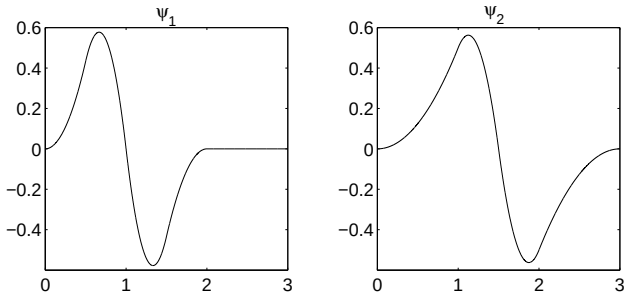

FIGURE A.1. Two antisymmetric generators of the quadratic spline tight frame with 1 vanishing moment and simple interior knots.

i	$\hat{q}_{-2,i}$	$\hat{q}_{-1,i}$	$\hat{q}_{0,i}$
1	0.288676		
2		0.353553	0.088388

TABLE A.2. Coefficients of boundary wavelets $\psi_{0,i}, i = 1, 2$, in expansion (3.21).

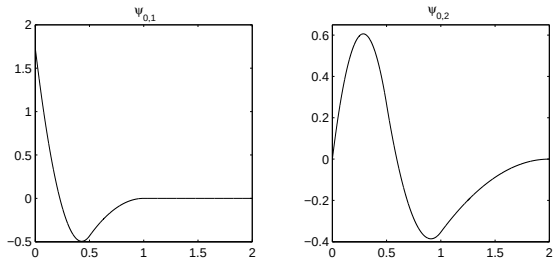

FIGURE A.2. Boundary wavelets of the quadratic spline tight frame with 1 vanishing moment and simple interior knots.

Remark A.1. *Note that the given two generators of interior wavelets are exactly the same to the two generators of the quadratic spline tight frame of* [**6**, Example 2].

A.2. Construction of a cubic spline tight frame with 2 vanishing moments ($m = 4, L = 2$)

We consider $n = 6$ for the interval and two knot vectors in (3.13) and (3.14). We begin with the 13×13 matrix Z_2 from representation (3.15) and perform the symmetric reductions using $T_{13,2,-1/6}$ to get

$$\tilde{Z}_2 := T_{13,2,-1/6} Z_2 T_{13,2,-1/6}^T.$$

Now we search for a factorization $\tilde{Z}_2 = BB^T$, with $B = [B_l, B_i, B_r]$, where B_i is the 13×7 block matrix that has the same structure as (3.24) with one more null row at the top and the bottom. A solution reads

$$a = \frac{\sqrt{11}}{16}, \quad b = \frac{\sqrt{3}}{16}, \quad c = \frac{\sqrt{3}}{9}, \quad d = \sqrt{\frac{13}{864}}.$$

Consequently we get the 13×17 matrix $B = [B_\ell, B_i, B_r]$ by applying the same method as in the previous examples. From the columns of the matrix $T_{13,2,1/6} B_i$ we obtain the coefficients (see Table A.3) of 7 interior wavelets

$$\psi_j(\cdot - k), \quad 1 \le j \le 3, \ 0 \le k \le 1, \quad \psi_1(\cdot - 2),$$

which are given by 3 symmetric generators $\psi_1 := \psi_{0,6}$, $\psi_2 := \psi_{0,7}$, and $\psi_3 := \psi_{0,8}$. The supports of ψ_1, ψ_2, ψ_3, are

$$\text{supp } \psi_1 = [0, 4], \quad \text{supp } \psi_2 = [0, 5], \quad \text{supp } \psi_3 = [1, 4]$$

and their graphs are shown in Figure A.3.

i	$\hat{q}_{0,5+i}$	$\hat{q}_{1,5+i}$	$\hat{q}_{2,5+i}$	$\hat{q}_{3,5+i}$	$\hat{q}_{4,5+i}$
1	0.034548	0.207289	0.034548		
2	0.018042	0.108253	0.228534	0.108253	0.018042
3			0.122663		

TABLE A.3. Coefficients of the interior wavelets $\psi_{0,5+i}$, $i = 1, 2, 3$, in expansion (3.21).

On the other hand, the columns of the matrix $T_{13,2,1/6} B_\ell$ provide the coefficients (see Table A.4) of the 5 boundary wavelets for the left endpoint of the interval. Their graphs are shown in Figure A.4.

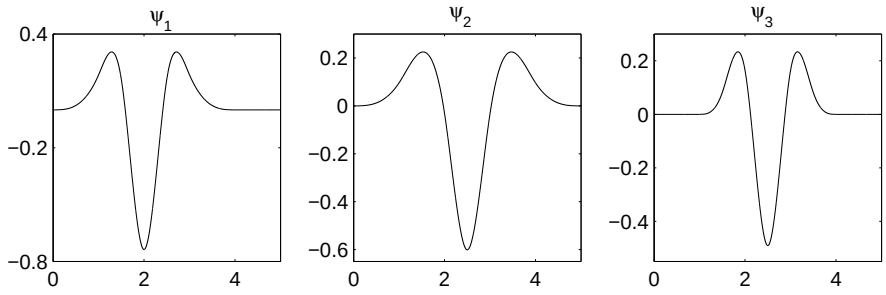

FIGURE A.3. Three symmetric generators of the cubic spline tight frame with 2 vanishing moments and simple interior knots.

i	$\hat{q}_{-3,i}$	$\hat{q}_{-2,i}$	$\hat{q}_{-1,i}$	$\hat{q}_{0,i}$	$\hat{q}_{1,i}$	$\hat{q}_{2,i}$
1	0.612372	0.153093				
2		1.096871	0.522319	0.087053		
3			1.739481	0.726565	0.224564	0.037427
4				2.151416	0.725354	0.120892
5				0.091642	0.549853	0.091642

TABLE A.4. Coefficients (*10) of boundary wavelets $\psi_{0,i}, i = 1, \ldots, 5$, in expansion (3.21).

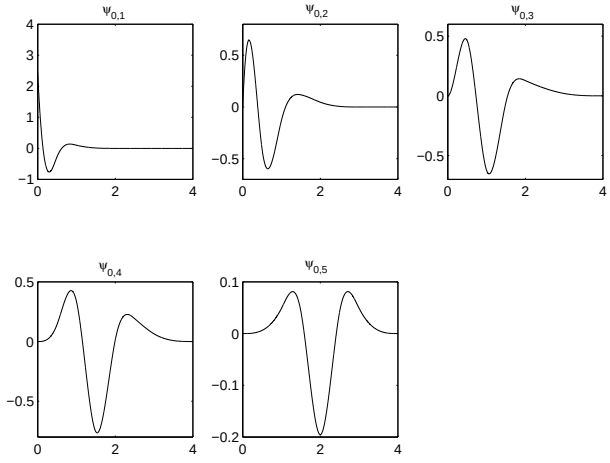

FIGURE A.4. Boundary wavelets of the cubic spline tight frame with 2 vanishing moments simple interior knots.

A.3. Construction of a quartic spline tight frame of 3 vanishing moments ($m = 5, L = 3$)

For the construction we choose $n = 9$ in (3.13)-(3.13). As in the former examples, we obtain the 19×19 matrix Z_3 from representation (3.15) and perform two

symmetric reductions to get

$$\tilde{Z}_3 = T_{19,4,-2/5} T_{19,3,-1/8} Z_3 T^T_{19,3,-1/8} T^T_{19,4,-2/5}.$$

Now, for a factorization $\tilde{Z}_3 = BB^T$, we set $B = [B_l, B_i, B_r]$, where the 19×10 block matrix B_i is given with 5 unknowns

$$B_i = \begin{pmatrix} 0 & & & & & & & & & \\ \vdots & & & & & & & & & \\ 0 & & & & & & & & & \\ a & & & & & & & & & \\ b & & d & & & & & & & \\ a & c & e & a & & & & & & \\ & & d & b & & & & & & \\ & & & a & c & & & & & \\ & & & & & \ddots & & & & \\ & & & & & & d & & & \\ & & & & & & c & e & a & \\ & & & & & & & d & b & \\ & & & & & & & & a & \\ & & & & & & & & 0 & \\ & & & & & & & & \vdots & \\ & & & & & & & & 0 & \end{pmatrix}.$$

B_i has 5 null rows at the top and the bottom. Using the system of equations from the 9th and 10th columns of $\tilde{Z}_3 = B_i B_i^T$, we get a solution

$$a = \sqrt{0.169271 \times 10^{-3}}, \quad d = \frac{5\sqrt{2}}{128}, \quad b = \sqrt{\frac{173}{12288} - 2d^2},$$
$$e = \left(\frac{107}{30720} - ab\right)/d, \quad c = \sqrt{\frac{121}{12800} - 2a^2 - e^2}.$$

Consequently, the coefficients of the 10 interior wavelets are given by the columns of the matrix $T_{19,3,1/8} T_{19,4,2/5} B_i$

$$\psi_j(\cdot - k), \quad 1 \le j \le 3, \ 0 \le k \le 2, \quad \psi_1(\cdot - 3),$$

and they are generated by the 3 antisymmetric generators $\psi_1 := \psi_{0,8}$, $\psi_2 := \psi_{0,9}$, and $\psi_3 := \psi_{0,10}$. Their coefficients, in expansion (3.21), are listed in the Table A.5, and their supports are

$$\text{supp } \psi_1 = [0, 6], \quad \text{supp } \psi_2 = [1, 6], \quad \text{supp } \psi_3 = [0, 7].$$

The graphs of the 3 antisymmetric generators are shown in Figure A.5.

The columns of the 19×7 matrix $T_{19,3,1/8} T_{19,4,2/5} B_\ell$ represent the coefficients (see Table A.6) of the boundary wavelets having multiplicities at the left endpoint 0. The graphs of the boundary wavelets for the left endpoint are shown in Figure A.6.

i	$\hat{q}_{0,i+7}$	$\hat{q}_{1,i+7}$	$\hat{q}_{2,i+7}$	$\hat{q}_{3,i+7}$	$\hat{q}_{4,i+7}$	$\hat{q}_{5,i+7}$	$\hat{q}_{6,i+7}$
1	0.060915	0.487321	1.014873	0.487321	0.060915		
2			0.107158	0.857267	0.107158		
3	0.027621	0.220971	0.687814	0.862121	0.687814	0.220971	0.027621

TABLE A.5. Coefficients (*10) of interior wavelets $\psi_{0,7+i}, i = 1, 2, 3$, in expansion (3.21).

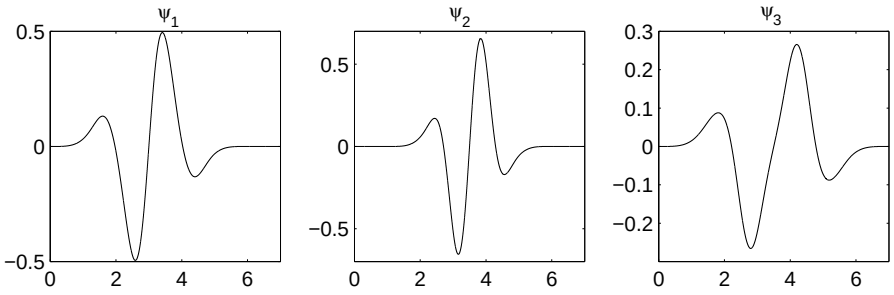

FIGURE A.5. Three antisymmetric generators of interior wavelets of the quartic spline tight frame with 3 vanishing moments and simple interior knots.

i	$\hat{q}_{-4,i}$	$\hat{q}_{-3,i}$	$\hat{q}_{-2,i}$	$\hat{q}_{-1,i}$	$\hat{q}_{0,i}$	$\hat{q}_{1,i}$	$\hat{q}_{2,i}$	$\hat{q}_{3,i}$	$\hat{q}_{4,i}$
1	0.108130	0.065534	0.010922						
2		0.261981	0.196515	0.068783	0.008598				
3			0.521353	0.337504	0.131162	0.033895	0.004237		
4				0.787054	0.561272	0.238378	0.070510	0.015510	0.001939
5					0.935485	0.619529	0.280960	0.077531	0.009691
6					0.119079	0.952636	0.267369	0.056491	0.007061
7					0.022096	0.176769	0.486114	0.176769	0.022096

TABLE A.6. Coefficients (*10) of the 7 boundary wavelets $\psi_{0,i}, i = 1, \ldots, 7$, in expansion (3.21).

A.4. Construction of a quintic spline tight frame with 6 vanishing moments ($m = 6, L = 6$)

We search for a quintic spline tight frames on $I = [0, 15]$, i.e. $n = 15$ in (3.13)-(3.14). As in the previous examples, we compute all matrices in representation (3.15). For a factorization of the 29×29 matrix Z_6 we apply three symmetric

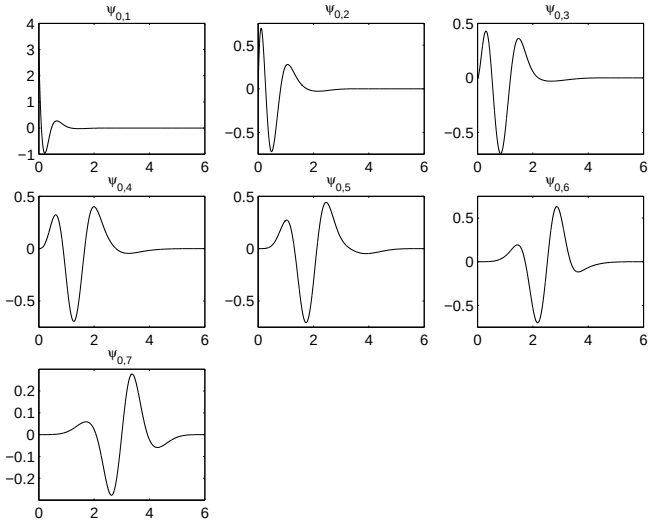

FIGURE A.6. Boundary wavelets of the quartic spline tight frame with 3 vanishing moments and simple interior knots.

reductions and get $\tilde{Z}_6$ by

$$\tilde{Z}_6 = T_{29,6,-\alpha_3} T_{29,5,-\alpha_2} T_{29,4,-\alpha_1} Z_6 T^T_{29,4,-\alpha_1} T^T_{29,5,-\alpha_2} T^T_{29,6,-\alpha_3},$$

where $\alpha_1 = 1/12,\ \alpha_2 = 9/35,\ \alpha_3 = 175/384.$

Now we suggest a factorization $\tilde{Z}_6 = BB^T$ by the matrix $B = [B_l, B_i, B_r]$, where B_i is the 29×16 block matrix given by

$$B_i = \begin{pmatrix}
0 & & & & & & & & & & & & & & & \\
\vdots & & & & & & & & & & & & & & & \\
0 & & & & & & & & & & & & & & & \\
a & & & & & & & & & & & & & & & \\
b & f & & & & & & & & & & & & & & \\
c & d & g & a & & & & & & & & & & & & \\
b & e & h & b & & & & & & & & & & & & \\
a & d & g & c & d & & & & & & & & & & & \\
 & & f & b & e & & & & & & & & & & & \\
 & & & a & d & & & & & & & & & & & \\
 & & & & & \ddots & & & & & & & & & & \\
 & & & & & & f & & & & & & & & & \\
 & & & & & & g & a & & & & & & & & \\
 & & & & & & h & b & & & & & & & & \\
 & & & & & & g & c & & & & & & & & \\
 & & & & & & f & b & & & & & & & & \\
 & & & & & & & a & & & & & & & & \\
 & & & & & & & 0 & & & & & & & & \\
 & & & & & & & \vdots & & & & & & & & \\
 & & & & & & & 0 & & & & & & & &
\end{pmatrix},$$

and B_i has 7 null rows at the top and the bottom. A possible solution of the factorization is obtained by letting

$$a = 0.651082 \times 10^{-4},\ b = 0.155501 \times 10^{-2},\ \ c = 0.484462 \times 10^{-2},\ d = 0.187213 \times 10^{-3},$$

$$e = 0.143774 \times 10^{-2},\ f = 0.296685 \times 10^{-2},\ g = 0.413488 \times 10^{-2},\ h = 0.108304 \times 10^{-1}.$$

As a result, the columns of the matrix $T_{29,4,\alpha_1}T_{29,5,\alpha_2}T_{29,6,\alpha_3}B_i$ give the coefficients of the 16 interior wavelets

$$\psi_j(\cdot - k), \quad 1 \le j \le 3, \ 0 \le k \le 4, \quad \psi_1(\cdot - 5),$$

and they are generated by the 3 symmetric generators (see Figure A.7) $\psi_1 := \psi_{0,12}$, $\psi_2 := \psi_{0,13}$, and $\psi_3 := \psi_{0,14}$. Their coefficients are given in the Table A.7 and their supports are

$$\text{supp } \psi_1 = [0, 10], \quad \text{supp } \psi_2 = [1, 11], \quad \text{supp } \psi_3 = [0, 11].$$

i	$\hat{q}_{0,i+11}$	$\hat{q}_{1,i+11}$	$\hat{q}_{2,i+11}$	$\hat{q}_{3,i+11}$	$\hat{q}_{4,i+11}$	$\hat{q}_{5,i+11}$	$\hat{q}_{6,i+11}$	$\hat{q}_{7,i+11}$	$\hat{q}_{8,i+11}$	$\hat{q}_{9,i+11}$	$\hat{q}_{10,i+11}$
1	0.001658	0.019897	0.107070	0.336420	0.682265	0.336420	0.107070	0.019897	0.001658		
2			0.001805	0.021663	0.101640	0.187099	0.101640	0.021663	0.001805		
3	0.002897	0.034768	0.188061	0.599465	1.227145	1.619062	1.227145	0.599465	0.188061	0.034768	0.002897

TABLE A.7. Coefficients(*100) of interior wavelets $\psi_{0,11+i}, i = 1, 2, 3$, in expansion (3.21).

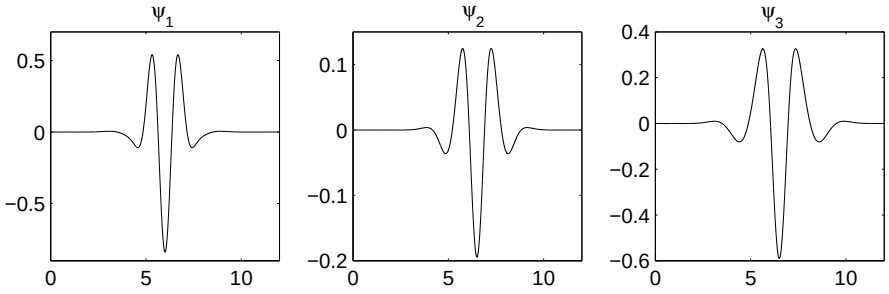

FIGURE A.7. Three symmetric generators of interior wavelets of the quintic spline tight frame with 6 vanishing moments and simple interior knots.

Now the coefficients of the 11 boundary wavelets for the left endpoint of the interval are found in the first 11 columns of the 29×11 matrix $T_{29,4,\alpha_1}T_{29,5,\alpha_2}T_{29,6,\alpha_3}B_\ell$. Table A.8 lists the coefficients in expansion (3.21) and Figure A.8 shows their graphs.

i	$\hat{q}_{-5,i}$	$\hat{q}_{-4,i}$	$\hat{q}_{-3,i}$	$\hat{q}_{-2,i}$	$\hat{q}_{-1,i}$	$\hat{q}_{0,i}$	$\hat{q}_{1,i}$	$\hat{q}_{2,i}$	$\hat{q}_{3,i}$	$\hat{q}_{4,i}$	$\hat{q}_{5,i}$	$\hat{q}_{6,i}$	$\hat{q}_{7,i}$	$\hat{q}_{8,i}$
1	0.1297	0.2712	0.2459	0.1095	0.0236	0.0020								
2		0.5244	0.9413	0.9299	0.5359	0.1773	0.0334	0.0028						
3			1.5236	2.4565	2.0941	1.1261	0.4326	0.1182	0.0207	0.0017				
4				2.8399	4.7083	4.1790	2.4199	0.9912	0.2995	0.0678	0.0108	0.0009		
5					4.3988	7.0284	6.3183	3.9763	1.8535	0.6439	0.1660	0.0320	0.0046	0.0004
6						5.6361	8.8393	7.9757	4.9753	2.2986	0.8046	0.2076	0.0354	0.0029
7						0.5451	6.5415	8.7155	7.2024	4.1913	1.7587	0.5103	0.0916	0.0076
8						0.1504	1.8052	7.8577	8.2460	5.6803	2.6394	0.8083	0.1481	0.0123
9						0.0726	0.8715	4.3191	10.2857	8.9272	4.5770	1.4647	0.2727	0.0227
10								0.0141	0.1687	0.7262	0.6719	0.2657	0.0528	0.0044
11								0.0005	0.0054	0.0264	0.0574	0.0264	0.0054	0.0005

TABLE A.8. Coefficients (*1000) of the 11 boundary wavelets $\psi_{0,i}, i = 1, \ldots, 11$, in expansion (3.21).

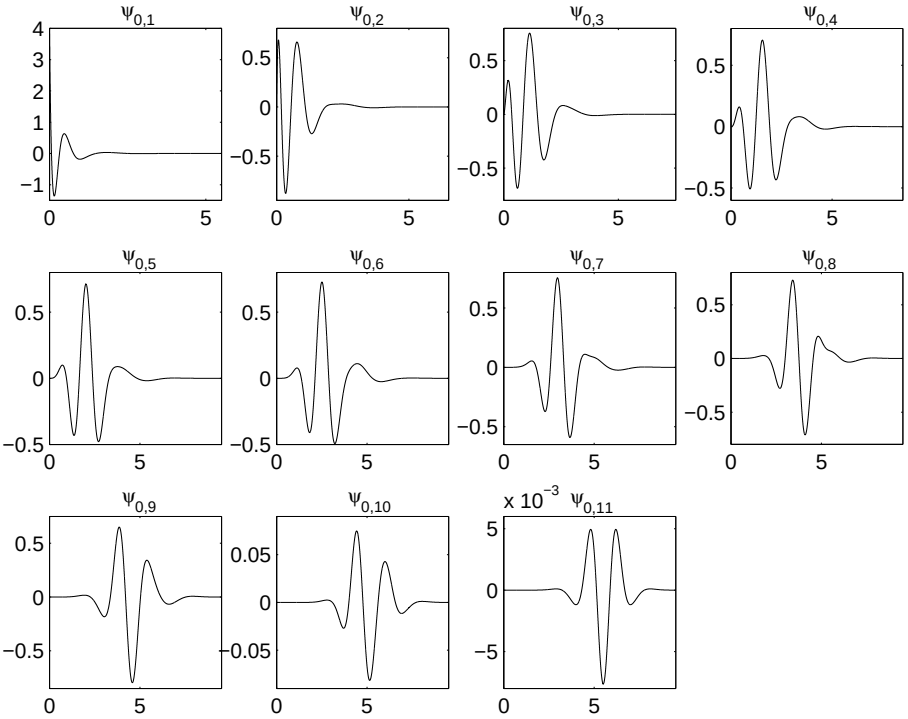

FIGURE A.8. Boundary wavelets of the quintic spline tight frame with 6 vanishing moments and simple interior knots.

Remark A.2. *In the work of Daubechies et al. ([***13***]) the three symmetric generators of a tight frame of* $L^2(\mathbb{R})$ *were introduced for the case* $m = 6, L = 6$. *The supports of them are the same as those of the three generators in this example.*

Bibliography

[1] C. de Boor, R. DeVore, and A. Ron, "Approximation from shift-invariant subspaces of $L_2(\mathbb{R}^d)$", Trans. Amer. Math. Soc. 341 (1994) 787-806

[2] P. L. Butzer and L. W. Trebels "Hilberttransformation, gebrochene Integration und Differentiation", (Forschungsber. des Landes Nordrhein-Westfalen **1889**) Westdeutsch. Verl., Köln und Opladen, 1968

[3] P. L. Butzer, "Fourier analysis and approximation", Birkhäuser, Basel und Stuttgart, 1971

[4] A. Cohen and I. Daubechies, "A stability criterion for biorthogonal wavelet bases and their related subband coding scheme", Duke Math. J. 68 (1992) 313-335

[5] C. K. Chui, "An introduction to wavelets", Academic Press, Boston, 1992

[6] C. K. Chui and W. He, "Compactly supported tight frames associated with refinable functions", Appl. Comput. Harmon. Anal. 8 (2000) 293-319

[7] C. K. Chui, W. He, and J. Stöckler, "Compactly supported tight and sibling frames with maximum vanishing moments", Appl. Comput. Harmon. Anal. 13 (2002) 224-262

[8] C. K. Chui, W. He, and J. Stöckler, "Nonstationary tight wavelet frames, I: Bounded Intervals", Appl. Comput. Harmon. Anal. 17 (2004) 141-197

[9] C. K. Chui, W. He, and J. Stöckler, "Nonstationary tight wavelet frames, II: Unbounded Intervals", Appl. Comput. Harmon. Anal. 18 (2005) 25-66

[10] C. K. Chui and X. Shi, "Bessel sequences and affine frames", Appl. Comput. Harmon. Anal. 1 (1993) 29-49

[11] C. K. Chui and J. Stöckler, "Recent development of spline-wavelet frames with compact support", in: G. V. Welland(Ed), Beyond Wavelets, Elsevier, New York, 2003, 151-214

[12] I. Daubechies, I. Guskov, and W. Sweldens, "Commutation for irregular subdivision", Constructive Approximation 15 (2001) 381-426

[13] I. Daubechies, B. Han, A. Ron, and Z. Shen, "Framelets: MRA-based constructions of wavelet frames", Appl. Comput. Harmon. Anal. 14 (2003) 1-46

[14] T. Eirola, "Sobolev characterization of solutions of dilation equations", Siam J. Math. Anal. 23 (1992) 1015-1030

[15] R. A. Gopinath, "The phaselet transform - An integral redundancy nearly shift-invariant wavelet transform", IEEE Trans. Signal Processing, 51 (2003) 1792-1805

[16] R. A. Gopinath, "Phaselets of framelets", IEEE Trans. Signal Processing, 53 (2005) 1794-1806

[17] E. Hernández and G. Weiss, "A first course on wavelets", CRC Press, New York, 1996

[18] N. Kingsbury, "Complex wavelets for shift invariant analysis and filtering of signals", Appl. Comput. Harmon. Anal. 10 (2001) 234-253

[19] W. Lawton, S. L. Lee, and Zuowei Shen, "Convergence of multidimensional cascade algorithm", Numerische Mathematik, 78 (1998) 427-438

[20] K. Y. Lee, and J. Stöckler, "Frame-Library: http://www.mathematik.uni-dortmund.de/lsviii/"

[21] S. Mallat, "A wavelet tour of signal processing", Academic Press, San Diego, 1998

[22] F. Natterer, "The mathematics of computerized tomography", Wiley, New York, 1986

[23] F. Natterer and F. Wübbeling, "Mathematical methods in image reconstruction", Siam, Philadelphia, 2001

[24] A. Petukhov, "Symmetric framelets", Constructive Approximation, 19(2) (2003) 309-328

[25] A. Ron and Z. Shen, "Affine systems in $L_2(\mathbb{R}^d)$: the analysis of the analysis operator", J. Functional Anal. 148 (1997) 408-447

[26] I. W. Selesnick, "Hilbert transform pairs of wavelet bases", IEEE Signal Processing Lett., 8 (2001) 170-173

[27] I. W. Selesnick, "The design of approximate Hilbert transform pairs of wavelet bases", IEEE Trans. Signal Processing, 50 (2002) 1144-1152

[28] I. W. Selesnick, "The double-density dual-tree DWT", IEEE Trans. Signal Processing, 52 (2004) 1304-1313

[29] W. Sweldens, "The lifting scheme: A custom-design construction of biorthogonal wavelets", Appl. Comput. Harmon. Anal. 3 (1996) 186-200

[30] S. Zhao, "Wavelet filtering for filtered backprojection in computed tomography", Appl. Comput. Harmon. Anal. 6 (1999) 346-373

[31] M. Vetterli and J. Kovačević, "Wavelets and subband coding", Prentice Hall, New Jersey, 1995